

**OPTIMISATION OF THE CLASSICAL SEMI-AUTOGENOUS  
AND BALL MILLING CIRCUIT USING THE ATTAINABLE  
REGION TECHNIQUE**

by

LUZUKO BASHE

submitted in accordance with the requirements for

the degree of

MAGISTER TECHNOLOGIAE

in the subject

ENGINEERING: CHEMICAL

at the

UNIVERSITY OF SOUTH AFRICA

SUPERVISOR: Prof FRANCOIS MULENGA

October 2019

## Declaration

Name: Luzuko Bashe

Student number: 64012867

Degree: Magister Technologiae in Chemical Engineering

Exact wording of the title of the dissertation as appearing on the electronic copy submitted for examination:

Optimisation of the classical semi-autogenous and ball milling circuit using the

attainable region technique

I declare that the above dissertation is my own work and that all the sources that I have used or quoted have been indicated and acknowledged by means of complete references.

I further declare that I submitted the dissertation to originality checking software and that it falls within the accepted requirements for originality.

I further declare that I have not previously submitted this work, or part of it, for examination at Unisa for another qualification or at any other higher education institution.

LUZUKO BASHE

October 2019

## **Dedication**

I dedicate this dissertation to my wonderful Wife who has been supporting and believing in me throughout this journey.

To my daughter for her inspiration and understanding that “Daddy has schoolwork to do” gave me the strength and motivation throughout this journey.

To my Mother, Father and Grandmother who always endorses education as a key to success in life.

Lastly, to everyone else that played different but important roles in this journey.

## **Acknowledgements**

First and foremost, I would like to thank our Heavenly Father for everything He has done for me. It is through You that I got this far, and I am eternally grateful for Your relentless blessings.

Secondly, I would like to thank Professor François Mulenga for believing in my abilities and continuous motivation. You have pushed my boundaries to higher levels, and I was privileged to have you as my mentor.

Lastly, I would like to thank the University of South Africa to allow me this opportunity to submit my dissertation.

## **Abstract**

The objective of this study was to improve the operation of the classical semi-autogenous and ball milling circuit also known as the SABC circuit. In order to achieve this goal, the challenges around this circuit were identified as the formation of critical sized material in a SAG mill. The size class considered for the critical sized material also known as pebbles was -100+23 mm. The attainable region (AR) method was used as an optimisation technique for the generated results using a computer simulation programme. MODSIM® demo version 3.6.22 is ore processing simulator that was used.

The research was divided into two sections, the first being the variation of feed flow rate ranging from 50 – 150 tph and ore feed size ranging between 100 and 600 mm. The second section compared the variation of the operating parameters of the SAG mill, which were mill filling, ball filling, ball size and mill speed. The AR technique graphically presented the results which indicated the best operating conditions to minimise pebble formation.

The effects of mill filling on a SAG mill indicate that a higher filling produces lower pebbles. Lower pebble generation also was observed at a higher ball filling. The influence of ball size indicated that the larger ball size was more effective in the reduction of pebbles. For mill speed the media displayed two common mode operations namely cascading at a low speed of 65% and cataracting at higher speed of 75%. The higher speed generated the least pebbles.

**Keywords:** Attainable region, semi-autogenous mill, ball mill, SABC circuit optimisation, pebbles, MODSIM®

## Table of contents

|   |           |
|---|-----------|
| <b>Declaration</b> .....  | v         |
| <b>Dedication</b> .....   | v         |
| <b>Acknowledgements</b> .....   | v         |
| <b>Abstract</b> .....   | v         |
| <b>List of figures</b> .....  | v         |
| <b>List of tables</b> .....   | v         |
| <b>List of symbols</b> .....  | v         |
| <b>Chapter 1 Introduction</b> .....   | <b>1</b>  |
| 1.1. Background and motivation .....  | 1         |
| 1.2. Justification and scope of the study .....                               | 2         |
| 1.3. Problem statement.....   | 3         |
| 1.4. Objectives and research questions .....                                  | 4         |
| 1.5. Dissertation outline .....   | 5         |
| <b>Chapter 2 Literature review</b> .....                                      | <b>7</b>  |
| 2.1. Introduction.....  | 7         |
| 2.2. Fundamentals of tumbling mills .....                                     | 7         |
| 2.3. Breakage mechanisms .....  | 10        |
| 2.4. Load behaviour in tumbling mills .....                                   | 12        |
| 2.5. Population balance model of milling.....                                 | 13        |
| 2.5.1. Selection function.....  | 15        |
| 2.5.2. Breakage function.....   | 17        |
| 2.5.3. Residence time distribution.....                                       | 19        |
| 2.6. Classical semi-autogenous mill, ball mill and cone crusher circuits..... | 21        |
| 2.6.1. Innovative configurations of the SABC circuits.....                    | 22        |
| 2.6.2. Pebble formation in comminution circuits.....                          | 24        |
| 2.6.3. Challenges faced during the design of SAG mills.....                   | 26        |
| 2.6.4. Optimisation of typical SABC circuits.....                             | 28        |
| 2.7. Attainable region theory in comminution operations .....                 | 33        |
| 2.8. Summary.....   | 36        |
| <b>Chapter 3 Research methodology and investigated design</b> .....           | <b>37</b> |

|   |           |
|---|-----------|
| 3.1. Introduction .....   | 37        |
| 3.2. Construction of the computer simulation model.....   | 38        |
| 3.3. Units modelled in MODSIM®.....   | 39        |
| 3.3.1. JAW1: Jaw crusher .....  | 39        |
| 3.3.2. SAGM: Semi-autogenous mill .....   | 40        |
| 3.3.3. SCR1: Single-deck vibrating screen.....  | 42        |
| 3.3.4. CYCA: Hydrocyclone.....  | 42        |
| 3.3.5. GMSU: Ball mill .....  | 44        |
| 3.3.6. CRSH: Cone crusher .....   | 45        |
| 3.4. Feed properties of material used .....   | 46        |
| 3.5. Simulation programme.....  | 47        |
| 3.6. Summary.....   | 50        |
| <b>Chapter 4 Simulation of the effects of pebble formation on the<br/>performance of the SABC circuit .....</b> | <b>51</b> |
| 4.1. Introduction.....  | 51        |
| 4.2. Simulation of the classical semi-autogenous/ball milling circuit .....                                     | 52        |
| 4.2.1. Simulated circuit for feed flow rate and ore feed size .....   | 56        |
| 4.2.2. Simulated circuit for operating parameters of the SAG mill .....   | 64        |
| 4.3. Energy consumption on the SAG mill closed circuit.....   | 64        |
| 4.4. Significance of the findings.....  | 65        |
| 4.5. Summary.....   | 67        |
| <b>Chapter 5 Attainable region analysis of the performance of the SABC<br/>circuit .....</b>                    | <b>68</b> |
| 5.1. Introduction.....  | 68        |
| 5.2. Construction of the attainable region .....  | 70        |
| 5.3. Effects of feed flowrate on the performance of the circuit .....   | 71        |
| 5.4. Effects of ore feed size on the performance of the circuit .....   | 75        |
| 5.5. Effects of load volume on the performance of the circuit .....   | 79        |
| 5.6. Effects of ball volume on the performance of the circuit .....   | 83        |
| 5.7. Effects of ball size on the performance of the circuit .....   | 87        |
| 5.8. Effects of ball mill speed on the performance of the circuit.....  | 91        |

|   |            |
|---|------------|
| 5.9. Concluding remarks .....                         | 95         |
| <b>Chapter 6 Conclusion and recommendations .....</b> | <b>96</b>  |
| 6.1. Introduction .....                               | 96         |
| 6.2. Overall summary of the findings .....            | 96         |
| 6.3. Future outlook .....                             | 100        |
| <b>List of references .....</b>                       | <b>101</b> |
| <b>Appendices .....</b>                               | <b>105</b> |

## List of figures

|             |  |    |
|-------------|--|----|
| Figure 1.1  | Typical semi-autogenous and ball milling circuit.....  | 2  |
| Figure 2.1  | Grinding methods .....   | 8  |
| Figure 2.2  | Illustration of the broad particle sizes typical of breakage by impact.....  | 11 |
| Figure 2.3  | Illustration of the narrow size spectrum of daughter particles and the remaining large rock produced as a result of breakage by attrition..... | 12 |
| Figure 2.4  | Different modes of operation of a tumbling mill.....   | 12 |
| Figure 2.5  | Mass balance for a single size fraction inside a mill .....  | 14 |
| Figure 2.6  | First-order and non-first-order breakage patterns.....   | 16 |
| Figure 2.7  | Cumulative percentage passing versus reduced size .....  | 18 |
| Figure 2.8  | The illustration of the mill with a schematic of the transportation model .....  | 20 |
| Figure 2.9  | Typical SABC circuit .....   | 21 |
| Figure 2.10 | SAG mill with high pressure grinding roll as a pebble crusher .....  | 23 |
| Figure 2.11 | Illustration of the specific rate of breakage in a SAG mill .....  | 25 |
| Figure 2.12 | Schematic of an AG mill with pebble ports.....   | 27 |
| Figure 2.13 | SAG mill with scats recycle.....   | 28 |
| Figure 2.14 | Crushing and screening circuit .....   | 30 |
| Figure 2.15 | Grinding circuit.....  | 31 |
| Figure 2.16 | An alternative configuration of the SABC circuit.....  | 32 |
| Figure 2.17 | Construction of the attainable region.....   | 35 |
| Figure 3.1  | Typical semi-autogenous/ball mill/crusher circuit.....   | 38 |
| Figure 3.2  | Jaw crusher parameters in MODSIM® .....  | 40 |
| Figure 3.3  | SAG mill parameters in MODSIM® .....   | 41 |
| Figure 3.4  | Screen parameters in MODSIM® .....   | 42 |
| Figure 3.5  | Hydrocyclone parameters in MODSIM® .....   | 43 |
| Figure 3.6  | Ball mill parameters in MODSIM® .....  | 44 |
| Figure 3.7  | Cone crusher parameters in MODSIM® .....   | 45 |
| Figure 3.8  | Feed properties in MODSIM® .....   | 47 |

|            |  |    |
|------------|--|----|
| Figure 4.1 | Simulation flow sheet on scenario 1 .....  | 56 |
| Figure 4.2 | Simulation flow sheet on scenario 2 .....  | 57 |
| Figure 4.3 | Simulation flow sheet on scenario 3 .....  | 58 |
| Figure 4.4 | Effects of particle size distribution of scenario 1 on the critical sized material .....   | 59 |
| Figure 4.5 | Effects of particle size distribution of scenario 2 on the critical sized material .....   | 60 |
| Figure 4.6 | Effects of particle size distribution of scenario 3 on the critical sized material .....   | 61 |
| Figure 4.7 | Energy usage in the SAG mill closed circuit .....  | 65 |
| Figure 5.1 | SAG mill in closed circuit .....   | 69 |
| Figure 5.2 | Milling kinetics of the SAG mill as a function of feed flow rate under the following simulation conditions: $J_T = 30\%$ , $J_B = 10\%$ , $d_B = 50$ mm, $\phi_c = 65\%$ of critical speed, and grate opening 40 mm with an ore feed of size -200+100 mm.....  | 71 |
| Figure 5.3 | Milling kinetics of the SAG mill as a function of feed flow rate under the following simulation conditions: $J_T = 30\%$ , $J_B = 10\%$ , $d_B = 50$ mm, $\phi_c = 65\%$ of critical speed, and grate opening 40 mm with an ore feed of size -400+200 mm.....  | 72 |
| Figure 5.4 | Milling kinetics of the SAG mill as a function of feed flow rate under the following simulation conditions: $J_T = 30\%$ , $J_B = 10\%$ , $d_B = 50$ mm, $\phi_c = 65\%$ of critical speed, and grate opening 40 mm with an ore feed of size -600+400 mm ..... | 73 |
| Figure 5.5 | Effects of feed flow of the SAG mill under the following simulated conditions: $J_T = 30\%$ , $J_B = 10\%$ , $d_B = 50$ mm, $\phi_c = 65\%$ of critical speed, and grate opening 40 mm .....   | 74 |
| Figure 5.6 | Milling kinetics of the SAG mill as a function of ore feed size under the following simulation conditions: $J_T = 30\%$ , $J_B = 10\%$ , $d_B = 50$ mm, $\phi_c = 65\%$ of critical speed, 40 mm grate opening, and a feed flow rate of 50 tph.....            | 75 |
| Figure 5.7 | Milling kinetics of the SAG mill as a function of ore feed size under the following simulation conditions: $J_T = 30\%$ , $J_B = 10\%$ , $d_B = 50$ , $\phi_c = 65\%$ of critical speed and grate opening 40 mm with a feed flow rate of 100 tph.....          | 76 |

|             |   |    |
|-------------|---|----|
| Figure 5.8  | Milling kinetics of the SAG mill as a function of ore feed size under the following simulation conditions: $J_T = 30\%$ , $J_B = 10\%$ , $d_B = 50$ , $\phi_c = 65\%$ of critical speed, and grate opening 40 mm with a feed flow rate of 100 tph.....                          | 77 |
| Figure 5.9  | Attainable region for the effects of ore feed of the SAG mill in the SABC circuit under the following simulated conditions: $J_T = 30\%$ , $J_B = 10\%$ , $d_B = 50$ mm, $\phi_c = 65\%$ of critical speed, and grate opening 40 mm.....  | 78 |
| Figure 5.10 | Milling kinetics of the SAG mill in the SABC circuit as a function of an ore feed of size -200+100 mm under the following simulation conditions: $J_B = 10\%$ , $d_B = 50$ mm, $\phi_c = 65\%$ of critical speed, and grate opening 40 mm with a feed flow of 100 tph .....     | 79 |
| Figure 5.11 | Milling kinetics of the SAG mill in the SABC circuit as a function of an ore feed of size -400+200mm under the following simulation conditions: $J_B = 10\%$ , $d_B = 50$ mm, $\phi_c = 65\%$ of critical speed, and grate opening 40 mm with a feed flow rate of 100 tph.....  | 80 |
| Figure 5.12 | Milling kinetics of the SAG mill in the SABC circuit as a function of an ore feed of size -600+400 mm under the following simulation conditions $J_B = 10\%$ , $d_B = 50$ mm, $\phi_c = 65\%$ of critical speed, and grate opening 40 mm with a feed flow rate of 100 tph.....  | 81 |
| Figure 5.13 | Attainable region for the effects of load volume of the SAG mill in the SABC circuit under the following simulated conditions: $J_B = 10\%$ , $d_B = 50$ mm, $\phi_c = 65\%$ of critical speed, and grate opening of 40 mm.....   | 82 |
| Figure 5.14 | Milling kinetics of the SAG mill in the SABC circuit as a function of an ore feed of size -200+100 mm under the following simulation conditions: $J_T = 30\%$ , $d_B = 50$ mm, $\phi_c = 65\%$ of critical speed, and grate opening 40 mm with a feed flow rate of 100 tph..... | 83 |
| Figure 5.15 | Milling kinetics of the SAG mill in the SABC circuit as a function of an ore feed of size -400+200 mm under the following simulation conditions: $J_T = 30\%$ , $d_B = 50$ mm, $\phi_c = 65\%$ of critical speed, and grate opening 40mm with a feed flow rate of 100 tph.....  | 84 |
| Figure 5.16 | Milling kinetics of the SAG mill in the SABC circuit as a function of an ore feed of size -600+400 mm under the following simulation conditions: $J_T = 30\%$ , $d_B = 50$ mm, $\phi_c = 65\%$ of critical speed, and grate opening 40 mm with a feed flow of 100 tph .....     | 85 |

|             |   |    |
|-------------|---|----|
| Figure 5.17 | Attainable region for the effects of the ball volumetric filling of the SAG mill in the SABC circuit under the following simulated conditions: $J_T = 30\%$ , $d_B = 50$ , $\phi_c = 65\%$ of critical speed, and grate opening 40 mm.....                                | 86 |
| Figure 5.18 | Milling kinetics of the SAG mill in the SABC circuit as a function of an ore feed of size -200+100mm under the following simulation conditions: $J_T = 30\%$ , $J_B = 10\%$ , $\phi_c = 65\%$ of critical speed, and grate opening 40 mm with a feed flow of 100 tph..... | 87 |
| Figure 5.19 | Milling kinetics of the SAG mill in the SABC circuit as a function of an ore feed of size -400+200mm under the following simulation conditions: $J_T = 30\%$ , $J_B = 10\%$ , $\phi_c = 65\%$ of critical speed, and grate opening 40 mm with a feed flow of 100 tph..... | 88 |
| Figure 5.20 | Milling kinetics of the SAG mill in the SABC circuit as a function of an ore feed of size -600+400mm under the following simulation conditions: $J_T = 30\%$ , $J_B = 10\%$ , $\phi_c = 65\%$ of critical speed, and grate opening 40 mm with a feed flow of 100 tph..... | 89 |
| Figure 5.21 | Attainable region for the effects of the ball size of the SAG mill in the SABC circuit under following simulated conditions: $J_T = 30\%$ , $J_B = 10\%$ , $\phi_c = 65\%$ of critical speed, and grate opening 40 mm .....   | 90 |
| Figure 5.22 | Milling kinetics of the SAG mill in the SABC circuit as a function of an ore feed of size -200+100mm under the following simulation conditions: $J_T = 30\%$ , $J_B = 10\%$ , $d_B = 50$ mm, and grate opening 40 mm with a feed flow of 100 tph.....                     | 91 |
| Figure 5.23 | Milling kinetics of the SAG mill in the SABC circuit as a function of an ore feed of size -400+200 mm under the following simulation conditions: $J_T = 30\%$ , $J_B = 10\%$ , $d_B = 50$ mm, and grate opening 40 mm with a feed flow of 100 tph.....                    | 92 |
| Figure 5.24 | Milling kinetics of the SAG mill in the SABC circuit as a function of an ore feed of size -600+400 mm under the following simulation conditions: $J_T = 30\%$ , $J_B = 10\%$ , $d_B = 50$ mm, and grate opening 40 mm with a feed flow of 100 tph.....                    | 93 |
| Figure 5.25 | Attainable region for the effects of the ball size of the SAG mill in the SABC circuit under the following simulated conditions: $J_T = 30\%$ , $J_B = 10\%$ , $d_B = 50$ mm, and grate opening 40 mm .....   | 94 |

## List of tables

|           |  |    |
|-----------|--|----|
| Table 1.1 | Process flow unit description .....  | 3  |
| Table 2.1 | Summary of SAG milling circuits .....  | 23 |
| Table 3.1 | Simulation programme for the SABC circuit .....                                      | 49 |
| Table 4.1 | Simulation programme for the SABC circuit for feed flow rate and ore feed size ..... | 53 |
| Table 4.2 | Simulation programme for the SABC circuit on SAG mill operating parameters .....     | 54 |
| Table 4.3 | Simulation results of the scenarios .....  | 63 |
| Table 4.4 | Operating parameters of the SAG mill.....  | 64 |

## List of symbols

| Symbol    | Description  | Units                  |
|-----------|--|------------------------|
| $a_i$     | Selection function parameters dependent on the properties of the material and the grinding conditions              | $\text{min}^{-1}$      |
| $B_{i,j}$ | Cumulative breakage distribution function for particles of size $j$ reporting to size $i$ after breakage           | -                      |
| $F$       | Feed rate of the mill of the solid particles   | $\text{kg}/\text{min}$ |
| $S_i$     | Selection function of particles of size $x_i$  | $\text{min}^{-1}$      |
| $S_{i,j}$ | Selection function of particles of size $x_i$ due to grinding balls of diameter $d_j$ present in a ball charge mix | $\text{min}^{-1}$      |
| $t$       | Grinding time used in each batch mill  | $\text{min}$           |
| $w$       | Total mass of the feed   | $\text{kg}$            |
| $w_i$     | mass fraction of unbroken material of size $i$ in the mill   | -                      |
| $x_i$     | Upper limit of particle size interval $i$  | $\text{mm}$            |

| Greek Symbol | Description   | Units        |
|--------------|---|--------------|
| $\alpha$     | Selection function  | -            |
| $\beta$      | Breakage function parameter characteristic of the material used whose values range from 2.5 to 5                            | -            |
| $\Phi_j$     | Breakage function fraction of fines that are produced in a single fracture event and is also dependant on the material used | -            |
| $\tau$       | Mean residence time   | $\text{min}$ |
| $\gamma$     | Breakage function material-dependent characteristic whose values are typically found to be between 0.5 to 1.5               | -            |
| $\mu$        | Selection function parameter dependent on mill conditions   | -            |

## Chapter 1 Introduction

### 1.1. Background and motivation

Comminution refers to methods of liberating valuable minerals from the natural host rock by mechanical size reduction to produce usable products. From a mineral processing perspective, the term encompasses the crushing and grinding of mineral ores.

Comminution is an important step of the mine value chain as it accounts for 8 % of the South African gross domestic product (Lehohla, 2017). With such a significant value, it is essential to enhance comminution processes while thriving to make them more economical and energy-efficient. Indeed, comminution operations are generally both expensive and energy intensive (Kawatra *et al.*, 2001). Opportunities of improvement are therefore pursued in view to use the lowest energy for greater throughput.

Coarse particles are generally inadequately liberated and lead to limited recovery; and thus, limited revenue in the subsequent separation stage. Finer grind, on the other hand, requires excessive energy that is not always mitigated by any possible increment in recovery (Zhang, 2016). These conflicting factors necessitate the use of optimisation tools that can integrate them in a flexible manner. The motivation for this is guided by the fact that Lynch and Morrison (1999) argued that SABC circuits are still optimised using trial and error techniques more than anything. The attainable region as an optimisation technique was exploited on a classical Semi-Autogenous, Ball mill and Crusher circuit known as SABC circuit. A typical SABC circuit is illustrated in Figure 1.1 which is used as the process flow diagram for this dissertation.



encompass SAG milling units. Table 1.1 below defines the units that are numbered in Figure 1.1.

Table 1.1: Process flow unit description

| Unit Number | Unit Description | Functionality  |
|-------------|------------------|----------------|
| 1           | Jaw Crusher      | Size reduction |
| 2           | Stockpile        | Mixing unit    |
| 3           | Mixer            | Mixing unit    |
| 4           | SAG Mill         | Size reduction |
| 5           | Screen           | Classifier     |
| 6           | Cone Crusher     | Size reduction |
| 7           | Sump             | Mixing unit    |
| 8           | Centrifugal Pump | Mass transfer  |
| 9           | Hydrocyclone     | Classifier     |
| 10          | Ball Mill        | Size reduction |

### 1.3. Problem statement

Semi-autogenous mills are central to the overall performance of SABC circuits; yet, their optimisation is challenging (Napier-Munn *et al.*, 1996). One reason is that their throughput rates are dependent on the hardness and particle size distribution of the feed (McCaffery *et al.*, 2006). The existence of the so-called ‘critical size’ of material in the circuit further exacerbates the problem (Zhang, 2016). Critical-size material or pebbles represents the fraction of the feed that does not self-break as readily as other size fractions. It therefore builds up in the SAG mill circuit especially if no crusher is present. In the case of Figure 1.1, it can be seen that the product from the SAG mill is screened so that the oversize material is recycled back to the SAG mill feed.

The attainable region is a graphical method used to identify the optimal region of a system. The approach is applied to the SABC circuit in the search for reduced energy consumption while preferentially producing a material within a predefined size range. A significant increase of the throughput can be achieved by means of minimising the formation of pebbles in a SAG mill. The application of the AR technique which uses objective functions rather than process equipment (Mulenga and Bwalya, 2015) can resolve this problem.

In an objective to obtain optimal process operation, this research study is essential to investigate on the significance of the SABC circuit in mineral processing. As mentioned earlier, the SAG mill is central to the SABC circuit and its major problem exists in the accumulation of the pebbles. This research is used to investigate on methods to minimise these critical sized particles to increase the overall efficiency of the SABC circuit.

#### 1.4. Objectives and research questions

The aim of the study is to apply the attainable region technique on the SABC circuit in anticipation to determine the optimal processing outcome under profound conditions. This is achieved through the following objectives:

- To investigate the effects of feed size distribution on the formation of critical size and performance of an SABC circuit
- To investigate the effects of feed rate on the energy consumption and throughput of an SABC circuit
- To determine the milling conditions that will guarantee optimal production of a material of a certain fineness using the attainable region technique

Through these objectives, it is expected that the graphical technique enables us to gain more insights in SABC optimisation beyond what is already known from traditional techniques. This is prepared by analysing the processing effects with

respect to ore feed size and production rate of a simulated SABC circuit. Furthermore, the circuit is under confined downstream parameters as the input conditions are subjected to change. Though the data generated in the research are simulation based, the parameters of the SABC circuit are most accurate to which a proposal of a laboratory scale of experiments could be done in the future. Finally, the research establishes a precedent for the use of the AR technique in the minerals industry as a tool of choice for the analysis and optimization of mineral processing circuits (Chimwani, 2014). Consequently, the objectives listed above would be achieved by answering the following questions:

- What effects do varied feed size distribution and feed rate have on the SABC circuit?
- What extent does pebble formation affect an SABC circuit?
- Can the attainable region methodology be used to find optimum operating conditions?

### 1.5. Dissertation outline

The dissertation is structured into 6 chapters. Chapter 1 is the introduction which describes the background, problem statement and objectives of the study.

Chapter 2 presents the literature review which includes a comprehensive delineation of the theory of milling and its fundamentals. The chapter also covers the classical SABC circuit with its optimisation methods and the application of attainable region theory in comminution operations.

Chapter 3 is the research methodology and investigated design which includes the construction of the computer simulation and classification on the parameters of the units that are assembled. The chapter considers the feed material used for simulation and the simulation programme with their respective operating conditions. The simulation programme consists of scenarios that have different

input conditions and operating parameters to produce output data for the research.

Chapter 4 is the simulation of the effects on pebble formation on the semi-autogenous and ball milling circuit which depicts the different simulations in their respective configuration and all the significant findings.

Chapter 5 is the presentation of the attainable region method and the discussion of this application. The AR technique is used on the results generated from the simulation programme. Its application enables us to determine the most favourable operating conditions for this system.

Chapter 6 concludes the study with a summary of significant findings while providing recommendations for future work.

## **Chapter 2 Literature review**

### **2.1. Introduction**

There exists a variety of circuit configurations that can be used for comminution. However, this literature review focuses on the SABC configuration. Relevant studies around the SABC circuit are reviewed with the aim of comprehending its operation and importance in comminution. The breakage mechanisms forming the basis of comminution operations are also discussed. The review highlights the performance of an SABC circuit with particular attention to the ever-present problem of pebble formation (Zhang, 2016). The fundamentals of milling circuits that underpin computer simulation software packages are then described. These include the selection function, the breakage function, the residence time distribution and the population balance model.

The chapter is concluded with the latest application of the attainable region technique in comminution. This technique is known as an approach derived from chemical reaction processes and that basically regards systems as made of reactants and products of interest. Its simplicity has attracted a lot of interest to be used as an optimisation tool for comminution operations. Associated findings and future avenues for research enquiry are also explored.

### **2.2. Fundamentals of tumbling mills**

Comminution is a generic term for the size reduction of materials with crushing and grinding being the two primary processes (Balasubramanian, 2017). The term milling, also known as grinding, refers to all the comminution operations designed to break mineral ore into smaller pieces by the action of abrasion, attrition, and impact using grinding media (Han, 2019). The size of the ore fed to a grinding unit

can range from 5 mm and 20 mm while the discharged product can be as fine as 150  $\mu\text{m}$ .

Comminution, and milling in particular, is commonly recognised as an energy intensive process (Umucu *et al.*, 2015). Several studies have attempted to quantify the amount of energy used in this process with contradictory findings (e.g. Daniel and Lewis-Gray, 2011; Tromans, 2008). However, there is a consensus that comminution energy typically accounts for between 35 % and 50 % of the total running costs of a mining operation (Curry *et al.*, 2014).

The main purpose of milling is to liberate individual minerals trapped in the rock fragments from the upstream crushing operation. Mineral liberation is done in preparation for the subsequent enrichment of the ore. Milling as a size reduction process may be carried out on either dry materials or slurries, i.e. mixtures of water and solid particles (Balasubramanian, 2017).

Figure 2.1 provides a summary of the types of grinding methods that can be used to achieve comminution at a milling stage. These are tumbling, stirring, and vibration. The scope of the review is limited to milling by tumbling action as is inherently found in ball mills, autogenous mills, and semi-autogenous mills.

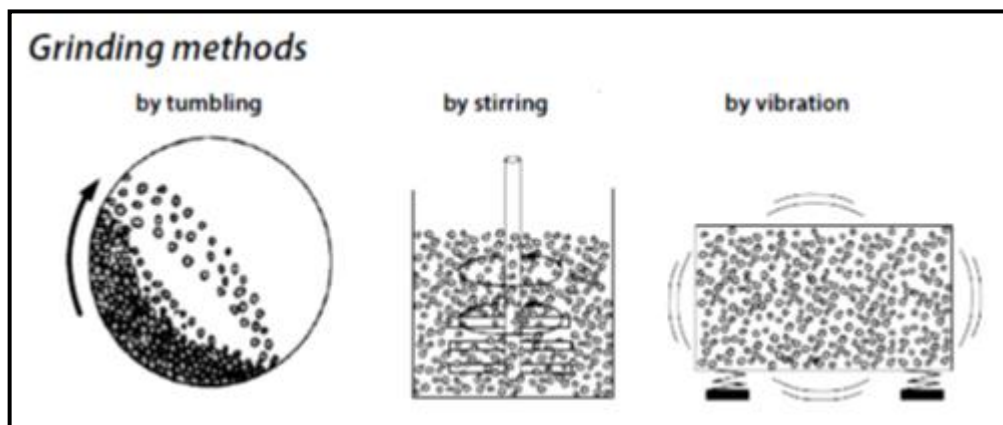


**Figure 2.1** Grinding methods (Balasubramanian, 2017)

Grinding mills are machines used in mineral processing for producing finely sized particles through impact, attrition, abrasion, and compression breakage. The

reliance on a combination of the above breakage mechanisms is generally dependent on the type of milling equipment used. It is also dictated by whether milling is done as a primary, secondary, or tertiary stage (Wikedzi, 2018). The following are the popularly milling units: autogenous mill, semi-autogenous mill, pebble mill, and ball mill. They are collectively referred to as tumbling mills because they perform grinding by tumbling (see Figure 2.1).

Autogenous mills or AG mills are rotating drums loaded with big lumps of rock that take the duty of breaking smaller rocks primarily by impact. The lumps, in turn, break through a process of self-grinding as result of repetitive tumbling. The tumbling action is such that the mill load is imparted with a cascading motion that throws larger ore particles around. Semi-autogenous mills, or SAG mills for short, apply the same principle as AG mills; however, spherical steel balls are used to assist with the grinding. This is to remedy to the presence of less competent rock lumps that can neither self-break well nor break smaller particles. AG and SAG mills find wide use in the primary stage of grinding.

Pebble mills are rotating drums that encourage mostly attrition between rock pebbles and ore particles. Rock pebbles are used as a substitute to steel balls where product contamination by iron from steel balls is to be avoided.

Ball mills consist of a horizontal rotating cylinder partially filled with grinding balls that bring about material grinding by attrition and impact. The combined breakage mechanisms grind the material down to the size fine enough to guarantee mineral liberation. That is why this type of mill is typically used just before the concentration of mineral ores. The next section discusses the breakage mechanisms that tumbling mills rely upon to effect comminution.

### 2.3. Breakage mechanisms

Milling is a highly energy-intensive process with the processing units being the most inefficient of the industry (Napier-Munn *et al.*, 1996). Milling has therefore

a great bearing on the operating costs of mineral processing plants. As such, it is important to describe the process well so that optimal operation can be obtained.

King (2001) has extensively discussed two breakage mechanisms prominent in tumbling mills: impact breakage and breakage by attrition. Impact breakage is most common in AG, SAG and ball mills while attrition frequently occurs in AG and SAG mills. Figure 2.2 illustrated the fracture pattern that can be expected from breakage by impact of a parent particle. The size range and size distribution of the daughter fragments formed is also provided along. Impact breakage is induced by the rapid application of compressive stress. It can be seen from Figure 2.2 that the offspring fragments are formed from the parent particle producing a broad size range. In a tumbling mill, impact breakage occurs in a series of steps in which the parent particle is fragmented followed directly by the consecutive fracturing of successively generated daughter fragments. This continues until all the energy available for fracture is dissipated.

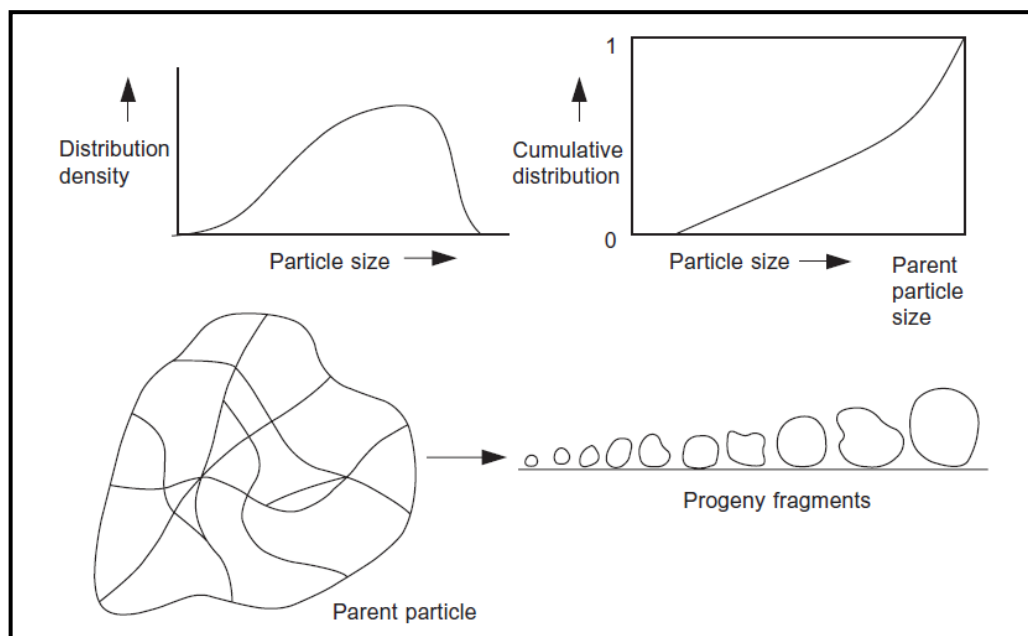


**Figure 2.2** Illustrates of the broad particle sizes typical of breakage by impact (after King, 2001)

Similarly, Figure 2.3 shows the result of breakage by attrition with minor size changes recorded for the parent particle. In contrast, numerous smaller particles are produced by rubbing of the parent particle against other particles or grinding balls. This type of breakage is more prevalent in AG and SAG mills where large particles are present to perform as breakage media while generating stresses that are not large enough to cause fracture.

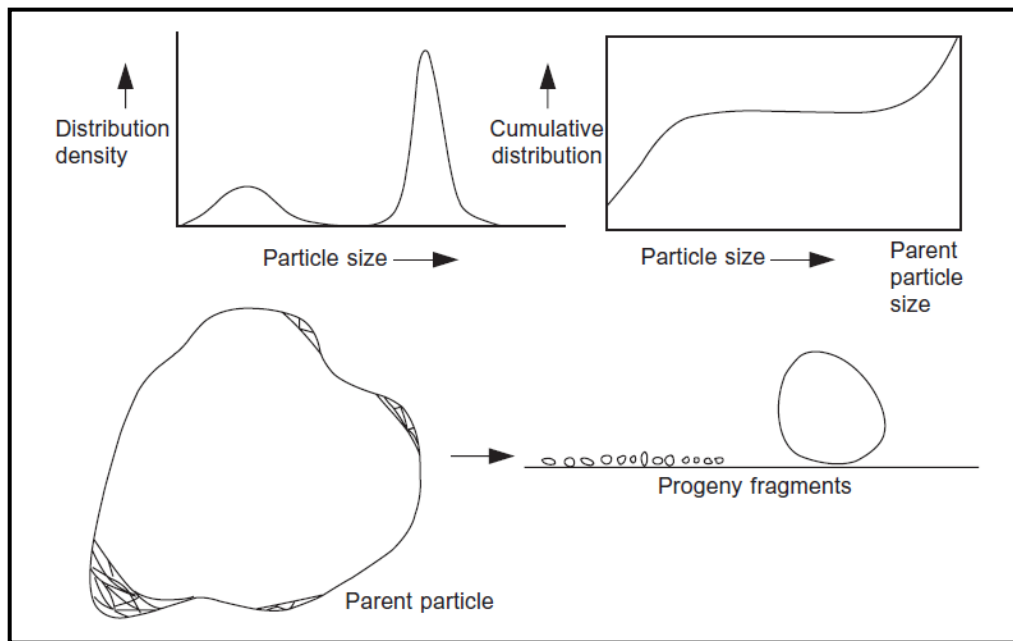


**Figure 2.3** Illustration of the narrow size spectrum of daughter particles and the remaining large rock produced as a result of attrition breakage (after King, 2001)

#### 2.4. Load behaviour in tumbling mills

Regardless of the grinding media used, tumbling mills generate breakage based on the behaviour of the load. Figure 2.4 illustrates the three types of behaviour descriptive of the en masse motion of the load. This motion is influenced by parameters such as the volumetric filling and the rotational speed of the drum.

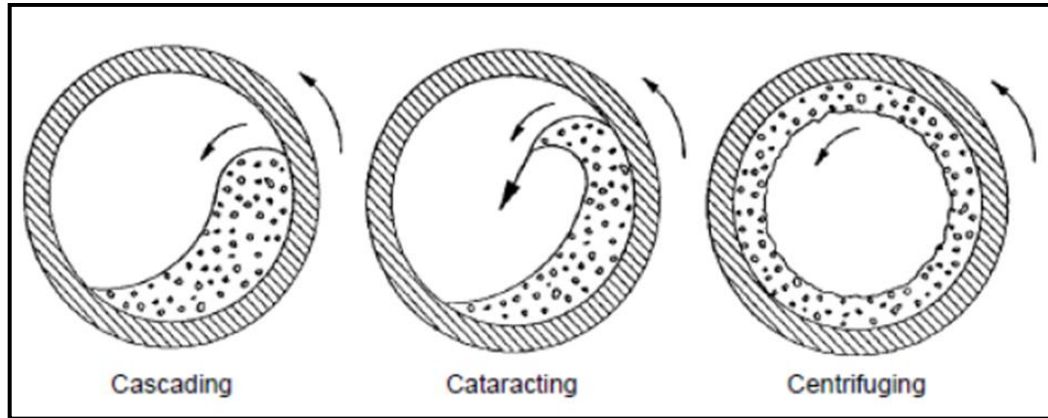


**Figure 2.4** Different modes of operation of a tumbling mill (Yulia *et al.*, 2016)

The mill load is said to be cascading when the charge material emerges from the highest point of the load (or shoulder of the load) and then rolls back down the surface of the charge to the toe of the load. This behaviour occurs at low mill speed and leads to the breakage of particles by attrition.

In the centrifuging behaviour, the mill is run at a speed higher than the critical speed. The latter is the theoretical speed at which a single ball loaded inside the mill starts to stick against the wall of the drum in a centrifuging motion (Austin *et al.*, 1984). Centrifuging occurs when the mill is operated at super-critical speeds; it reduces the mill diameter and causes part of the charge to become inactive.

Cataracting occurs at mill speed that is less than the critical speed but greater than cascading speeds. This behaviour is experienced by the portion of the charge that is elevated high enough in the mill around the shoulder before falling back down to the toe in free flight motion (see Figure 2.4). It is desired that the high potential energy of cataracting grinding media be converted into impact breakage of particles around the toe of the load.

## 2.5. Population balance model of milling

The accurate modelling of material breakage is critical to achieving good design, operation and control of milling circuits (Koka and Trass, 1987). The most widely

accepted milling model is built around the population balance modelling framework (Yekeler, 2007). This was introduced by Epstein (1947) with further development by many including Austin *et al.* (1983), Herbst and Fuerstenau (1968 & 1972), Kelsall *et al.* (1969), and Whiten (1974). Modern simulation software packages such as JKSIMMet™ and MODSIM® are computer-rendered scripts of the population balance model (Napier-Munn *et al.*, 1996; King, 2012).

The population balance model applied to comminution processes describes particles that are transformed from their parent size range into smaller daughter particles (Anticoi *et al.*, 2018). A detailed understanding of grinding is essential for modelling such a mechanism. A mass balance can be considered to derive the actual model for a particular size fraction  $i$  within a mill with the transport into a breakage zone, breakage in and transport out of the zone (Napier-Munn *et al.*, 1996; King, 2001) as shown in Figure 2.5.

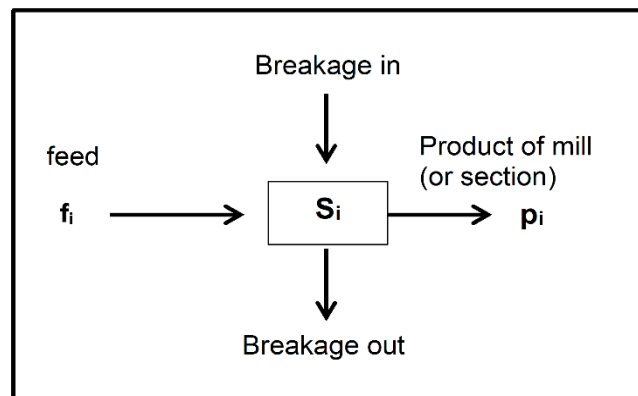


**Figure 2.5** Mass balance for a single size fraction inside a mill  
(Napier-Munn *et al.*, 1996)

It follows that:

$$\text{Feed in} + \text{Breakage in} = \text{Product out} + \text{Breakage out} \quad (2.1)$$

This essential behaviour suggests that the process is a combination of two actions taking place simultaneously inside the mill (Gupta and Yan, 2006). These processes are known as the selection function and the breakage function. The formation of

the population balance model requires these two functions, as they provide a foundation for the modelling of the grinding process. It describes material breakage in mills (Reid, 1965; Kelsall and Reid, 1965; Austin, 1971 & 1972; Mike, 1975) based on size-mass balances on narrow size intervals of the particulate mass. In relations to the selection and breakage function parameter, the particulate masses are subjected to breakage in the mill and are formulated (Koka and Trass, 1988). The selection function and breakage function are two functions that lead to the formation of the population balance model, with Austin (1971) and Lucky (1972) considering that the parameter of these function could be used to investigate the kinetics of size reduction in mills.

### 2.5.1. Selection function

This model is called first order rate model (Napier-Munn *et al.*, 1996). This is because it assumes that the formation of the ground material per unit time within the mill depends only on the mass of the size fraction which is present in the mill contents.

The selection function or breakage rate is defined as the rate at which material is broken out of a particular discretized size class (Austin *et al.*, 1984). This rate is presented as the chart of breakage probability versus a system variable such as grinding time. The breakage of a given size fraction of material usually follows a first-order law (Austin, 1972):

$$\frac{dw_i}{dt} = -S_i w_i(t) \quad (2.2)$$

where  $w_i(t)$  represents the mass fraction of unbroken material of size  $i$  in the mill at time  $t$

$S_i$  is the rate of disappearance of material of size  $i$ , also known as selection function.

The pattern for first-order and non-first-order breakage can be illustrated in Figure 2.6. As the mass fraction decreases with time in a linear form it reaches a stage where the breakage decelerates or accelerates. Non-first-order grinding usually occurs when coarse particles are being ground (Chimwani, 2014) and in this case of breakage it is referred to be abnormal breakage.

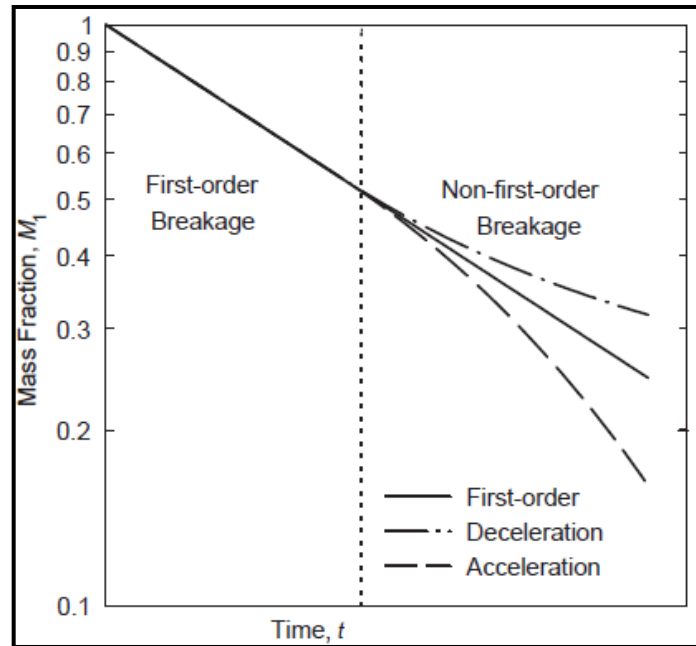


**Figure 2.6** First order and non-first-order breakage patterns (Bilgili *et al.*, 2006)

Austin *et al.* (1984) suggested that the most important point is how the breakage rate changes with respect to particle size, thus able to show the rate of disappearance of particles as a function of size is given by:

$$S_i = a_i x_i^\alpha \quad (2.3)$$

where  $x_i$  is the upper limits of the size interval [in mm] indexed by  $i$

$a_i$  and  $\alpha$  are model parameters dependent on the properties of the material and the grinding conditions.

A generalised model proposed by Austin *et al.* (1984) to define the selection function is described below:

$$S_i = a_i x_i^\alpha \frac{1}{1 + \left(\frac{x_i}{\mu}\right)^\Lambda} \quad (2.4)$$

where  $x_i$  is the upper limits of the size interval [in mm] indexed by  $i$

$\Lambda$  and  $\alpha$  are positive constants which are dependent on material properties;

$a_i$  is a parameter dependent on mill conditions and material properties,  
which indicates the rate of grinding;

$\mu$  is a parameter dependent on mill conditions.

### 2.5.2. Breakage function

Kelly and Spottiswood (1990) defined the breakage function, also called the primary breakage distribution function, as the average size distribution resulting from the fraction of a single particle. The distribution of sizes is produced after a single step of breakage of a particle. Austin *et al.* (1984) proposed an empirical model to describe the primary breakage distribution function of a particle of size  $j$  reporting to size  $i$ :

$$b_{i,j} = \frac{\text{mass of particles from class } j \text{ broken to size } i}{\text{mass of particles of class } j \text{ broken}} \quad (2.5)$$

However, Austin *et al.* (1984) established that the usage of the cumulative breakage function would be more suitable in describing the breakage distribution function. This method is defined as follows:

$$B_{i,j} = \sum_{k=n}^i b_{k,j} \quad (2.6)$$

where  $B_{i,j}$  represents the weight fraction of the material leaving the top size interval  $j$  going to all size fractions finer than size  $i$ .

$k$  represents the finest size fraction into which particles breaking from top size  $j$  can reach.

From the definition in Equation (2.6), Austin *et al.* (1984) demonstrated that the cumulative breakage function can be express as a function of particle size:

$$B_{i,j} = \Phi_j \left( \frac{x_{i-1}}{x_j} \right)^\gamma + (1 - \Phi_j) \left( \frac{x_{i-1}}{x_j} \right)^\beta \quad (2.7)$$

where  $\Phi_j$  represents the fraction of fines that are produced in a single fracture event and is also dependant on the material used.

$\gamma$  represents a material-dependent characteristic whose values are typically found to be between 0.5 to 1.5.

$\beta$  is a parameter characteristic of the material used whose values range from 2.5 to 5.

Austin *et al.* (1984) explains the formula as  $\Phi_j$ ,  $\gamma$ , and  $\beta$  being model parameters that depend on the properties of the material. Furthermore, an assumption for the breakage function to be normalizable was considered by Austin *et al.* (1984) as it considers the breakage distribution function as independent to the initial particle size. Therefore, in this case  $\Phi_j$  is not a function of the parent size as seen in Figure 2.7. Austin *et al.* (1984) and King (2001) found that for many materials and for simulation purposes it has been proven acceptable while arguable in essence.

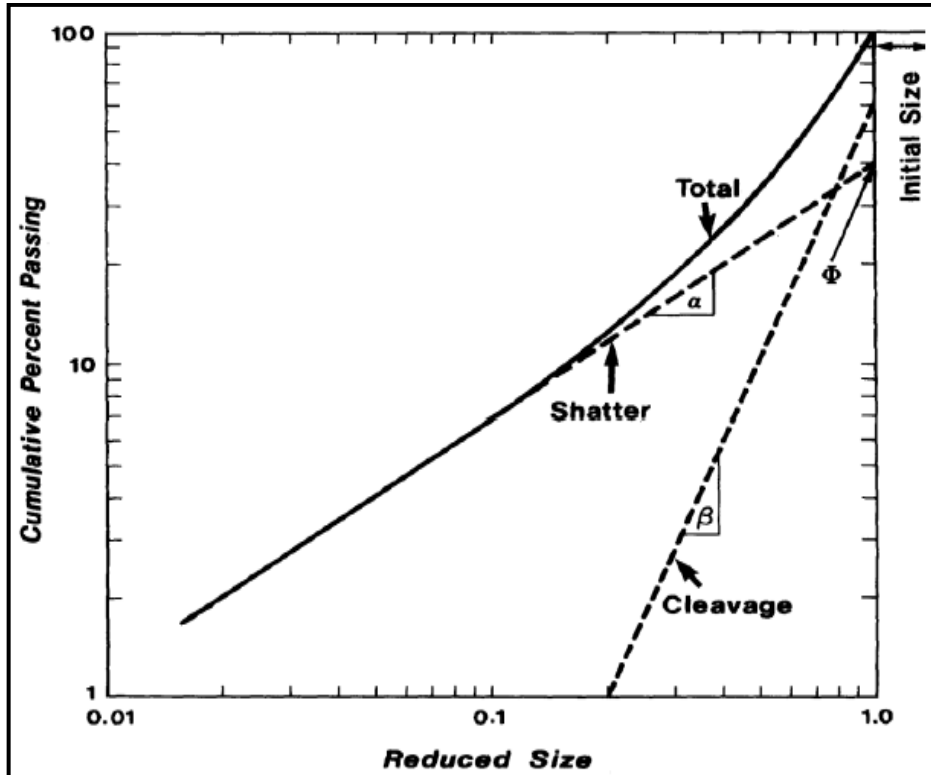


**Figure 2.7** Cumulative percentage passing versus reduced size  
(Kelly and Spottiswood 1990)

The breakage function for AG and SAG mills as described by King (2001) is determined essentially by the impact energy level and the  $t_{10}$  method. The  $t_{10}$  method is the fraction of the daughter particles that are smaller than  $1/10^{\text{th}}$  of the parent size. In self-breakage the impact energy is a function of the lump size and the height of the drop. It is calculated as the potential energy of the lump at half the inside diameter of the mill. The average energy calculated for impact breakage as the net specific power input to the mill charge.

### 2.5.3. Residence time distribution

The residence time of the material in a mill can vary as some particles of the material could leave immediately, whereas some may stay for longer period. Therefore, a residence time distribution (RTD) function exists that can be measured by tracer tests. Experimentally in a grinding system, a dynamic tracer

test can be used to measure the residence time distribution function (King, 2001). It is usually introduced in sections of a mill to determine appropriate time intervals (Napier-Munn, 1999). Given a mill containing two different physical states namely liquid and solid they would therefore share two different residence time distributions as the solids would experience a greater resistance to flow than the liquid. Nevertheless, King (2001) found that although the two phases have significantly different mean residence times, the behaviour of each phase is consistent. Cho (2013) noted that various forms to describe the RTD of grinding mills are used in presentation of the RTD in a functional form. Using an equation recommended by Austin *et al.* (1984) that is expressed by the following:

$$E(t) = 1 - \exp\left(-\frac{t}{\tau}\right) \quad (2.8)$$

where  $E(t)$  represents the cumulative fraction of traced feed, while  $t$  represents the time taken after it has been fed into the mill and  $\tau$  represents the mean residence time calculated as follows:

$$\tau = \frac{W}{F} \quad (2.9)$$

with  $W$  being the mass of material in the mill while  $F$  is the feed rate of the mill of the solid particles.

Size reduction and material transport are the two processes that occur simultaneously in a mill. The residence time distribution of a full-scale mill can be modelled as two equally small fully mixed reactors followed by one large fully mixed reactor. Using a schematic of the transportation model established by Austin *et al.* (1984), a dead zone was considered by Makokha *et al.* (2011) as seen in Figure 2.8. The addition of this dead zone was to consider the non-ideal flow delays that occurred due to the system dynamics (Makokha *et al.* 2011).

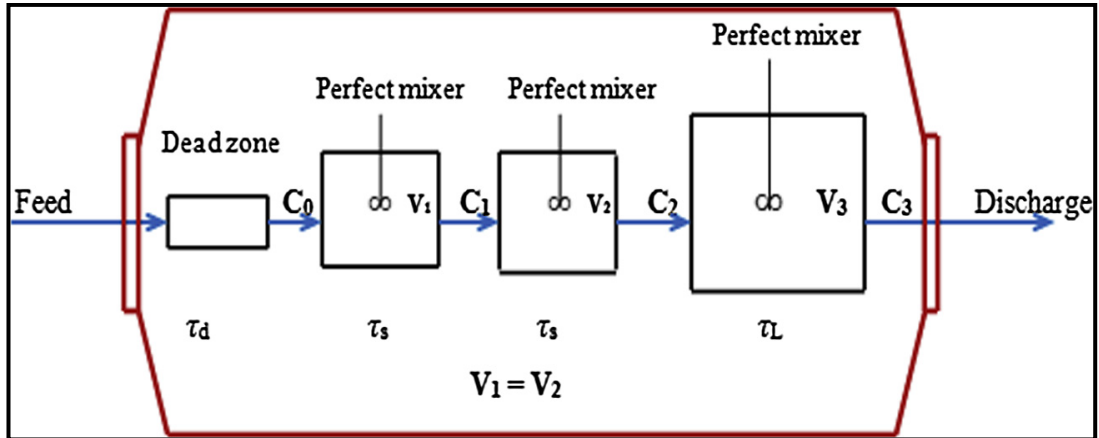


**Figure 2.8** The illustration of the mill with a schematic of the transportation model (Makokha et al., 2011)

The variables in Figure 2.8 are described as the following:

$\tau_L$  represents the partial residence time of the large fully mixed reactor;

$\tau_s$  represents the partial residence time of the smaller fully mixed reactor;

$\tau_d$  represents the partial residence time of the dead time zone;

$c_{i,j}$  represents the transformation matrix used for the generation of the transfer function matrix;

$v_{i,j}$  describes the volume of the larger fully mixed and smaller fully mixed reactors.

## 2.6. Classical semi-autogenous mill, ball mill, and crusher circuits

A typical SABC circuit consists of a primary crusher, a semi-autogenous mill, and a ball mill. The primary crushing is usually done by a jaw crusher (unit 1) as shown in Figure 2.8. This unit breaks down the run-of-mine ore (stream 1) from rocks as large as 1 m in diameter into fragments of size usually around 20 cm. The SAG mill then processes the stockpiled product (unit 2) from the jaw crusher and grinds it finer.

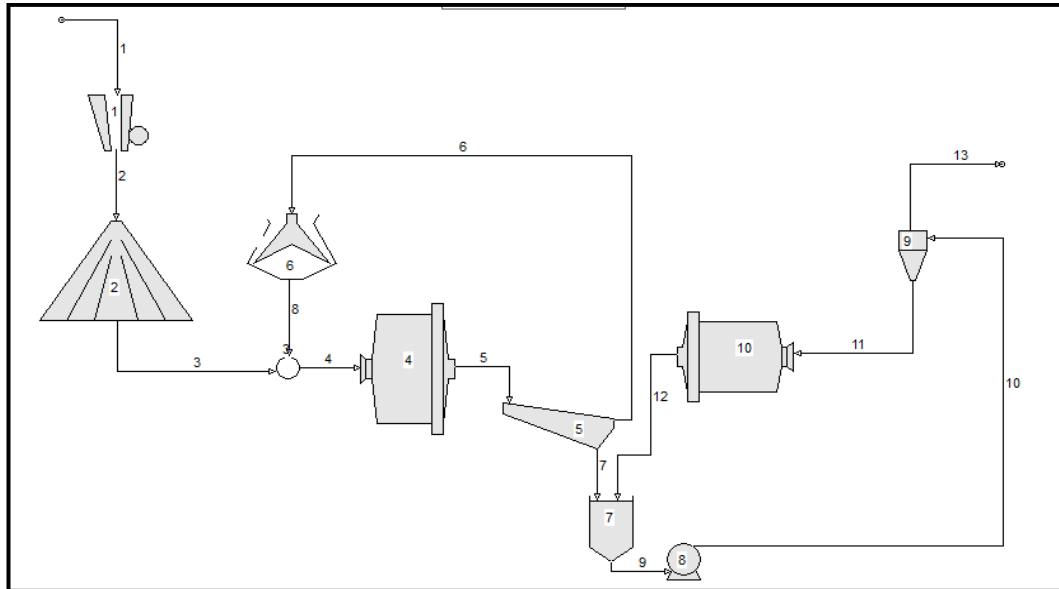


**Figure 2.9** Typical SABC circuit

The fraction of the discharged product that does not meet the size requirements as well as the critical-size fraction (i.e. stream 6) are handled by a cone crusher and fed back to the SAG mill. The product from the SAG milling section (stream 7) finally goes to a hydrocyclone that splits it into the oversize (stream 11) and the undersize (stream 13) fractions. The oversized fraction is recycled around the ball mill for further grinding while the undersize is the final product from the SABC circuit sent for subsequent separation by froth flotation for example.

The classical circuit configuration in Figure 2.8 is common as it usually produces a significant increase in throughput and energy efficiency due to the removal of the critical size material (Wills and Finch, 2016).

### 2.6.1. Innovative configurations of the SABC circuits

Rosario (2010) suggested that another recent development in pebble crushing is the additional of HPGRs (High Pressure Grinding Roll) rather than a cone crusher to treat the pebble product (see Figure 2.9). The replacement of the cone crusher by a HPGR can produce a much finer and more uniform product. The usage of a HPGR as a pebble crusher can thereby decrease the ball mill power requirements.

In doing so, Gupta and Yan (2006) have claimed that the final product was more amenable to flotation and leaching circuits that follow in some operations.

The application of the high-pressure grinding roll for industrial comminution has attracted the attention of many researchers (Schonert, 1988; Norgate and Weller, 1994; Fuerstenau and Kapur, 1995). This is primarily ascribed to its low specific energy, its low steel consumption, its ability to operate at high capacity, and its high ratio of reduction compared to the conventional tertiary grinders.

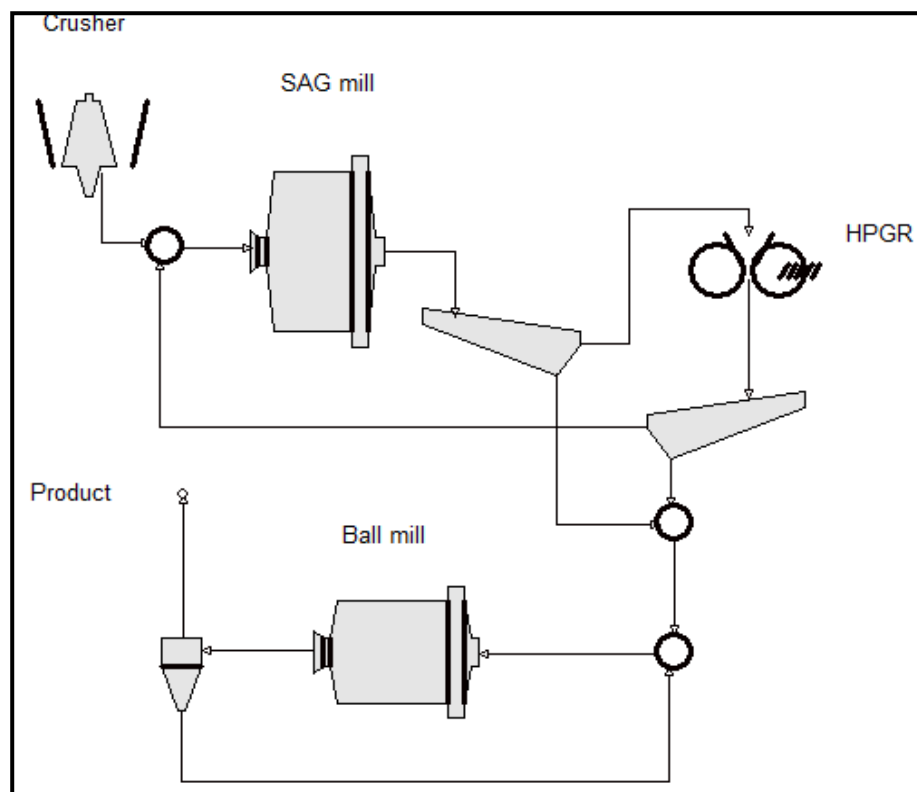


**Figure 2.10** SAG mill with HPGR as a pebble crusher (Wikedzi, 2018)

It is well known that there are various circuit configurations that consist of a SAG and ball mills. Lane *et al.* (2002) summarised this as shown in Table 2.1 as a way of providing a simple comparison of the different comminution circuits. The primary mill may be operated in open circuit or in a closed circuit by using a screen or a hydrocyclone. Operating the primary mill in a closed circuit can improve the efficiency for some operations or may facilitate a reduction in the product size of the mill.

**Table 2.1** Summary of SAG milling circuits (after Lane *et al.*, 2002)

|                          | SAG milling circuits                           |                                |  |
|--------------------------|--|--------------------------------|--|
| Crushing                 | Single stage crush                             | Single stage crush             | One- or two-stage crush  |
| Primary milling          | Single stage SAG mill                          | SAG mill                       | SAG mill and pebble crush  |
| Secondary milling        |  | Ball mill                      | Ball mill  |
| Examples of existence    | Cosmos Nickel Mine                             | Macraes Gold Mine              | Cadia Hill Copper/Gold Mine, Northparkes Mines and Fimiston Gold Mine. |
| Maintenance requirements | Low  | Moderate                       | Moderate-High  |
| Operability and issues   | Variation in ore competency an issue           | Current benchmark              | Pebble crushing impacts on SAG mill                                    |
| Applicability            | Low to moderate throughput and competency feed | OK for moderate competency ore | Ok for moderate to high competency ore                                 |

### 2.6.2. Pebble formation in comminution circuits

Comminution circuits consist of several types of size reduction units like crushers, SAG mills and ball mills. Mills in particular must be capable of treating these units separately but also in a circuit (Mwanga, 2014). Meer (2019) noted that the most frequent bottleneck in the operation of AG and SAG mills is the generation of critical size pebbles. Their subsequent requirements of re-crushing result in an extra burden for the mill. This is in the form of a recirculating load of harder and more abrasive material. Critical size of material is the dominant factor when mined ore is hard, competent and amenable to impact breakage to an acceptable size according to Wipf (1996). Zhang (2016) defines the critical-size material (also known as pebbles or scats) as a representation of material that does not self-break

as readily as other sizes. Powell *et al.* (2015) further clarifies on critical size as a build-up of material established from the use of AG and SAG mills which can drop throughput to half (Morrell and Valery, 2001), as these pebbles occupy a large volume within the mill therefore contributing a large mill power draw (Wikedzi, 2018).

Self-breakage plays an important role in AG and SAG milling. King (2001) explains its mechanisms as the larger the particle and greater its height of fall in the mill, the larger its probability of self-breakage on impact. Particles smaller than 10 mm have negligible breakage probabilities; and consequently, very low values of the specific rate of self-breakage. Parameters like pebble handling, transfer size between SAG and ball mill handling of slimes may be more important for the throughput estimate than the actual grind ability (Mwanga, 2014). Although, pebble formation found in SAG mills shows evidence of grind ability issues, Dance (2016) has questioned the worth of returning the pebbles to the mill, as they have proven themselves to be hard, resilient and challenging.

In Figure 2.10, King (2001) explains the decrease in specific rate of breakage as particles that are too large to be properly compressed during an impact event. This phenomenon is important for both AG and SAG mills. As the coarse feed supplies various particles in this size range and an intermediate size range exists in the mill. The condition therefore makes these particles too large to suffer impact breakage but also too small to suffer self-breakage. The particles in this size range accumulate in the mill as neither break nor discharge.

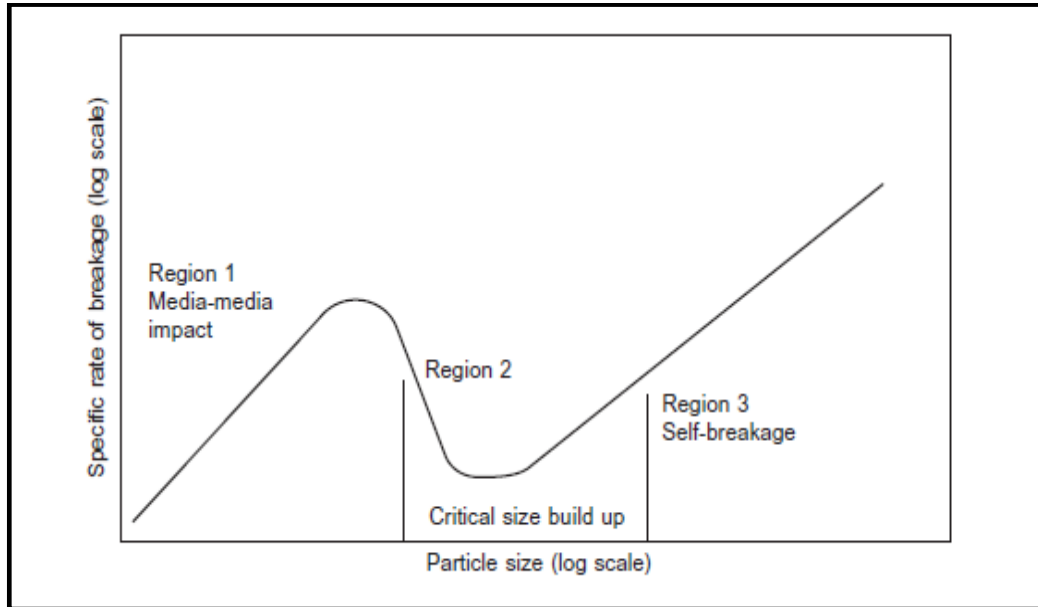


**Figure 2.11** Schematic illustration of the specific rate of breakage in SAG mill  
(King, 2001)

### 2.6.3. Challenges faced during the design of SAG mills

Critical size rocks ranging from 12 mm to 75 mm in AG mills reduce breakage rate therefore a significant solution to this problem is required. As a result of this, Rosario (2010) recommends the addition of steel balls in the mill and to recycle the critically size material through the crusher and back into the mill. SAG mills have pebble ports designed to discharge pebbles or critical size materials which are crushed using a closed-circuit. This design assists the elimination of critical size material resulting in a higher throughput and a more stable or constant flow (Koivistoinen, 1995). Wikedzi (2018) noted that the use of AG and SAG mills have grown popularity in the comminution industry and overtaking rod and ball mill configured circuits. This is due to the economic purpose as the expense of steel balls and rods which contribute highly to wear of liners.

Rosario (2010) expressed that inclusion of a pebble discharge (see illustrated in Figure 2.11) has become almost standard in the design of grinding circuit. The pebble discharge makes it a cost-effective way of increasing the throughput of

existing plants and as a power efficient circuit design for new plants. Its popularity lies in its selectivity, as the feed to the crusher is typically only that material which builds up in the mill and which by definition the mill finds hard to break (Napier-Munn *et al.*, 1996).

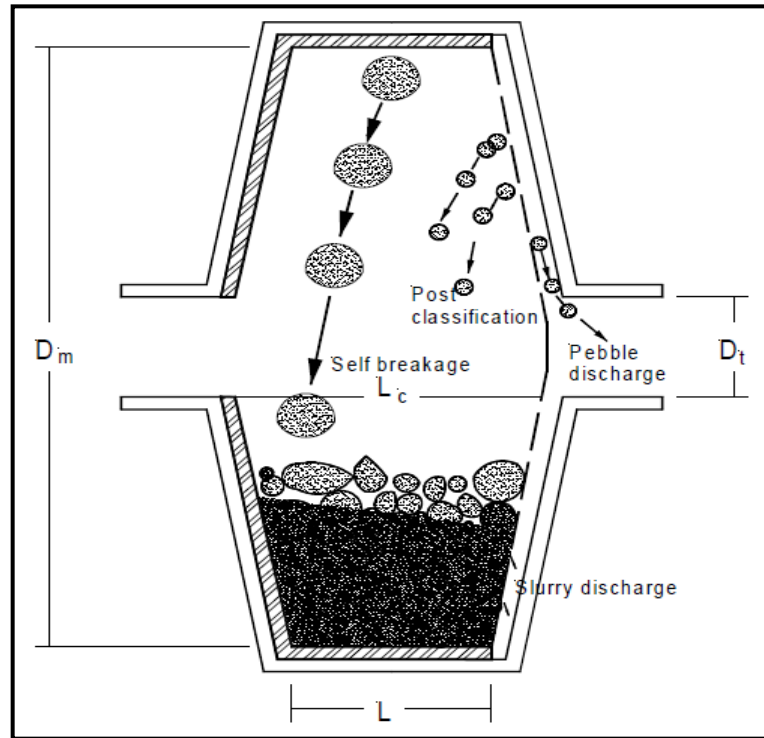


**Figure 2.12** Schematic of an AG mill with pebble ports (King, 2001)

Using current practices, Figure 2.12 is a SAG mill closed with a crusher to control the amount of pebbles or scats in the circuit. The pebble material is removed from the mill load by product classification and ports in the mill discharge and trammel screen (Meer, 2009). The pebbles are then crushed separately by a cone/pebble crusher and fed back to be blended in with the mill feed. Even though the solution on pebble control was found through the circulation of the pebbles as crushed feed, new difficulties were discovered. This is when the steel balls exit the mill and enter the crushing circuits (Koivistoinen, 1995). Additional ways are required to improve this in order to maximize plant operational effectiveness in terms of throughput and energy (Meer, 2019). Thus, maximising pebble extraction and crushing was a key performance criterion to be addressed.

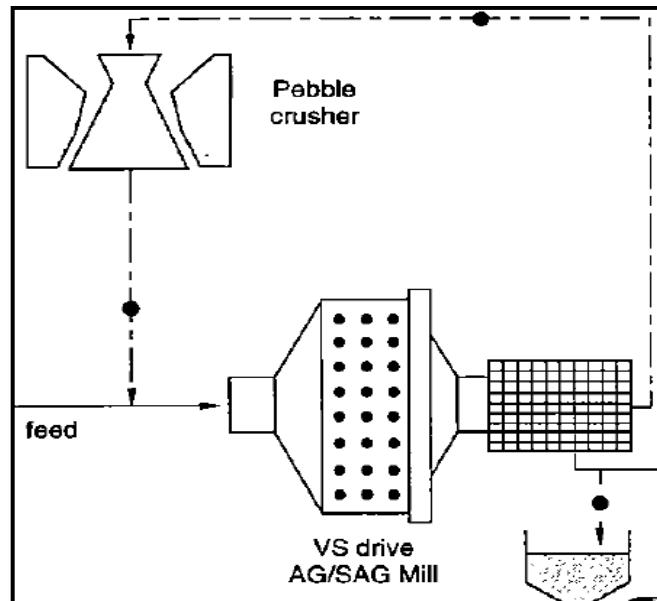


**Figure 2.13** SAG Mill with scats recycle (Napier-Munn *et al.*, 1996)

#### 2.6.4. Optimisation of typical SABC circuits

Process optimisation should be considered as a continuous exercise aimed to ensure that better operating efficiency is achieved. Napier-Munn *et al.* (1996) recognized that the optimisation criteria of a SAG circuit are primarily plant-based. However, the following generic factors are targeted: throughput, grind size, power consumption, and steel consumption. Zhang (2016) found that SABC circuits have many advantages which include a simple flow sheet arrangement, a small footprint, easy expansion, and high potential for energy-efficient operation. The greatest barrier to their full adoption in the industry has been the logistical challenge in controlling and operating them optimally.

Dance *et al.* (2014) were able to show that optimisation typically involves three steps: the theoretical and practical knowledge of the process, the definition of the methodology by which to apply this knowledge to the objective of optimisation, and a baseline by which to judge the outcome of the optimisation effort. Valery *et al.* (2006) focused on these principles in an attempt to reduce cost per tonne of ore treated so as to increase the profitability of the operation. This was conducted

through various adjustments which include grinding efficiency improvements using a ball size mixture. The mixture consisted of 70 mm and 38 mm with a ratio of 50:50. Furthermore, an increase in ball mill power was attained through a combined effect of increased ball charge from 30% to 44% and a mill speed of 74%.

The ultimate objective of the SABC circuit is to reduce the ore size down to the level that guarantees sufficient liberation of the valuable components of the ore for easy concentration. The conventional approach to the optimisation of a circuit is to optimise units independently (see for example Dance *et al.*, 2014; Napier-Munn *et al.*, 1996; Valery *et al.*, 2006). However, Hlabangana *et al.* (2018) found that this approach does not essentially produce an optimum system. There are several factors that can influence the outcome of the optimisation as the SABC circuit consists of multiple processing units. The alternative approach would be to determine first the size requirements of the product from the SABC circuit. This is because product size is known to affect ore recovery at the concentration stage (Wills and Napier-Munn, 2005). The next section discusses critical aspects of conventional optimisation of SABC circuit while the last section delves on the global optimisation.

The approach to optimisation is important as it determines the method to be used when seeking to improve the circuit. Three possible methods are discussed as far as SABC circuits are concerned. The first method is to optimize the circuit units in isolation to produce its best operating conditions. The second approach is to consider the downstream stages of the production chain and to incorporate their requirements into the optimisation. The third method is to consider a global view of the process flow and optimize it using a criterion such as minimal consumption of energy. Napier-Munn *et al.* (1996) further explains these approaches in three case studies that involves two different comminution circuits with case study 1 focusing on the crushing process and case studies 2 and 3 concentrating on the grinding process. These two circuits are seen in Figures 2.13 and 2.14 respectively.

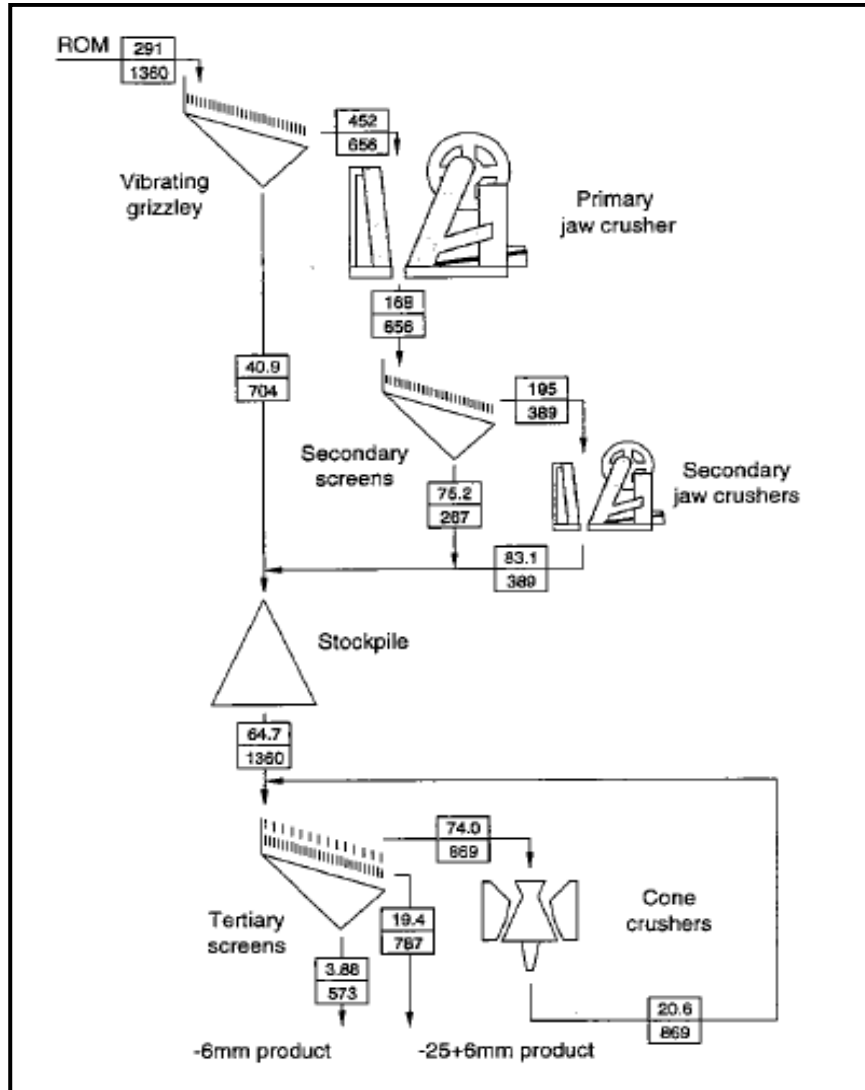


**Figure 2.14** Crushing and screening circuit (Napier-Munn *et al.*, 1996)

In the first case study the improvements on the throughput by 10 % and an increase in the amount of products in the specified range were successfully achieved using different alterations on the circuit. These alterations include the following:

- Increase feed rate by 10 %
- Increase the aperture of the primary scalper from 100 mm to 120 mm
- Increase secondary crusher power from 552 kW to 628 kW
- Adjust the closed-side setting of the tertiary crusher from 25 mm to 32 mm

- Reduce the tertiary crusher (CCS) from 32 mm to 28 mm to comply with the limited specifications.

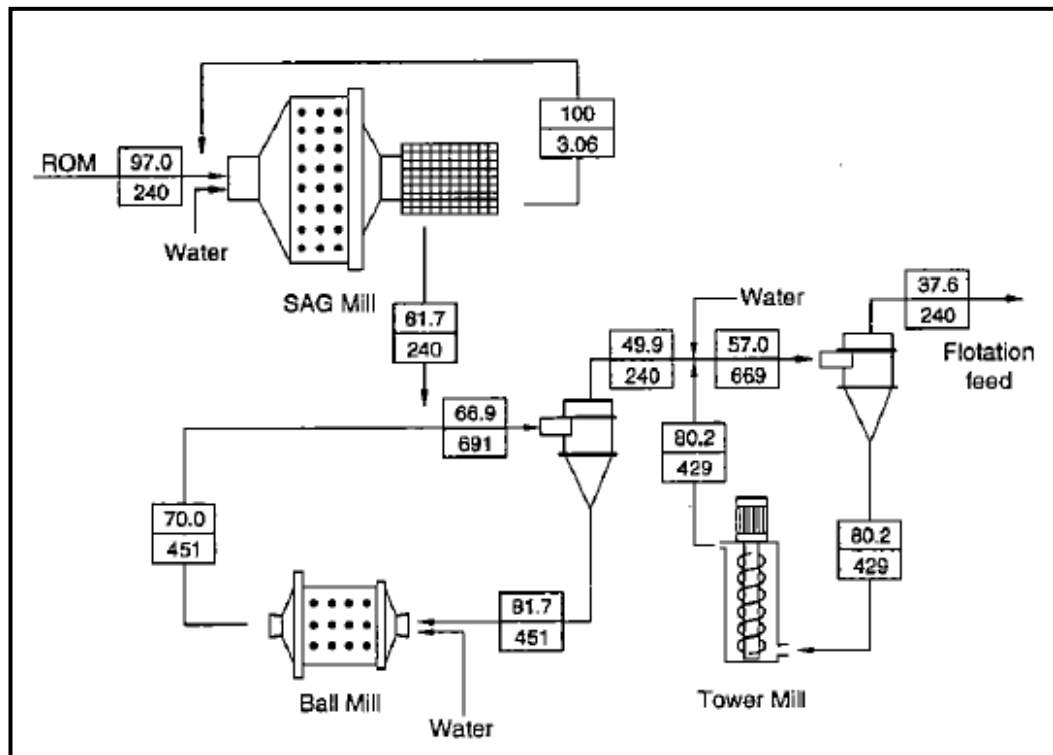


**Figure 2.15** Grinding circuit (Napier-Munn *et al.*, 1996)

In the second case study the objective was to improve the product size of the circuit which was completed in various stages, this resulted from an improvement on the final ground size from 64  $\mu\text{m}$  to 31  $\mu\text{m}$ . In the last case study, information from case study 2 was used in an objective to improve the circuit throughput from 240 to 288 tons per hour (tph) at a constant product size. Using the last approach it was discovered that not only was the objective achieved but further improvements were revealed to further improve the current product size.

In an optimisation case study of the SABC circuit, Hart *et al.* (2001) theorised that it is possible to increase the throughput by 10% by discharging the crushed pebbles into the ball mill rather than recycling the pebbles into the SAG mill as seen in Figure 2.15. The application to this idea was confirmed through a series of plant trials by means of increasing the new feed rate by 0.3 tph during the trial for every ton per hour of crushed pebbles not returned to the mill. Hart *et al.* (2001)



resulted to an increase in the discharge rate of pebbles, the efficiency of the SAG mill and the processing capacity of fresh ore. Additional improvements was the replacement of the HP Series pebble crusher with a TC84 crusher and the addition of a 100 m<sup>3</sup> pebble bin which assisted the circuit on its irregular recirculation of pebbles around the SAG mill as an accumulation of uncrushed pebbles caused over-loading of the mill power draw.

## 2.7. Attainable region theory in comminution operations

The theory of the attainable region (AR) has been applied successfully in various fields of chemical engineering for the purpose of optimisation (Danha *et al.*, 2015). Though its use is primarily in the optimisation of reactor networks (Metzger *et al.*, 2009), Chimwani (2014) found it to be a flexible and versatile graphical analysis tool for the optimisation of industrial ball milling operations. The power of the AR technique lies in its ability to represent only the variables of interest in a process. This basically means that milling parameters can be overlooked while focus is made around the fundamental breakage process. Mulenga *et al.* (2016) consequently suggested that the focus for the optimisation of comminution circuits should be on meeting the size requirements for effective separation downstream. This is a different and more holistic approach to optimising circuits in contrast to optimisation based on a single-point size specification as is currently the case. This then helps determine the set of all achievable size distributions plotted as an attainable region. Note that in the case of comminution operations, the feed material to be comminuted would be considered as the reactant and the product would depend on the downstream process.

Figure 2.16 exemplifies the application of the AR technique to a batch mill. The first step is to identify the fundamental process taking place inside the reactor. Comminution, flotation, leaching, classification and mixing are some fundamental processes encountered in mineral processing (Hlabangana *et al.*, 2017). In the case under consideration, comminution or breakage is the only fundamental process

taking inside the batch mill. The second step is to select the state variables characterising the output state of the system. The state variables can come in the form of concentration, mass fractions, reaction conversion or recovery. The case in point and comminution in general use mass fractions of the feed and the product as the state variables. As illustrated in Figure 2.16, Hlabangana *et al.* (2016) started off with a feed of size between 5600  $\mu\text{m}$  and 4000  $\mu\text{m}$ . They then defined the target product size range as 4000  $\mu\text{m}$  and 300  $\mu\text{m}$ . This is because a product size between 300  $\mu\text{m}$  and 38  $\mu\text{m}$  is considered ideal for froth flotation. The two aforementioned state variables were defined: the first is the mass fraction  $M_1$  of the product falling between sizes 5600  $\mu\text{m}$  and 4000  $\mu\text{m}$ ; the second is the mass fraction  $M_2$  of the product falling between 4000  $\mu\text{m}$  and 300  $\mu\text{m}$ . Afterwards,  $M_1$  and  $M_2$  were tracked as functions of milling times as shown in Figures 2.16(a) and 2.16(b). The third step is now to construct the candidate attainable region, that is, to plot  $M_1$  versus  $M_2$  as seen in Figure 2.16(c). Finally, the last step is used to find the optimal point of the AR path and it is generally on the boundary of the attainable region. In the case of Figure 2.16(c), the optimum is point K which corresponds to the maximum possible production of particles between sizes 4000  $\mu\text{m}$  and 300  $\mu\text{m}$ . Also note point Z representing the product identified as points X and Y in sub-Figures 2.16(a) and 2.16(b) respectively.

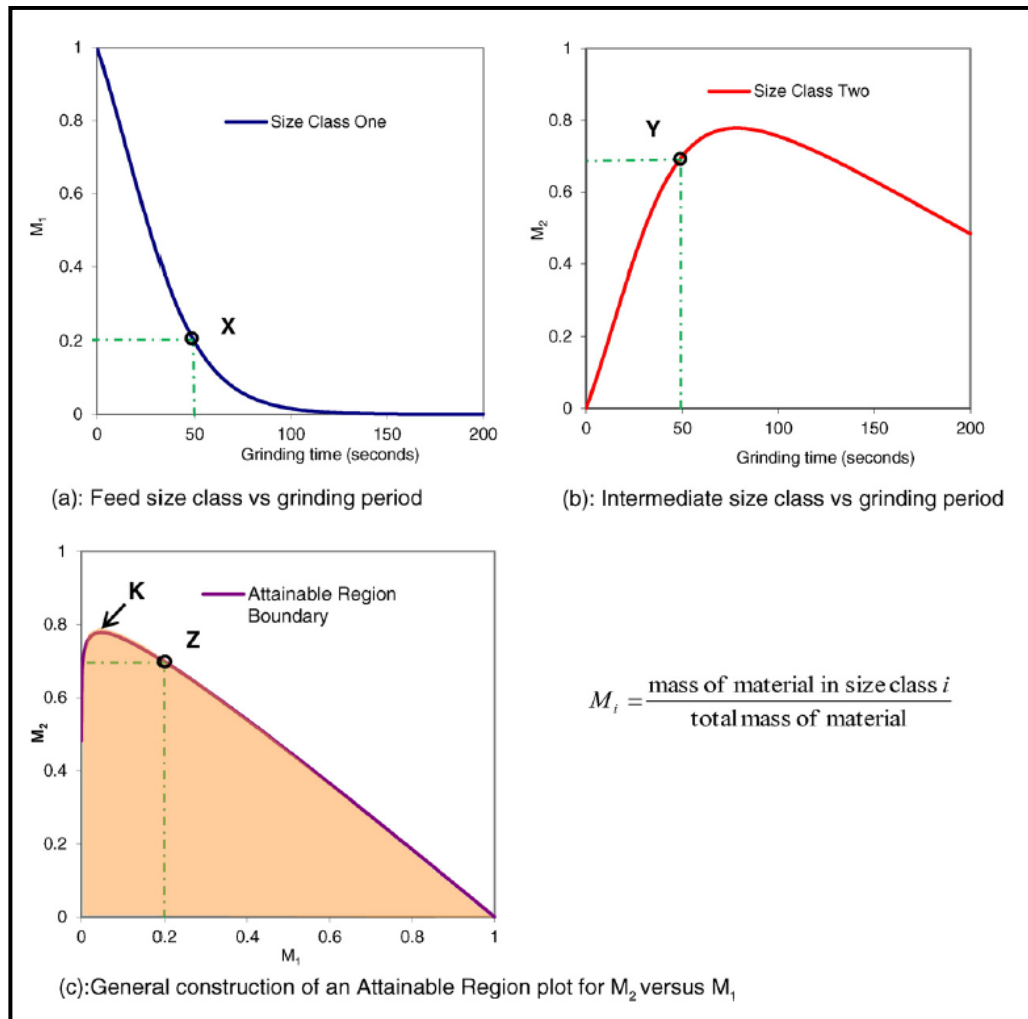


**Figure 2.17** Construction of the attainable region (Hlabangana *et al.*, 2016)

The AR technique can be extended to objective functions such as product size, energy consumption, and total operating cost. Although the technique has been applied in batch settings, Danha *et al.* (2015) noted that the extension of the technique has yet to reach industrial settings entailing other operations such as leaching, flotation or smelting. The sequel of work by Mulenga *et al.* (2015 & 2016) are the only practical cases where the AR method has been applied to ball milling circuits. It is therefore hoped that the present dissertation can contribute to paving a niche for the application of the AR paradigm to industrial comminution operations. That is why the technique is extended from single-stage ball milling circuit to a typical SABC circuit.

## 2.8. Summary

The present literature review has highlighted the importance of SABC circuit configurations. This type of circuit was found to rely on comminution through the action of self-break, abrasion, attrition and impact. The chapter has also covered key elements around the formation, handling and reduction of pebbles in SAG milling systems.

In terms of the modelling of the grinding process, the selection and breakage functions were identified to form the basis of the population balance model. The population balance modelling framework indeed was established to be central to the simulation program later used in this dissertation.

The three classical approaches to the optimisation of SABC circuits were discussed by means of cases studies. The first case study covered the optimisation of an SABC circuit in isolation to produce the best operating conditions. The second case study involved the inclusion of requirements of a downstream stage to the optimisation exercise. The last case study reflected on the global view of the process and to optimise a total production criterion. The review of process optimisation techniques was complemented with the attainable region technique. The technique was initially intended for chemical process optimisation. However, when used in comminution, the analysis looks at breakage into and out of size three different size classes. The simplicity of the technique was also here found to be attractive as an alternative to classical optimisation techniques. Further explorative work is done in subsequent chapters in this light.

## Chapter 3 Research methodology and simulation programme

### 3.1. Introduction

This chapter describes the techniques employed to build the simulation model of a SABC circuit using MODSIM® version 3.6.22 demo. MODSIM® is a simulation software specialising in ore processing. It is used to calculate mass and energy balances for a circuit amongst others.

A computer simulation model is an invaluable tool used to study for instance the dynamics of a system. It can also be used to conduct sensitivity analysis of different effective elements on the performance of the system (Dindarloo *et al.*, 2016). As far as mineral processing is concerned, a computer model is used to predict the effects of changes in specific operating parameters on the performance of the circuit (Maria, 1997).

A simulation model can therefore be regarded as a tool that enables the evaluation of the performance of an existing circuit. A proposed circuit can also be evaluated under different configurations and conditions. From this point of view, simulation is used before an existing system is altered or a new system is built. This approach presents several advantages; for example, the chances of failure to meet specifications are reduced. Unforeseeable bottlenecks can also be prevented while poor utilisation of resources is avoided.

It is in line with the above that this dissertation seeks to identify by simulation the factors and parameters that could lead for optimised performance of a typical SABC circuit. The main motivation for pursuing the simulation route is that models of operations underpinning comminution circuits are reasonably well developed (Umucu *et al.*, 2012). The construction of the SABC circuit was implemented in MODSIM® so as to simulate different scenarios in line with the objectives of this research. MODSIM® was found to be an easy to follow and user-friendly program that can meet the user's requirements. The program can accurately identify an

input error that is placed in the circuit, guiding the user to review their input variables and constraints.

### 3.2. Construction of the computer simulation model

King (2012) described MODSIM® as a unique software that can simulate the liberation of minerals during comminution operations. This aspect is becoming increasingly relevant to plant managers that seek greater operating and plant efficiency. In addition to this, MODSIM® calculates a detailed mass balance for any ore dressing plant. This can be in terms of total flow rates of water and solids, particle size distributions of the solid phase of individual streams, distributions of particle composition, and the average assay of the solid phase.

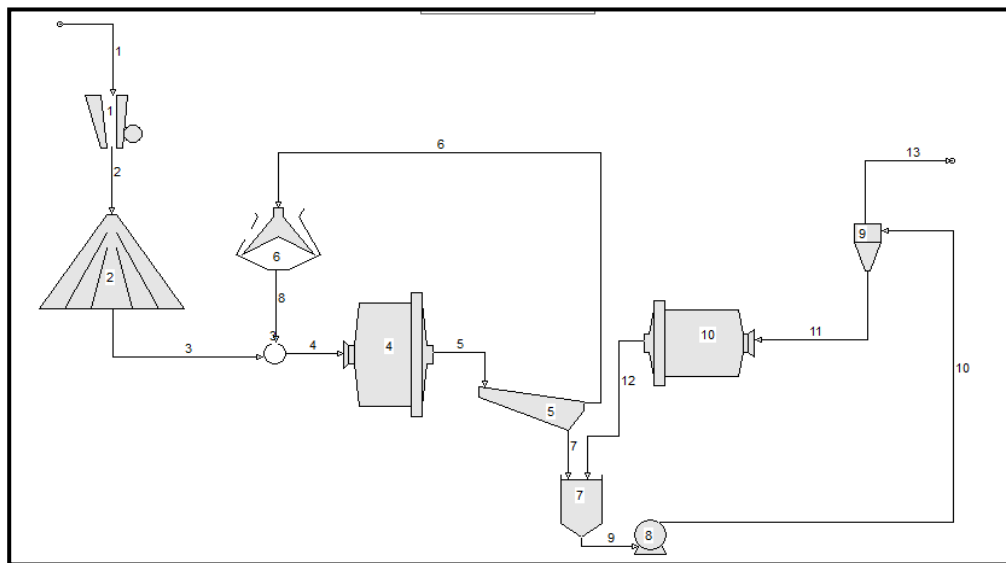


**Figure 3.1** Typical semi-autogenous-ball mill crusher circuit

As illustrated in Figure 3.1, the SABC circuit that is simulated in this work consists of 6 different operational units: the jaw crusher, the SAG mill, the vibrating screen, the cone/pebble crusher, the ball mill, and the hydrocyclone. Each unit requires the definition of a MODSIM® performance model as close as possible to reality. These are presented below with relevant information. Note that the stockpile (unit 2), and the mixing unit 3, the sump (unit 7), and the centrifugal pump (unit 8) have

no model behind them. They are treated as mass transfer units similar to a stream; hence, they are not included in the description that follows.

### 3.3. Units modelled on MODSIM®

#### 3.3.1. JAW1: Jaw crusher

The jaw crusher in Figure 3.1 labelled unit 1 has the primary function of reducing large size rock by repetitive compression. MODSIM® offers three options of jaw crushing models for the purpose of simulation. They are identified in the simulator by the following acronyms: JAW1, JAW2 and EMJC. The first two models (i.e. JAW1 and JAW2) have similar parameters that only differ with the standard size distribution as JAW1 is assumed to use the Nordberg process machinery reference manual May 1976 and JAW2 using Samancor's Mamatwan plant. The model EMJC known as the Empirical Model for Jaw and Gyratory Crushers uses detailed parameters that are not measured in this research. The JAW1 crusher considers the open side setting of the crusher which determines the maximum size of material that can be accepted in the crusher (King, 2001). This is based on the idea that larger material is crushed to a predefined sized distribution and smaller material passes straight through the crusher. This unit also requires the work index to be used by the crusher. The parameters considered for this unit are seen in Figure 3.2.

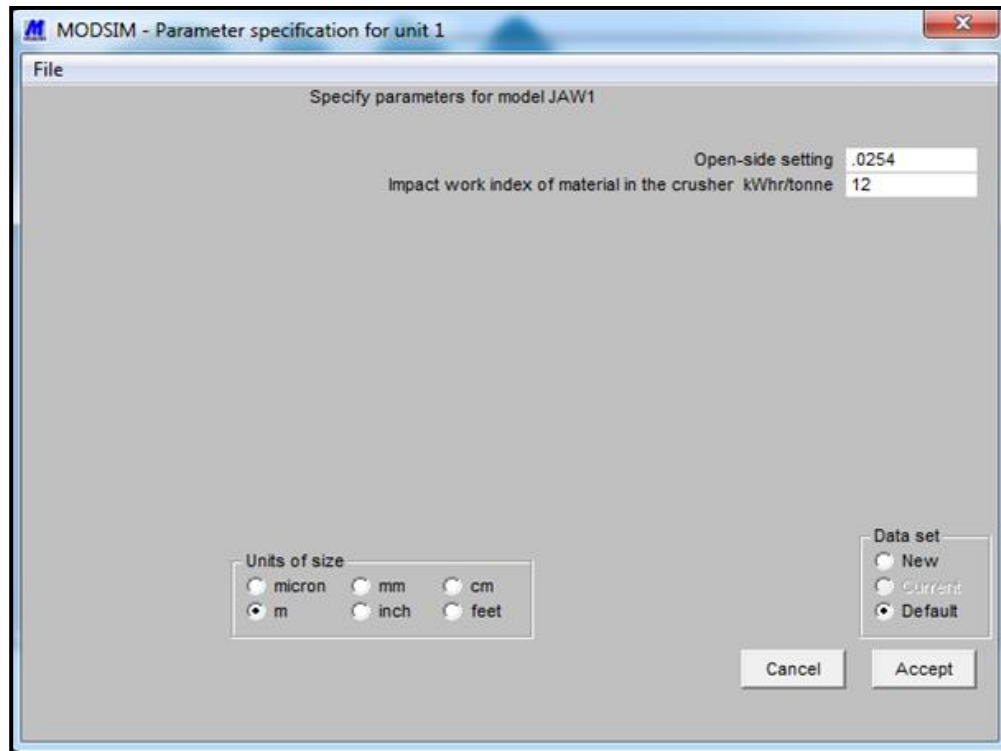


**Figure 3.2** Jaw crusher parameters in MODSIM®

### 3.3.2. SAGM: Semi-autogenous mill

The semi-autogenous milling unit 4 in Figure 3.1 can be modelled in MODSIM® in four different ways: as a fully autogenous mill (FAGM), as a semi-autogenous mill (SAGM), as a fully-autogenous mill with a trommel screen (FAGT), or as a semi-autogenous mill with a trommel (SAGT).

Based on the objectives set out for this work, unit 4 should represent the behaviour of semi-autogenous mill in line with what a SABC circuit stands for. That is why SAGM in MODSIM® was selected to be the model behind the semi-autogenous mill.

Figure 3.3 illustrates the input parameters that need to be defined for the SAGM model. King (2012) describes three distinct breakage processes that are modelled; namely, surface attrition, impact breakage, and self-breakage. Surface attrition is described as stresses that are not large enough to fracture or break the large ore particles in the mill as the parent particle barely varies in size but producing small

particles. The rate of attrition as described by Napier-Munn *et al.* (1996) can be measured using a tumbling test. Using the standard Austin breakage and selection functions the impact fracture is modelled. The breakage function for impact and self-breakage as described by King (2012) is determined mainly by the impact energy level and the  $t_{10}$  method which describes characteristic size reduction (Napier-Munn, 1999) for this the model. King (2012) further defines self-breakage as a result of a single particle that shatters on impact after falling freely in the mill; consequently, the impact energy is a function of the lump size and the height of the drop.

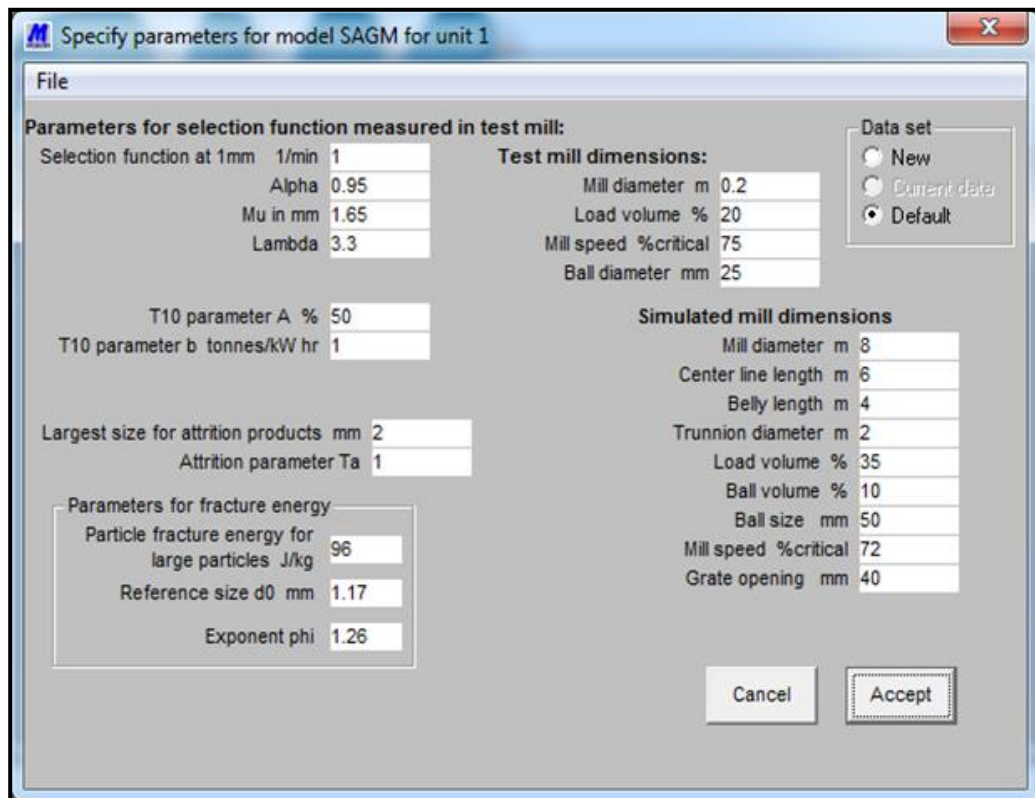
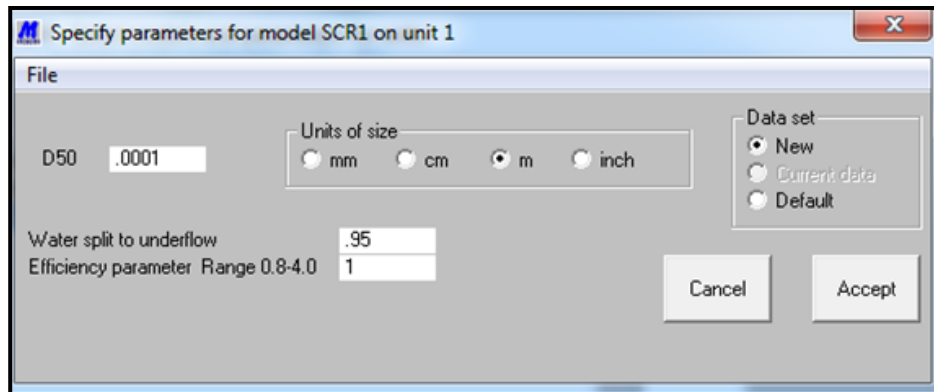


Figure 3.3 SAG mill parameters in MODSIM®

### 3.3.3. SCR1: Single deck vibrating screen

Screening is the passing of material through its openings to the required particle size. This model was used due to its simplicity of information required to classify the size particles. There are 5 models of screens found on MODSIM®: SCR1 for

single-deck vibrating screen; SCR2 for single-deck vibrating screen; KSCN for kinetic model for the vibrating screen; PSCN for probability screen; and SCRN for single-deck vibrating screen. The SCR1 model was selected for this model as its primary function is to classify the size particles and is a simple ideal model for wet screening. Figure 3.4 contains of the input parameters that are considered in the unit model SCR1.



**Figure 3.4** Screen parameters in MODSIM®

There are three parameters required for this model. The median size which is also known as D50, is the parameter that controls the size passing of the particles. King (2012) noted that the efficiency is mainly established by the actual feed loading on the screen relative to the rate feed capacity.

### 3.3.4. CYCA: Hydrocyclone

A hydrocyclone is a device used to separate particles in a liquid suspension based on their different sizes. The simulator program MODSIM® has two models of hydrocyclone: CYCA and CYCL. Similar to the single-decking vibrating screen SCR1, the simplicity of the CYCA model is used instead of the CYCL model. This is due to the fact that CYCL is complex and requires so many input parameters relating to the design and size of the hydrocyclone. So, unless an actual plant is being modelled and technological information of the hydrocyclone is available, CYCA is preferred (King, 2012). The input parameters to be considered in the CYCA model are illustrated in Figure 3.5.

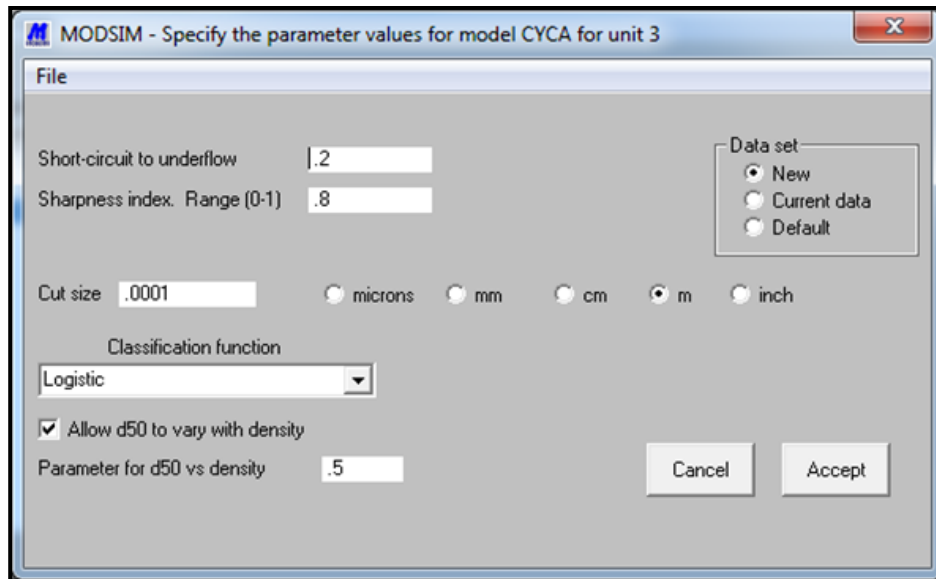


**Figure 3.5** Hydrocyclone parameters in MODSIM®

There are numerous empirical distribution functions that can represent the size distribution of particle populations accurately in practice. Note in Figure 3.5 the classification function of the hydrocyclone set at the “Logistic” option when the “Exponential sum” and the “Rosin-Rammler” are also available. The exponential sum function is found suitable for a dense-medium cyclone. The “Rosin-Rammler” type is often used for product size distributions with the parameters of the distribution varying with the product size. Preference was given to the logistic function since it can be linearized by using the appropriate coordinate systems (King, 2012).

A classification function provides a realistic depiction of the performance of a classification device. It defines the probability that an individual particle enters the oversize stream that leaves the classifier. The classification function is defined as the mass fraction of material in size interval in the feed which finally leaves in the oversize stream.

### 3.3.5. GMSU: Ball mill

Similar to the SAG mill, this unit is used to grind the ore into a finer size. This is the simplest model for the ball mill using the selection and breakage functions (King,

2012). Equations (2.2) and (2.5) are used in this unit as the selection and breakage function respectively. Figure 3.6 illustrates the parameters that were considered in this unit. MODSIM® has various models for a ball milling: GMIL, MILL, HFMI, HFML, HFSU, GMI1, GMSU, UMIL, and SB16. The GMSU model was used as it models the effect of the ball size distribution. The residence time distribution of the mill is presented as three mixing reactor series which is more in line with reality. Austin *et al.* (1984) showed that joining the scale-up equation with the description of the distribution of residence time in the mill enables successful construction the simulation model for the steady-state continuous operation. Most importantly, the GMSU model assumes that post-classification is present and that the mill load is perfectly mixed.

**Specify parameters for model GMSU for unit 1**

File

Parameters for selection function in test mill:

Specific rate of breakage at 1mm S1 1/min: 1.3

Particle size exponent alpha: .491

Size coefficient for maximum breakage rate mu mm: 2

Exponent for rate of decrease of selection function Lambda: 2

Parameters based on:  Representative size  Upper mesh size

Data set:  New  Current data  Default

Units of size:  meters  Feet

Mill dimensions:

|  | Test mill | Full scale mill |
|--|-----------|-----------------|
| Mill diameter                                    | .38       | 5               |
| Mill length                                      | .38       | 5.5             |
| Ball load %                                      | 40        | 40              |
| Fraction of media filled by solids U (Dry basis) | .4        | .4              |
| Mill speed as percentage of critical             | 74        | 74              |
| Make-up ball size mm                             | 18.75     | 50              |

Use standard ball size distribution

Ball size distribution

Number of sizes: 1

| Ball size | % in charge |                                     |
|-----------|-------------|-------------------------------------|
| 22.4      | 100.00      | <input checked="" type="radio"/> mm |
|           |             | <input type="radio"/> cm            |
|           |             | <input type="radio"/> m             |
|           |             | <input type="radio"/> inch          |

Parameters for breakage function:

Beta: 3.2

Gamma: .52

Delta: 0

Phi at 5mm: .158

Fractional residence times:

Perf. Mixed Region 1: .0137

Perf. Mixed Region 2: .2123

Perf. Mixed Region 3: .774

Allow for post classification  Allow for overfilling

Classification function

Transport model

Specific gravity of media: 7.8

Choose a liberation model:  None  Liberation  Beta function

Make Andrews-Mika diagram on exit using the beta function model.

Cancel Accept

**Figure 3.6** Ball mill parameters in MODSIM®

### 3.3.6. CRSH: Cone crusher

The cone crusher is used to break down the oversized material coming from the SAG mill discharge. This model is based on the crushing zone and internal classification behaviour described by Whiten *et al.* (1973). The unit has 3 cone crushing units: CRSH, CRS1 and SHHD. The CRSH model was selected for this process as its purpose is to eliminate the pebble rocks found in the process. The input parameters considered for the cone crusher unit are seen in Figure 3.7.

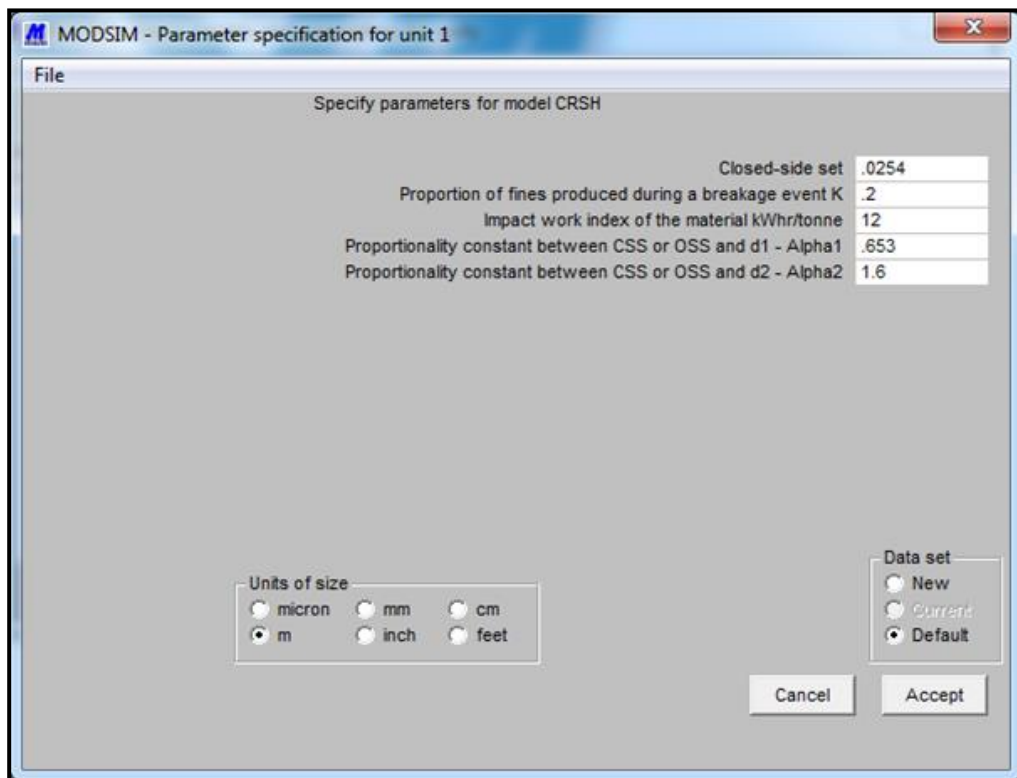


**Figure 3.7** Cone crusher parameters in MODSIM®

There are four parameters that are considered in this unit. The variables of the unit require a significant power usage which can be adjusted in order to break down the pebble particles. The Bond equation expresses the work done between the toughness of the material and the power required in the crusher. The closed-side setting (CSS) determines the product size distribution as all particles experience at least one closed-side phase during passage through the crusher with no particle falling through during a single open-side period. Proportionality constant between CSS or OSS and d1 (Alpha1) is identified as the smallest size

particle that can be retained in the crushing zone during the opening phase of the cycle and  $d_2$  (Alpha2) is the largest particle that can fall through the crushing zone during the opening phase of the cycle. These are parameters that are characteristic of the crusher and are determined primarily by the setting of the crusher (King, 2001).

### 3.4. Feed properties of material used

The South African mining industry has been mainly associated with gold, understandably, as this is due to the early existence of gold mines in the country. The recognition in the South African mining industry brought the popularity of other minerals such as platinum, coal (from Eskom), diamonds, etc. However, base metals have never received prominence, although they have formed part of the industry's contribution for decades. This includes the production of copper from Palabora Mining, nickel from Nkomati Nickel and copper, zinc and lead from Vedanta Resources formerly known as Black Mountain Mining. The characteristic of the ore is an important factor to consider in mineral processing as it dictates the amount of energy used. Base metal is a term that refers either to metals inferior in value to those of gold and silver, or to metals that are more chemically active than gold, silver and the platinum metals. A base metal is more common and inexpensive metal as opposed to a precious metal such as gold or silver. The appropriate term for base metal is nonferrous ore metals which include metals such as copper, lead, zinc, aluminium and tin. Chalcopyrite is the principle ore mineral of copper (George *et al.*, 2017). Its chemical composition is Copper iron sulphide ( $\text{CuFeS}_2$ ) with a relative density of  $4.19 \text{ g/cm}^3$ . Table 3.1 shows the mineral that was used in this simulation programme.

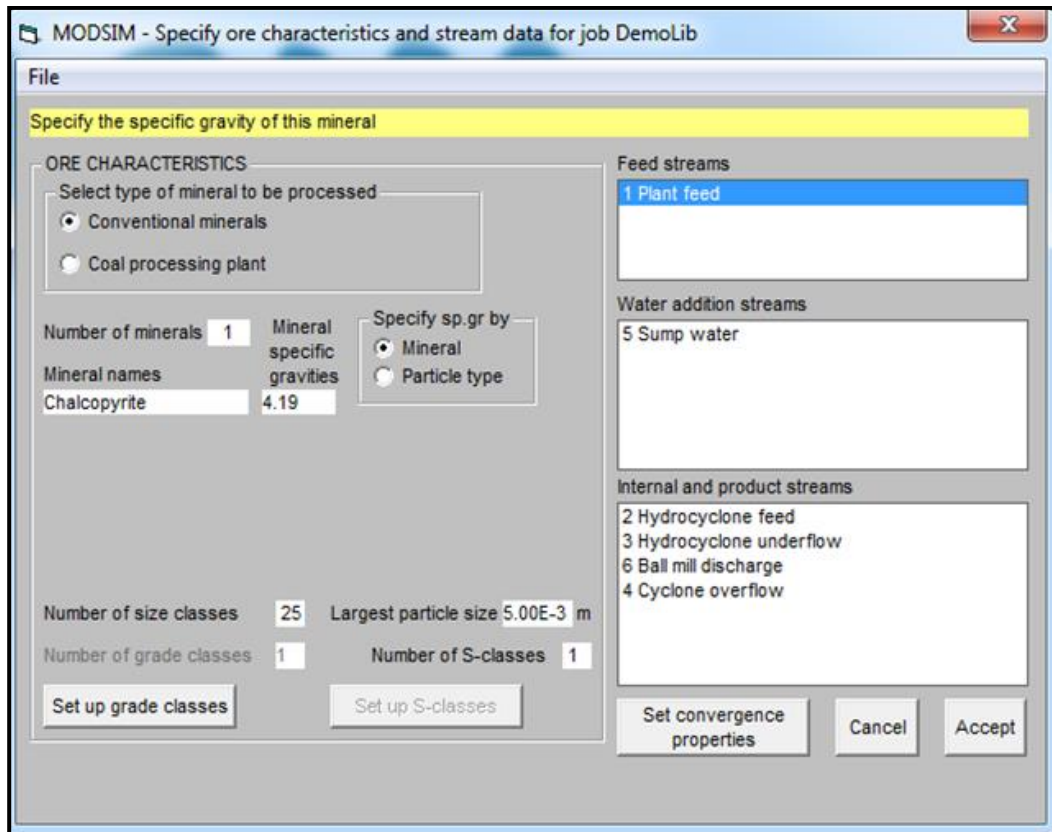


**Figure 3.8** Feed properties in MODSIM®

### 3.5. Simulation programme

The regulatory of critical sized ore is one of the principal motivations that govern this research. Therefore, the crucial area is not only around the final ground but also around the SAG mill as the pebbles form around the sector of the circuit. To optimise the SABC circuit, different scenarios on the circuit feed are created to form different processing conditions as seen in Table 3.1. The attainable region approach is then used to explore avenues of effective optimisation of the selected SABC circuit. A simple and approximate computer model of the circuit is built in MODSIM® for the purpose.

Table 3.1 illustrates the operating conditions for which the results are generated. The operating conditions make up the input data to the simulation model while the results are collected as output data for later analysis. The input data basically forms the different scenarios in the circuit and the output is the consequence of

those changes. The first column is the different scenario that is simulated. The second column consists of the independent variable which is the feed size particle of the ore which is used ranging between 100 mm and 600 mm with the feed flow containing 3 different flows. The third column is the fixed variables which are constant throughout the different scenarios. This constant variable includes the water feed measured by the solid percentage in the stream. The fourth column represents the operating parameters of the SAG mill with respect to the different scenarios. These variables consist of the load volume, ball volume, ball size, mill speed and grate opening. Similar to the fourth column, the fifth and last column represent the operating parameters of the screen and cone crusher and their varied variables of d50 and the closed-side setting (CSS) respectively. The purpose of the size increase is to observe the effectiveness of the size reduction and the increased flow is to determine the rate at which it can produce these fine particles. The input changes generated data that is used to form a parameter that determine the feasible region which determines the optimal condition in this circuit.

**Table 3.1** Simulation programme for the SABC circuit

| Input parameters     |                            |                               | Operating parameters |                 |                |                |                    |                      |              |
|----------------------|----------------------------|-------------------------------|----------------------|-----------------|----------------|----------------|--------------------|----------------------|--------------|
| Independent variable |                            | Fixed variable                | SAG Mill             |                 |                |                |                    | Screen               | Cone Crusher |
| Plant feed (tph)     | Chalcopyrite ore size (mm) | Water feed (% slurry content) | Load volume (%)      | Ball volume (%) | Ball size (mm) | Mill speed (%) | Grate opening (mm) | d <sub>50</sub> (mm) | CSS (mm)     |
| 50                   | -200+100                   | 60                            | 30                   | 10              | 50             | 65             | 40                 | 0.023                | 0.001        |
| 50                   | -400+200                   | 60                            | 35                   | 12              | 75             | 70             | 40                 | 0.023                | 0.001        |
| 50                   | -600+400                   | 60                            | 40                   | 14              | 100            | 75             | 40                 | 0.023                | 0.001        |
| 100                  | -200+100                   | 60                            | 30                   | 10              | 50             | 65             | 40                 | 0.023                | 0.001        |
| 100                  | -400+200                   | 60                            | 35                   | 12              | 75             | 70             | 40                 | 0.023                | 0.001        |
| 100                  | -600+400                   | 60                            | 40                   | 14              | 100            | 75             | 40                 | 0.023                | 0.001        |
| 150                  | -200+100                   | 60                            | 30                   | 10              | 50             | 65             | 40                 | 0.023                | 0.001        |
| 150                  | -400+200                   | 60                            | 35                   | 12              | 75             | 70             | 40                 | 0.023                | 0.001        |
| 150                  | -600+400                   | 60                            | 40                   | 14              | 100            | 75             | 40                 | 0.023                | 0.001        |

According to Hlabangana (2012) in order to guarantee high mineral recovery and low operational cost, the desire for most concentrators is to function under an optimal design configuration. Together with that, it is understood that unit operations used in mineral processing perform effectively within a certain particle size range. Mulenga *et al.* (2016) have recommended an effective size range of 5 – 500  $\mu\text{m}$  for froth flotation and 20 – 600  $\mu\text{m}$  for a high intensity wet magnetic separation. For the purpose of this research, the size class considered for downstream process was 75 - 300  $\mu\text{m}$ . The critical sized material found by many researchers is listed below. Based on their findings, the critical size range 23 – 100 mm is calculated as the average and is preferred for this study. The following size ranges were considered by various researches are for critical size range: 25 – 50 mm (Napier-Munn, 1996; Gupta and Yan, 2006), 12 – 75 mm (Rosario, 2010), 30 – 90 mm (Powell *et al.*, 2015), 25 – 40 mm (Wikedzi, 2018), and 25 – 90 mm (Meer, 2019).

### 3.6. Summary

The classical SABC circuit was simulated using a simulation programme as presented in Table 3.1. There were in total 81 simulations completed using MODSIM® as described in this chapter. The mineral properties simulated were that of chalcopyrite which has a specific gravity of 4.19  $\text{g}/\text{cm}^3$ .

## **Chapter 4 Simulation of the effects of pebble formation on the performance of the SABC circuit**

### **4.1. Introduction**

The outcomes of the MODSIM® simulations are presented and interpreted in this chapter for the SABC circuit. The data was generated by means of the simulation programme described in the previous chapter. The simulation programme consisted of a combination of input variables that formed different scenarios. This entailed feed rates to the circuit ranging between 50 and 150 metric tons per hour (tph) and ore feed sizes between 100 and 600 mm. The motivation for the simulation work was to investigate the existence of critical size particles formed in a SAG mill. As mentioned in the previous chapter, the size range 23 – 100 mm was considered as the critical size particles formed in the SAG mill for this research. Understanding the consequence of pebble formation in a circuit, as described in this literature review. This size range was classified by the vibrating screen to the cone crusher for further size reduction.

There were 81 scenarios simulated which are divided in two sections. The first section covers the flow rates and ore feed size. The second section considers the operating parameters of a SAG mill. The division is based on a simplified discussion of these results. The optimisation of this circuit comes from many forms which involves the understanding of the circuit and the current bottlenecks that exists. Through this information we can identify and highlight sections that can improve the performance of this circuit.

Particle size reduction is the primary motivation of the comminution. However, energy usage has an influence on the design and operation of a circuit. In this chapter, the minimisation of pebble formation was monitored together with the energy consumption of the SAG mill and cone crusher.

#### 4.2. Simulation of the classical semi-autogenous/ball milling circuit

The first section was a simulation on feed flow rate and ore feed size variation using Table 4.1. The results displayed figures that show how the circuit was simulated having an ore feed size of 200 mm, 400 mm, and 600 mm respectively. Correspondingly, the flowrates were 50 tph, 100 tph, and 150 tph. The operating parameters were constant throughout the scenarios as the objective was to have varied plant feed and ore size.

**Table 4.1** Simulation programme for the SABC circuit for feed flow rate and ore feed size.

| Input parameters |                      |               | Operating parameters |                  |                  |                |                |                    |                      |              |
|------------------|----------------------|---------------|----------------------|------------------|------------------|----------------|----------------|--------------------|----------------------|--------------|
|                  | Independent variable |               | Fixed variable       | SAG Mill         |                  |                |                |                    | Screen               | Cone Crusher |
| Scenario         | Plant feed (tph)     | Ore size (mm) | Water feed (% solid) | Mill filling (%) | Ball filling (%) | Ball size (mm) | Mill speed (%) | Grate opening (mm) | d <sub>50</sub> (mm) | CSS (mm)     |
| 1                | 50                   | -200+100      | 60                   | 30               | 10               | 50             | 65             | 40                 | 0.023                | 0.001        |
| 2                | 50                   | -400+200      | 60                   | 30               | 10               | 50             | 65             | 40                 | 0.023                | 0.001        |
| 3                | 50                   | -600+400      | 60                   | 30               | 10               | 50             | 65             | 40                 | 0.023                | 0.001        |
| 4                | 100                  | -200+100      | 60                   | 30               | 10               | 50             | 65             | 40                 | 0.023                | 0.001        |
| 5                | 100                  | -400+200      | 60                   | 30               | 10               | 50             | 65             | 40                 | 0.023                | 0.001        |
| 6                | 100                  | -600+400      | 60                   | 30               | 10               | 50             | 65             | 40                 | 0.023                | 0.001        |
| 7                | 150                  | -200+100      | 60                   | 30               | 10               | 50             | 65             | 40                 | 0.023                | 0.001        |
| 8                | 150                  | -400+200      | 60                   | 30               | 10               | 50             | 65             | 40                 | 0.023                | 0.001        |
| 9                | 150                  | -600+400      | 60                   | 30               | 10               | 50             | 65             | 40                 | 0.023                | 0.001        |

**Table 4.2** Simulation programme for the SABC circuit on SAG mill operating parameters

| Input parameters     |               |                      | Operating parameters |                  |                |                |                    |                      |              |
|----------------------|---------------|----------------------|----------------------|------------------|----------------|----------------|--------------------|----------------------|--------------|
| Independent variable |               | Fixed variable       | SAG Mill             |                  |                |                |                    | Screen               | Cone Crusher |
| Plant feed (tph)     | Ore size (mm) | Water feed (% Solid) | Mill filling (%)     | Ball filling (%) | Ball size (mm) | Mill speed (%) | Grate opening (mm) | d <sub>50</sub> (mm) | CSS (mm)     |
| 100                  | -200+100      | 60                   | 30                   | 10               | 50             | 65             | 40                 | 0.023                | 0.001        |
| 100                  | -200+100      | 60                   | 35                   | 10               | 50             | 65             | 40                 | 0.023                | 0.001        |
| 100                  | -200+100      | 60                   | 40                   | 10               | 50             | 65             | 40                 | 0.023                | 0.001        |
| 100                  | -200+100      | 60                   | 30                   | 12               | 50             | 65             | 40                 | 0.023                | 0.001        |
| 100                  | -200+100      | 60                   | 30                   | 14               | 50             | 65             | 40                 | 0.023                | 0.001        |
| 100                  | -200+100      | 60                   | 30                   | 10               | 75             | 65             | 40                 | 0.023                | 0.001        |
| 100                  | -200+100      | 60                   | 30                   | 10               | 100            | 65             | 40                 | 0.023                | 0.001        |
| 100                  | -200+100      | 60                   | 30                   | 10               | 50             | 70             | 40                 | 0.023                | 0.001        |
| 100                  | -200+100      | 60                   | 30                   | 10               | 50             | 75             | 40                 | 0.023                | 0.001        |

Table 4.2 depicts a sample of the second section that was simulated for an ore size of -200 +100 mm. Ore feed sizes -400 +200 mm and -600 +400 mm were also simulated. The main variation was the operating parameters around the section known as the pebble formation. These units include the SAG mill, vibrating screen and the cone/pebble crusher. The plant feed was constant at 100 tph with parameters varying on the mill filling, ball filling, ball size and mill speed.

The general depiction of the simulated SABC circuits is given in this section, with stream 1 being the feed to the circuit dry-crushed in a jaw crusher (unit 1). The product of the crusher is stream 2 which has the same flowrate but different ore size as the particles have undergone size reduction. Ultimately, this stream feeds to a stockpile (unit 2) to collect all the crushed ores.

Stream 3 feeds the mixer together with the stream 14 which supplies water on a flowrate to sustain a slurry ratio of 60% solid and 40% liquid, the return of the crushed pebbles from stream 7. Stream 4 is the feed to the SAG mill where the first stage of milling takes place which involves wet grinding. Stream 5 is the discharge of the SAG mill that enters a classification unit known as the vibrating screen (unit 5). This unit separates the oversized material which is stream 6 and undersized particles being stream 8 respectively. The purpose of stream 6 is to recycle oversized particles by feeding it to a cone crusher (unit 6) that breaks the critical size particles formed in the SAG mill. Stream 7 is fed into the mixer as the ground pebbles.

Stream 8 is the undersized particles that feed the sump (unit 7). Using a centrifugal pump (unit 8), stream 9 is the suction and stream 10 is the discharge of the pump to a hydrocyclone (unit 9). The hydrocyclone classifies the oversized particles (stream 11) and undersize particles (stream 13). Stream 13 is the product size of the circuit and stream 11 is the recycled particles that are fed back into the ball mill (unit 10). The ball mill performs a secondary grinding on the ore feed and discharges it into the sump via stream 12.





this indicates that the higher ore feed size required different operating parameters for the ball mill.

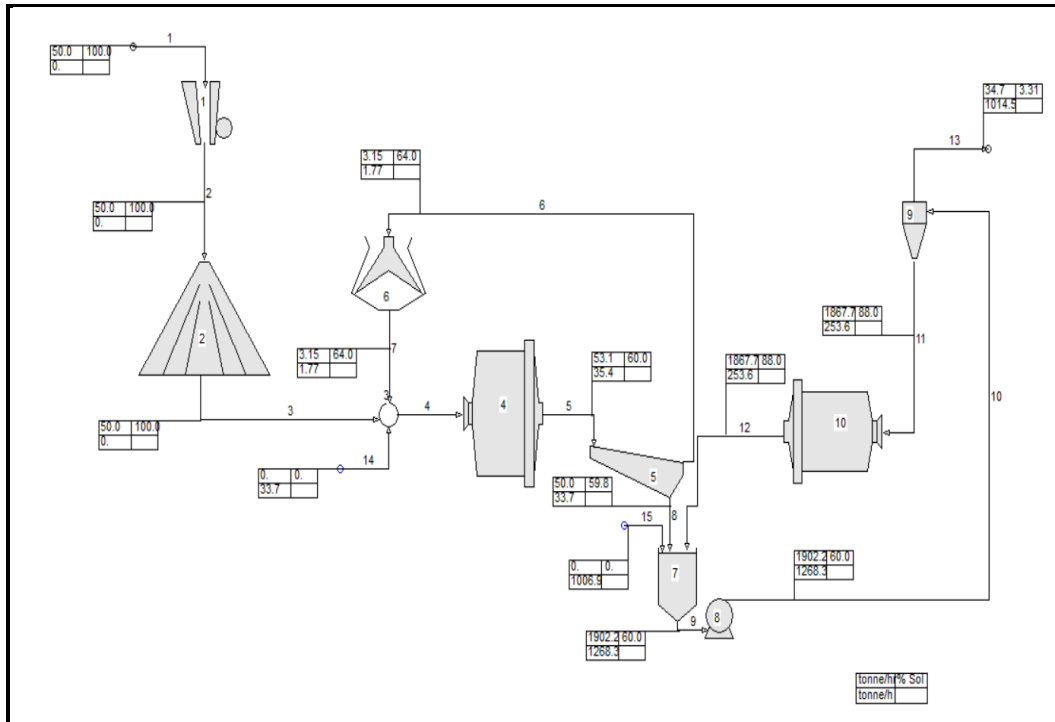


**Figure 4.3** Simulation flow sheet on scenario 3

The distribution function for a particular property defines quantitatively how the values of that stream are distributed among the particles in the entire population. The best known and most widely used distribution function is the particle size distribution function (King, 2001). This function is defined by mass fraction of that portion of the population that consists of particles with size less than or equal to the size of the particle. The particle size distributions in Figures 4.4, 4.5 and 4.6 illustrate the cumulative percentage plotted as a function of the passing particle size. The streams displayed are around the SAG mill, vibrating screen and cone crusher specifically streams 3, 4, 5, 6 and 7. Each figure represents the particle size distribution of the different scenarios; namely, scenarios 1, 2 and 3.

Figure 4.4 displays the particle size distribution (PSD) of scenario 1 on streams 3 – 8, this can be considered as a SAG mill closed circuit. The results indicate that the circuit experiences significant changes in the SAG mill between stream 4 and

stream 5. Stream 4 has a changing PSD that ranges from 5% to 100% while stream 5 ranges from 95 % to 100 %.

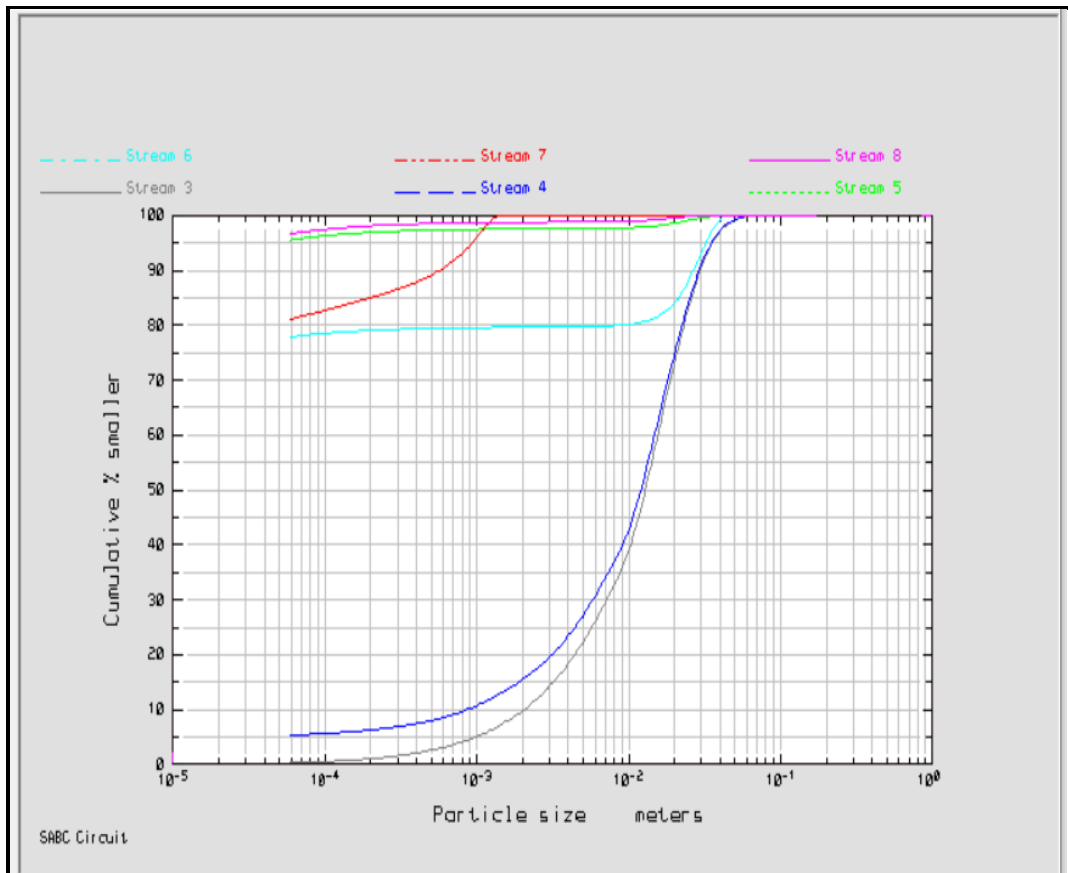


**Figure 4.4** Particle size distribution of scenario 1 on the critical sized material

In Figure 4.5 is the PSD of scenario 2 on streams 3 – 8. Similar to Figure 4.4, the results show that the circuit experiences a significant change in stream 4 and stream 5. Stream 4 experiences a PSD ranging from 5% to 100% while stream 5 ranges from 96 % to 100 %.

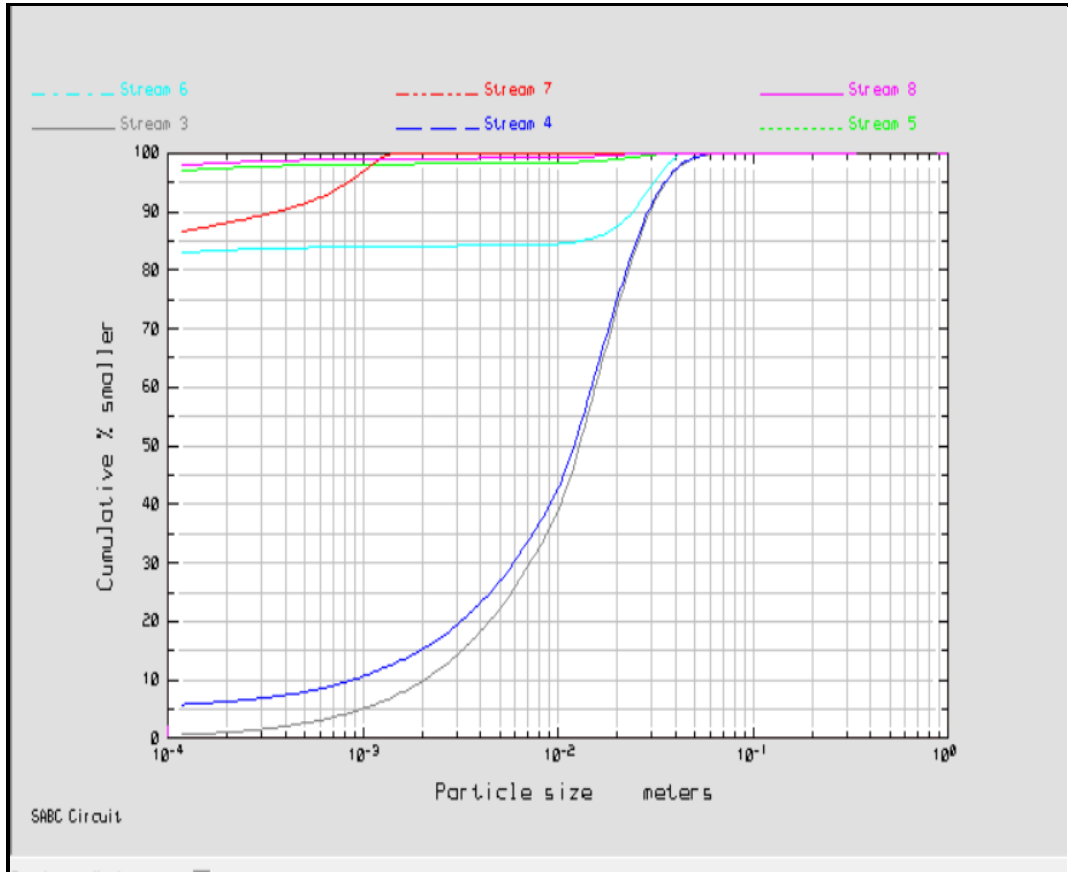


**Figure 4.5** Particle size distribution of scenario 2 on the critical sized material

Figure 4.6 displays the PSD of scenario 2 on streams 3 – 8, this can be considered as a SAG mill closed circuit. The results indicate that the circuit experiences significant changes in the SAG mill between stream 4 and stream 5. Stream 4 experiences a PSD ranging from 6% to 100% and stream 5 ranges from 97% to 100%.

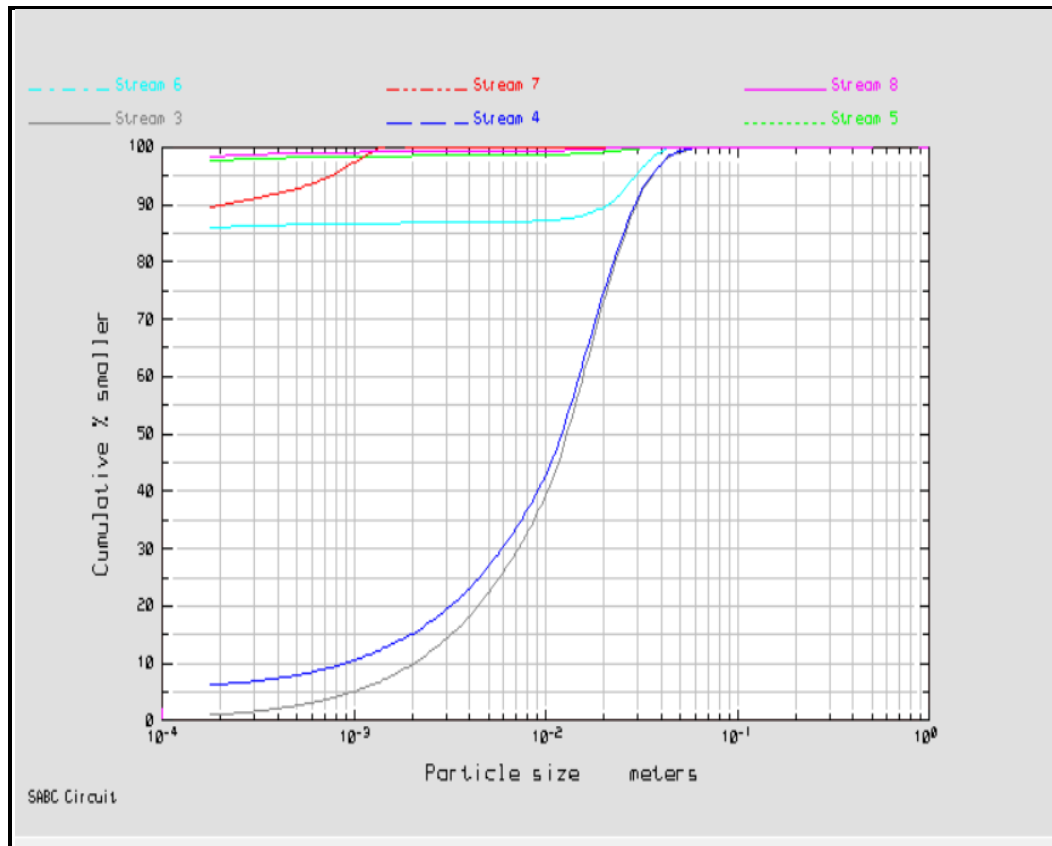


**Figure 4.6** Particle size distribution of scenario 3 on the critical sized material

It is evident that the particle size distribution for these scenarios project similar trends with no major differences. In general, the size distribution graph varies significantly when the streams undergo a size reduction unit such as a SAG mill and a cone crusher. These were streams 4 and 5 for the SAG mill. For the cone crusher, it was between stream 6 and 7. Based on Figures 4.4 – 4.6, the ore feed size appears to be the major factor that defines the shape of the PSD. In relation to the respective scenarios, the PSD of the smaller sized ore feed which is in scenario 1 generates a slightly broader curve whereas the bigger sized ore feed which is scenario 3 produced a narrower shaped curve. This signifies that scenario 1 produces greater range size of particles to that of scenario 3.

This section covers scenarios 4, 5 and 6 has a circuit feed of 100 tph in all the simulated circuits. However, all these scenarios have different ore size ranges, i.e. -400 +200 mm and -600 +400 mm respectively. In Table 4.3, it is noted that the feed (stream 4) and product (stream 5) of the SAG mill were at 108 tph with a

flowrate of 8 tph recycled (stream 6) through the cone crusher. A notable trend in these scenarios was an increase in flow around the stream 9 and stream 12 as the ore feed increases. The overall implications to the circuit resulted in a reduction in throughput. Therefore, an increase in ore size at constant feed flow rate and operating parameters for this circuit resulted in a deterioration of throughput. The section that covers scenarios 7, 8 and 9 has a circuit feed of 150 tph in all the simulated circuits. Similar to the abovementioned section, the scenarios have different ore size ranges. It is noted in Table 4.3 that the SAG mill produces (stream 5) a product at 164 tph while the cone crusher receives a flow rate of 13 tph. Parallel to 100 tph, the trend in this section illustrates a reduction in the overall throughput as the ore feed size increases with unproductive circuit operations.

**Table 4.3** Simulation results of the scenarios

|           |                  | Scenarios |     |      |     |     |      |
|-----------|------------------|-----------|-----|------|-----|-----|------|
|           |                  | 4         | 5   | 6    | 7   | 8   | 9    |
| Stream 1  | Flowrate(tph)    | 100       | 100 | 100  | 150 | 150 | 150  |
|           | Slurry (% solid) | 100       | 100 | 100  | 100 | 100 | 100  |
| Stream 2  | Flowrate(tph)    | 100       | 100 | 100  | 150 | 150 | 150  |
|           | Slurry (% solid) | 100       | 100 | 100  | 100 | 100 | 100  |
| Stream 3  | Flowrate(tph)    | 100       | 100 | 100  | 150 | 150 | 150  |
|           | Slurry (% solid) | 100       | 100 | 100  | 100 | 100 | 100  |
| Stream 4  | Flowrate(tph)    | 108       | 108 | 108  | 163 | 164 | 164  |
|           | Slurry (% solid) | 60        | 60  | 60   | 60  | 60  | 60   |
| Stream 5  | Flowrate(tph)    | 108       | 108 | 108  | 163 | 164 | 164  |
|           | Slurry (% solid) | 60        | 60  | 60   | 60  | 60  | 60   |
| Stream 6  | Flowrate(tph)    | 8         | 8   | 8    | 13  | 14  | 14   |
|           | Slurry (% solid) | 69        | 69  | 69   | 71  | 71  | 71   |
| Stream 7  | Flowrate(tph)    | 8         | 8   | 8    | 13  | 14  | 14   |
|           | Slurry (% solid) | 69        | 69  | 69   | 71  | 71  | 71   |
| Stream 8  | Flowrate(tph)    | 100       | 100 | 100  | 150 | 150 | 150  |
|           | Slurry (% solid) | 59        | 59  | 59   | 59  | 59  | 59   |
| Stream 9  | Flowrate(tph)    | 130       | 230 | 4007 | 199 | 348 | 5756 |
|           | Slurry (% solid) | 60        | 60  | 60   | 60  | 60  | 60   |
| Stream 10 | Flowrate(tph)    | 130       | 230 | 4007 | 199 | 348 | 5756 |
|           | Slurry (% solid) | 60        | 60  | 60   | 60  | 60  | 60   |
| Stream 11 | Flowrate(tph)    | 30        | 129 | 3935 | 49  | 198 | 5652 |
|           | Slurry (% solid) | 63        | 81  | 88   | 65  | 81  | 88   |
| Stream 12 | Flowrate(tph)    | 30        | 129 | 3935 | 49  | 198 | 5652 |
|           | Slurry (% solid) | 63        | 81  | 88   | 65  | 81  | 88   |
| Stream 13 | Flowrate(tph)    | 100       | 100 | 73   | 150 | 150 | 105  |
|           | Slurry (% solid) | 59        | 45  | 3    | 59  | 45  | 3    |

#### 4.2.2. Simulated circuit for operating parameters of a SAG mill

It is common practice to operate a SAG mill in a closed circuit. This is due to the inevitable challenge of pebble formation. However, this can be achieved through comprehending the essential mechanisms of its operation. Therefore, selecting the operating parameters of a SAG mill is critical to its operation. This section focuses on the SAG mill closed-circuit operation, which was simulated having an ore feed size of 200 mm, 400 mm and 600 mm respectively. Correspondingly, the flowrate was constant at 100 tph. However, the main variation was the operating parameters around the SAG mill in order to minimise critical sized material. These parameters include mill filling, ball filling, ball size and mill speed. The variation of these parameters is displayed in Table 4.4. The results in this section are used in Chapter 5 for the attainable region technique to determine the best operating condition for the parameter being simulated.

**Table 4.4** Operating parameters of the SAG mill closed circuit.

| Operating parameter | Mill filling (%) |    |    | Ball filling (%) |    |    | Ball size (mm) |    |     | Mill speed (%) |    |    |
|---------------------|------------------|----|----|------------------|----|----|----------------|----|-----|----------------|----|----|
|                     | 30               | 35 | 40 | 10               | 12 | 14 | 50             | 75 | 100 | 65             | 70 | 75 |
|                     |                  |    |    |                  |    |    |                |    |     |                |    |    |

#### 4.3. Energy consumption on the SAG mill closed circuit

Energy consumption can dictate the operation of a circuit, as cost-effective measures in Comminution are always considered. Mill operation can measure its efficiency through energy consumption (Napier-Munn *et al.*, 1999). Figure 4.7 depicts the energy usage in the simulated circuit for feed flowrate and ore feed size variations. The x-axis shows the different scenarios and the y-axis shows the power consumption in kW. The blue bars indicate the net power consumption in the SAG mill. The red bars indicate the estimated power requirement in the Cone crusher. Based on Figure 4.7, the SAG mill operation was constant throughout all the scenarios. For the Cone crusher, however, the energy requirement varies. At 50 tph the trend shows the decline in energy consumption as the ore feed size increases. The ore feed size for -200 +100 mm reaches a combined energy

consumption of 7400 kW. For -400 +200 mm, the combined energy consumption was 7380 kW and for -600+400 mm, the combined energy consumption was 7360 kW. The energy consumption for 100 tph and 150 tph feed flow rate were constant at 7390 kW and 7405 kW respectively.

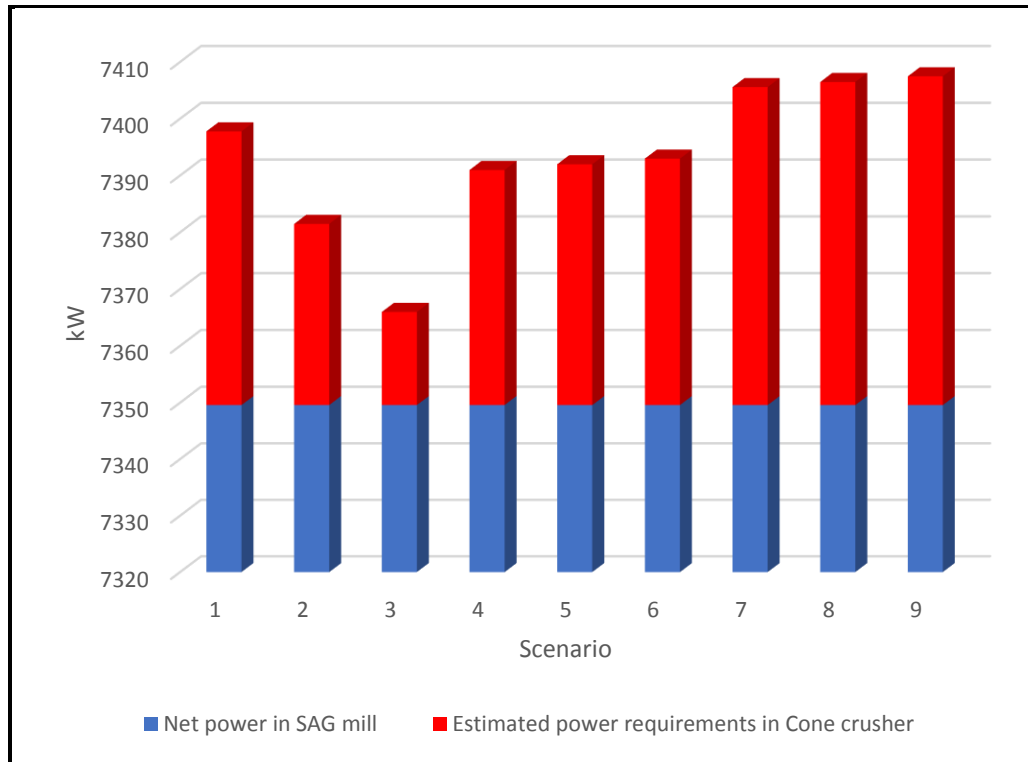


**Figure 4.7** Energy usage in the SAG mill closed circuit

#### 4.4. Significance of the findings

In this chapter, simulations were adopted and carried out as part of the computer-based experimental programme. The methodology was aimed at accomplishing the objectives of this research by generating data that forms critical sized material.

The main purpose of a mineral processing plant is to separate the valuable compounds from the other valueless material, gangue (Napier-Munn *et al.*, 1990). In this framework, there are many variables and operating systems that affect the liberation of these valuable minerals. The SABC circuit is one circuit that is used for this application. There were 81 scenarios that were simulated using MODSIM®

3.6.22 Demo version. The focus was around the SAG mill closed circuit which consisted of a SAG mill, vibrating screen and cone crusher. The purpose was to minimise the handling of critical sized material. The simulation program found in illustrates the input variables ranging from 50 tph to 150 tph and the ore size ranging from 100 mm to 600 mm. It also displays the independent operating parameters together with the fixed variables in the circuit.

The energy usage increases as the ore size and flow rates increase in the SAG mill. Extraordinarily for the cone crusher, the energy usage in scenario 3 is less than that of scenario 1 which has a smaller ore feed size. The PSD of scenarios 1-3 in relation to the energy used on the cone crusher and its effectiveness is observed. Evertsson (2000) discusses the breakage behaviour of rock fragmentation in Jaw, cone and gyratory crushers identifying compression, impact and attrition crushing as the critical factors in these size reduction units. Through his research, it established that the compression ratio is the primary effect for breakage behaviour with force and energy being the secondary effect. The compression ratio describes how much the rock material is compressed at a certain location in the crushing event. Based on figures 4.4 – 4.6, we notice that the crushing efficiency was greater at a lower energy used, this was due to type of crushing that occurred in the cone crusher. In figure 4.6, it is evident that the media experienced significant attrition motion rather than compression crushing as seen in figure 4.4.

The slurry of the SAG mill closed circuit throughout the scenarios displayed similar data, as the mill operated in a 60% solid content. The cone crusher operated on a slurry content ranging from 65% (in solid) in scenario 1 to 64% (in solid) in scenario 3. Napier-Munn et al (1996) revealed the importance of slurry density in size reduction units which have the ability to control the grinding action. However, the increase in water addition affects the grinding ability of the mill due to the reduced interaction of the smaller particles(media) with the balls.

#### 4.5. Summary

The results produced were successfully completed. The 81 scenarios were separated in two sections according to input variables and operating parameters. The simulation flow sheets presented in the various figures depicts the detail flow rate of each stream. Energy consumption was constant for the SAG mill at all the scenarios and increased in the cone crusher as ore size increased.

## Chapter 5 Attainable region analysis of the performance of the SABC circuit

### 5.1 Introduction

The attainable region (AR) technique was originally intended for chemical process optimisation using reactants and product concentrations. Later, it was discovered that this concept can be extended to other fields of chemical engineering such as comminution. The underlying assumption was that since milling is a comminution operation, it can be considered as a rate process to which size classes break down from larger to smaller sizes in a manner parallel to reactor system (Danha *et al.*, 2015).

The concept of the AR theory is to use the values of the output values that were achieved from the specified feed and limiting parameters. This results or output values can then be applied graphically to a geometric space in which the achievable points were found (Hlabangana *et al.*, 2016). The benefit of this method is that it neglects milling parameters and focuses on the breakage process, which permits the attainment of a specific objective function (Khumalo *et al.*, 2006). The objective function is a fundamental expression that relates the output variables to the input variables in a process. The overall intention of the AR technique is to establish values of the input variables that will give result to optimum conditions of the output variables (Hlabangana, 2018).

The choice of operating parameters in this research was based around pebble formation in a SAG mill and its implications to the overall circuit. The effects of critical sized material were highlighted in Chapter 2 and the AR method was applied in this chapter from data produced using MODSIM® (see Chapter 4). The purpose of this method is to highlight the best form of operations used from the simulation program. The results were graphically displayed through the AR technique to highlight the optimal operation.

A variety of scenarios were simulated to illustrate the significance of simulated semi-autogenous and ball milling circuit. The simulation circuit were divided into 9 different scenarios that had different input parameters and operating conditions. The altered independent parameters ranged from flow rates to ore sizes. The different operating parameters of the SAG mill were mill filling, ball filling, ball size, mill speed and grate openings.

The SAG mill was the central component that governs this research due to the formation of critical sized particles. This involved the closed circuit of the SAG which includes vibrating screen and cone crusher, also referred to as the pebble crusher, as seen in Figure 5.1.

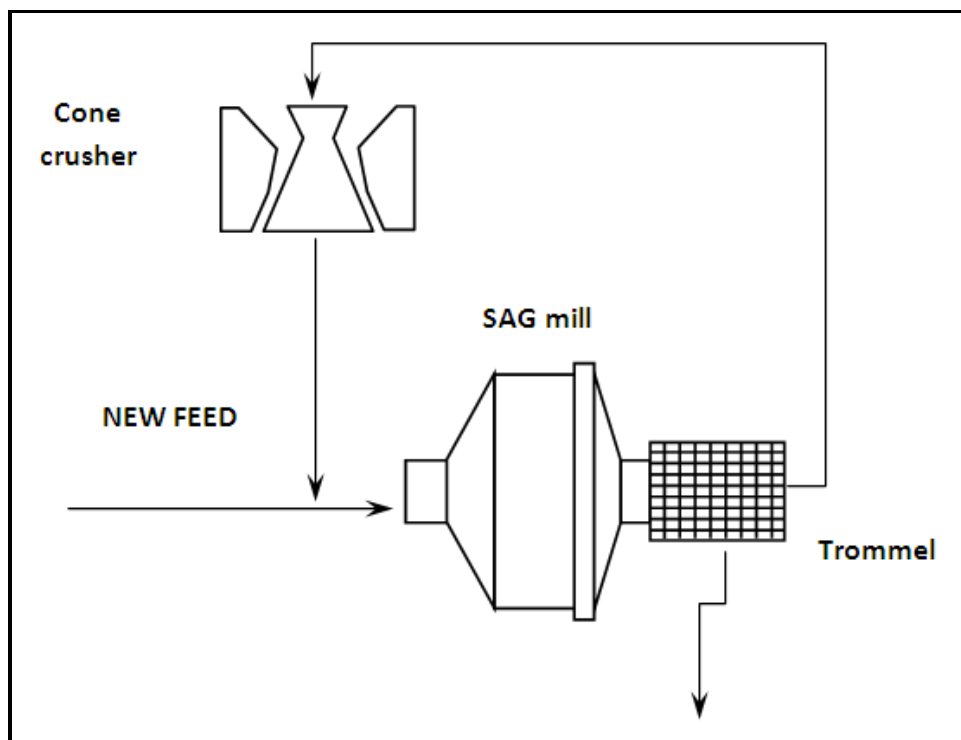


**Figure 5.1** SAG mill in closed circuit

As described in the literature review, the attainable region path is formed in three steps. The first step is to determine the fundamental process taking place and, in this case, it is a comminution circuit which entails size reduction, mixing and classification. The second step is to select the state variables characterising the output state of the system. The state variables in this case are mass fractions

defined as feed size, intermediate size and fines. The third and final step is to find the optimal point of the AR path which is generally on the boundary of the attainable region.

## 5.2 Construction of the attainable region path

To apply the attainable region technique, the ore material was grouped into a three different size classes in order to monitor how breakage occurs. As discussed in Chapter 3, the critical sized material for the research was -100 +23 mm. Therefore, the different classes were defined as follows:

- The feed size class or the material of size falling between 100 mm and 23 mm. The mass fraction of material in this class is labelled  $m_1$
- The middling size class constituted of particles of size between 23 mm and 4.7 mm. The corresponding mass fraction of material in this class is labelled  $m_2$
- The fines size class  $m_3$ , which is defined as the mass fraction of the material passing through screen size 4.7 mm.

Since the objective function of the research refers to the minimisation of critical sized material the focus was around mass fractions  $m_1$  and  $m_2$ . The critical sized material was analysed through streams 3 and 7 under various operating conditions that were described in Chapter 3. The pebbles were generated in the SAG mill, classified in the vibrating screen then ground in the cone crusher. Contrast to using the grinding rate with the residence time in a grinding unit to determine the breakage, this research traces the size reduction and classification over the SAG mill, vibrating screen and cone crusher.

## 5.3 Effects of feed flow rate on the performance of the circuit

The results represent the scenarios that were simulated at flow rates 50 tph, 100 tph and 150 tph for ore feeds ranging from 100 – 600 mm. The purpose was to

study the effects of flow rate around a SAG mill closed circuit. Figures 5.2 – 5.4 represent the different ore feed sizes that were simulated at -200 +100 mm, -400 +200 mm and -600 +400 mm respectively.

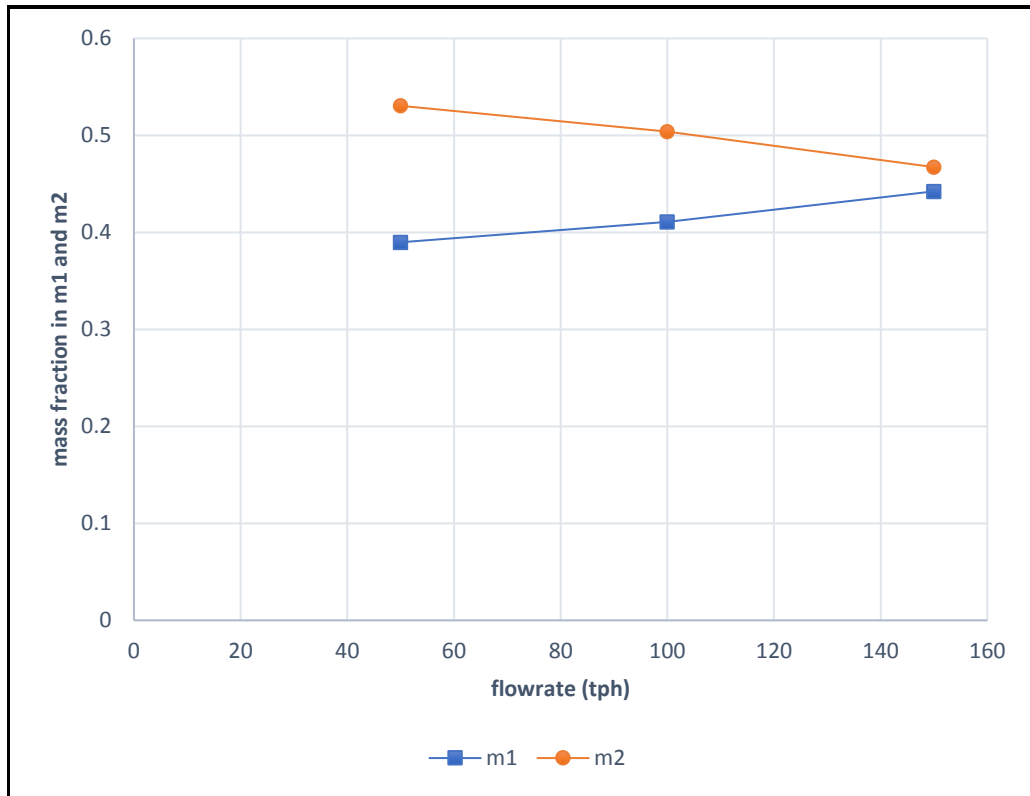


**Figure 5.2** Milling kinetics of a SAG mill in a SABC circuit as a function of feed flow rate under the conditions:  $J_T = 30\%$ ,  $J_B = 10\%$ ,  $d_B = 50$ ,  $\Phi_c = 65\%$  and grate opening 40 mm with an ore feed of -200+100 mm.

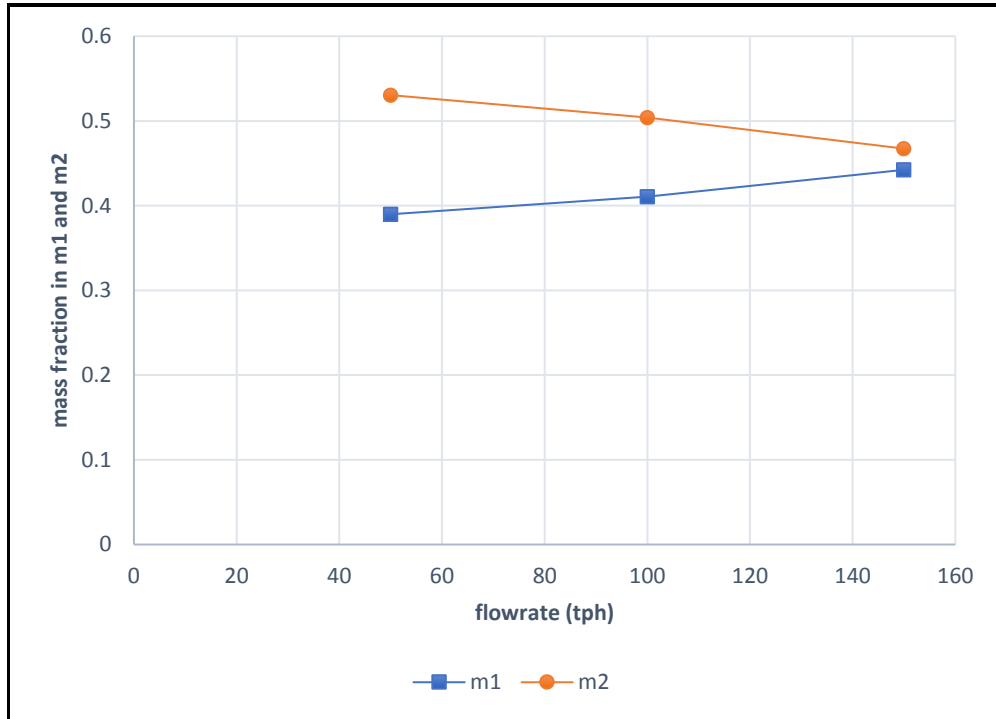


**Figure 5.3** Milling kinetics of a SAG mill in a SABC circuit as a function of feed flow rate under the conditions:  $J_T = 30\%$ ,  $J_B = 10\%$ ,  $d_B = 50$ ,  $\Phi_c = 65\%$  and grate opening 40 mm with an ore feed of -400+200 mm.

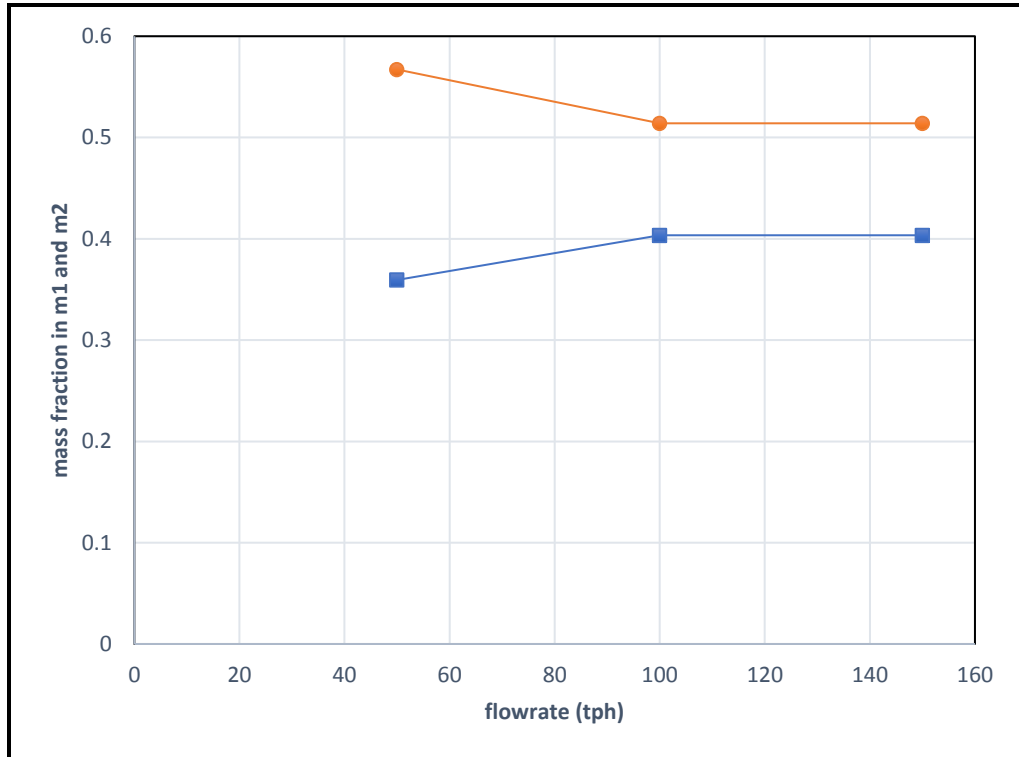


**Figure 5.4** Milling kinetics of a SAG mill in a SABC circuit as a function of feed flow rate under the conditions:  $J_T = 30\%$ ,  $J_B = 10\%$ ,  $d_B = 50$ ,  $\Phi_c = 65\%$  and grate opening 40 mm with an ore feed of -600+400 mm.

Using the results from Figures 5.2 – 5.4, the attainable region was formed as seen in Figure 5.5. It represents 9 simulations that operated on the same operating conditions having a  $J_T$  of 30%,  $J_B$  of 10%,  $d_B$  of 50 mm,  $\phi_c$  of 65% and grate opening of 40 mm. However, they had different input variables. Based on the graph, the formation of critical sized material was at its highest on a flow rate of 150 tph representing 45% of  $m_1$ . In contrast, the maximised point for the section was 57% which represents the scenario with an ore feed of -600 +400 mm and a flow rate of 50 tph.

Based on Figures 5.2 - 5.4, the bigger ore sized material which was -600+400 mm experienced a different breakage mechanism than the smaller sized material of -200+100 mm and -400+200 mm in the SAG mill. This mechanism favours breakage by attrition on the bigger sized material rather than breakage by impact.

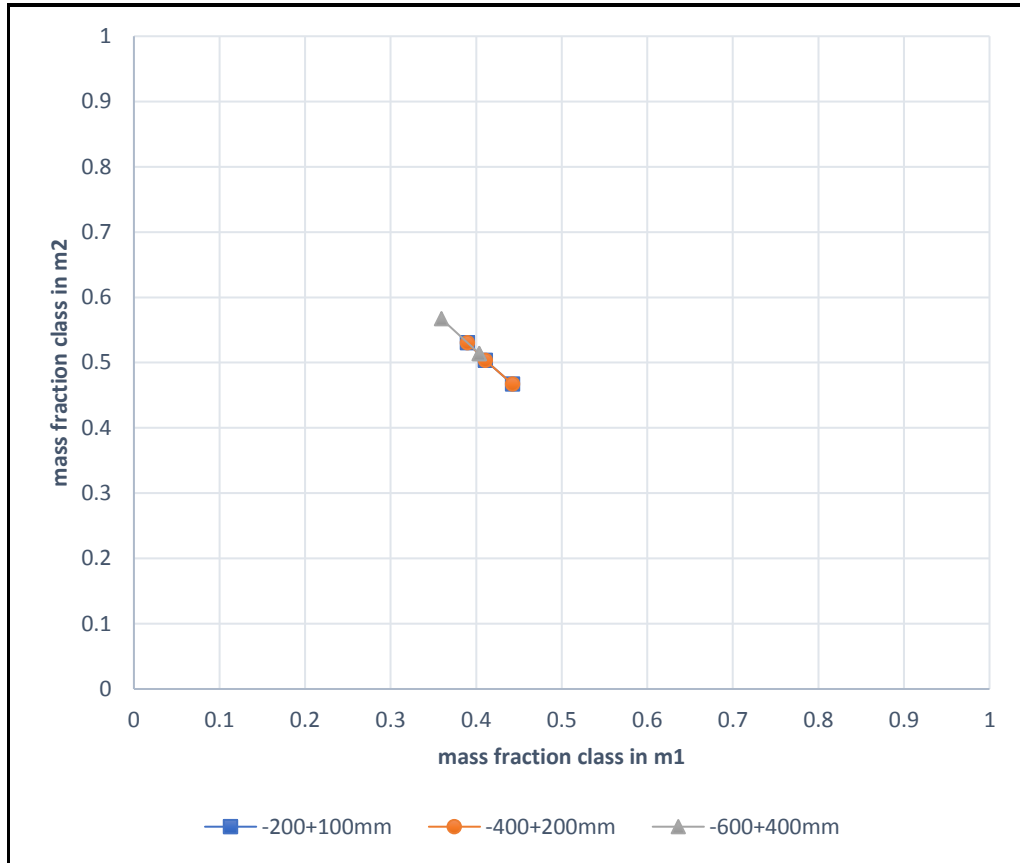


**Figure 5.5** The Attainable Region summary presenting the effects of feed flow of a SAG mill in an SABC Circuit under simulated conditions:  $J_T = 30\%$ ,  $J_B = 10\%$ ,  $d_B = 50$  mm,  $\Phi_c = 65\%$  and grate opening 40 mm.

#### 5.4 Effects of ore feed size on the performance of the circuit

The results represent the scenarios that were simulated at ore feed sizes -200+100 mm, -400 +200 mm and -600 +400 mm for feed flow rates ranging from 50 – 150 tph. The purpose was to observe the effects of ore feed size around a SAG mill closed circuit. Figures 5.6 – 5.8 represent the different feed flow rates that were simulated at 50 tph, 100 tph and 150 tph respectively.

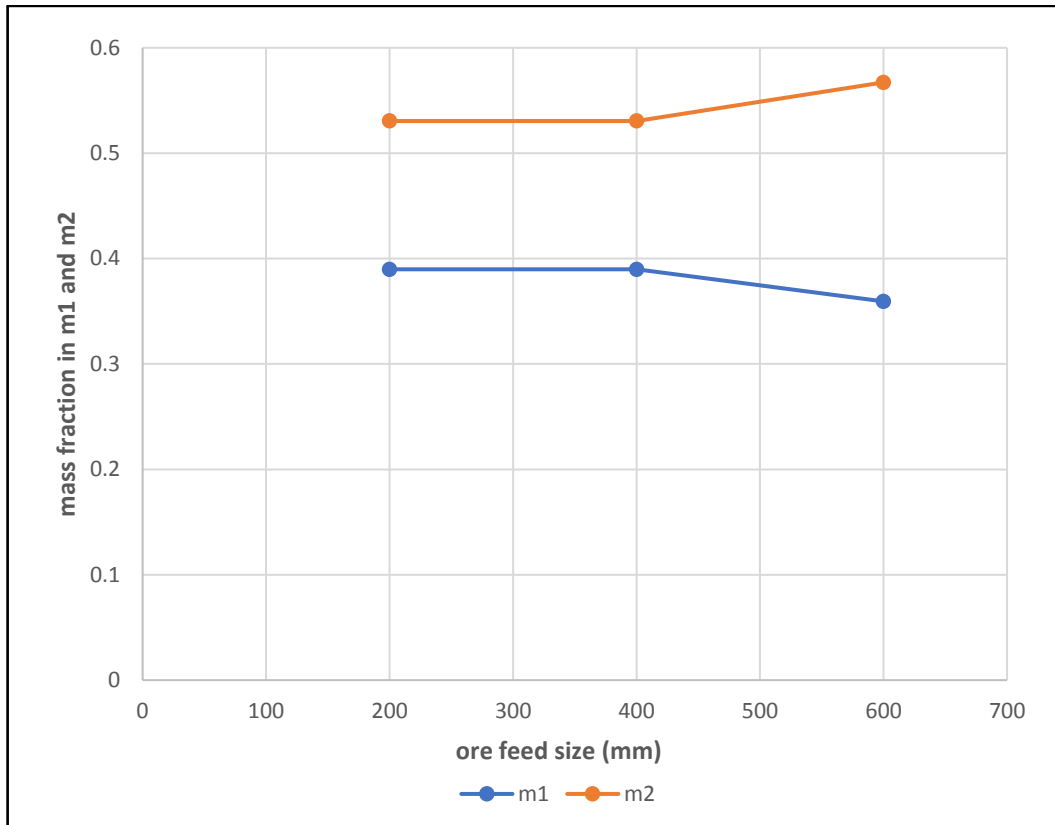


**Figure 5.6** Milling kinetics of a SAG mill in a SABC circuit as a function of ore feed size under the following conditions:  $J_T = 30\%$ ,  $J_B = 10\%$ ,  $d_B = 50$  mm,  $\Phi_c = 65\%$  of critical speed, 40 mm grate opening, and 50 tph feed flow rate.

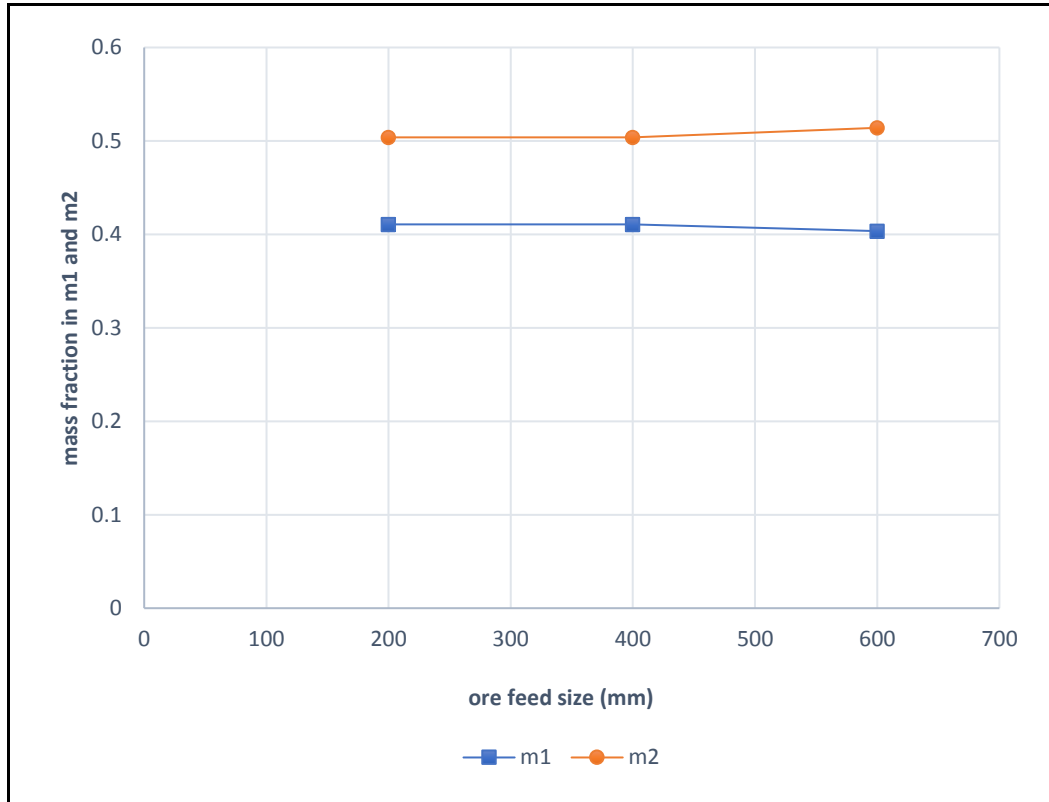


**Figure 5.7** Milling kinetics of a SAG mill in a SABC circuit as a function of ore feed size under the conditions:  $J_T = 30\%$ ,  $J_B = 10\%$ ,  $d_B = 50$ ,  $\Phi_c = 65\%$  and grate opening 40 mm with a feed flow rate of 100 tons/hr.

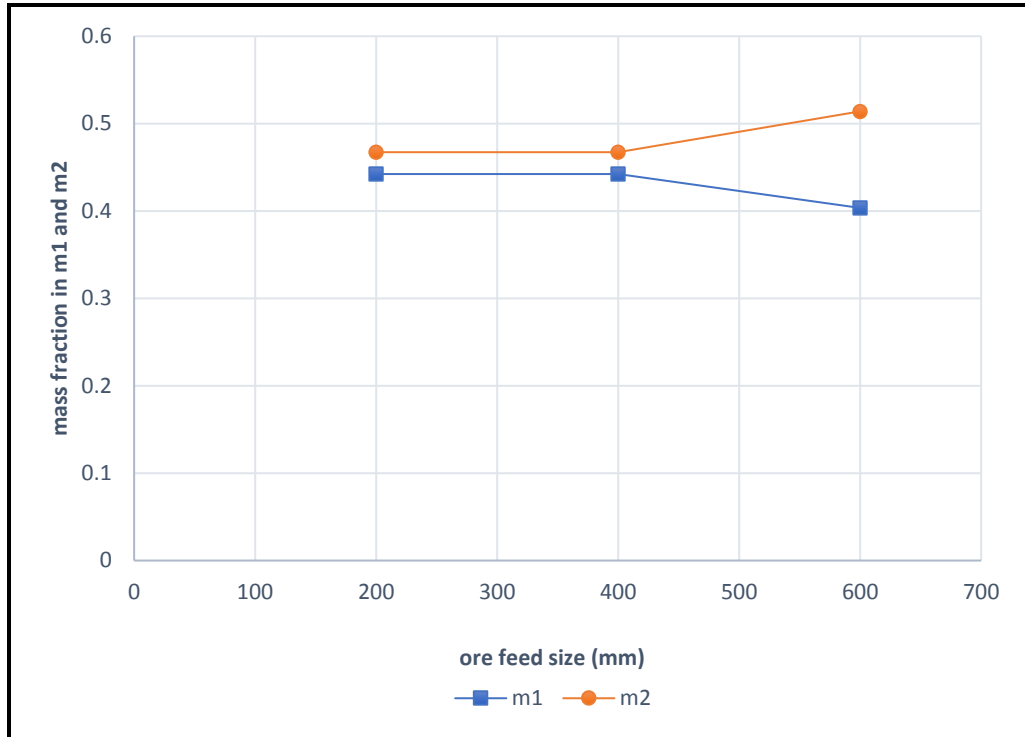


**Figure 5.8** Milling kinetics of a SAG mill in a SABC circuit as a function of ore feed size under the conditions  $J_T = 30\%$ ,  $J_B = 10\%$ ,  $d_B = 50$ ,  $\Phi_c = 65\%$  and grate opening 40 mm with a feed flow rate of 100 tons/hr.

Figure 5.9 represents the attainable region that was formed by the results of Figures 5.6 – 5.8. It represents 9 simulations that operated on the same operating conditions having a mill filling of 30%, ball filling of 10%, ball size of 50 mm, mill speed of 65% and grate opening of 40 mm, however, they had different input variables. Based on the graph, the formation of critical sized material was at its highest on a flow rate of 150 tph representing 44% of  $m_1$ . In contrast, the maximised point for the section was 58% which represents the scenario with an ore feed of -200 +100 mm and a flow rate of 50 tph.

Based on Figures 5.6 – 5.8, the ore size -200+100 mm and -400+200 mm formed identical results at different flow rates. Seemingly, the bigger sized ore particle experienced a different breakage mechanism than the smaller sized particles in the SAG mill. This mechanism favours breakage by impact on the bigger sized material rather than attrition breakage consequently generating lower critically sized material.

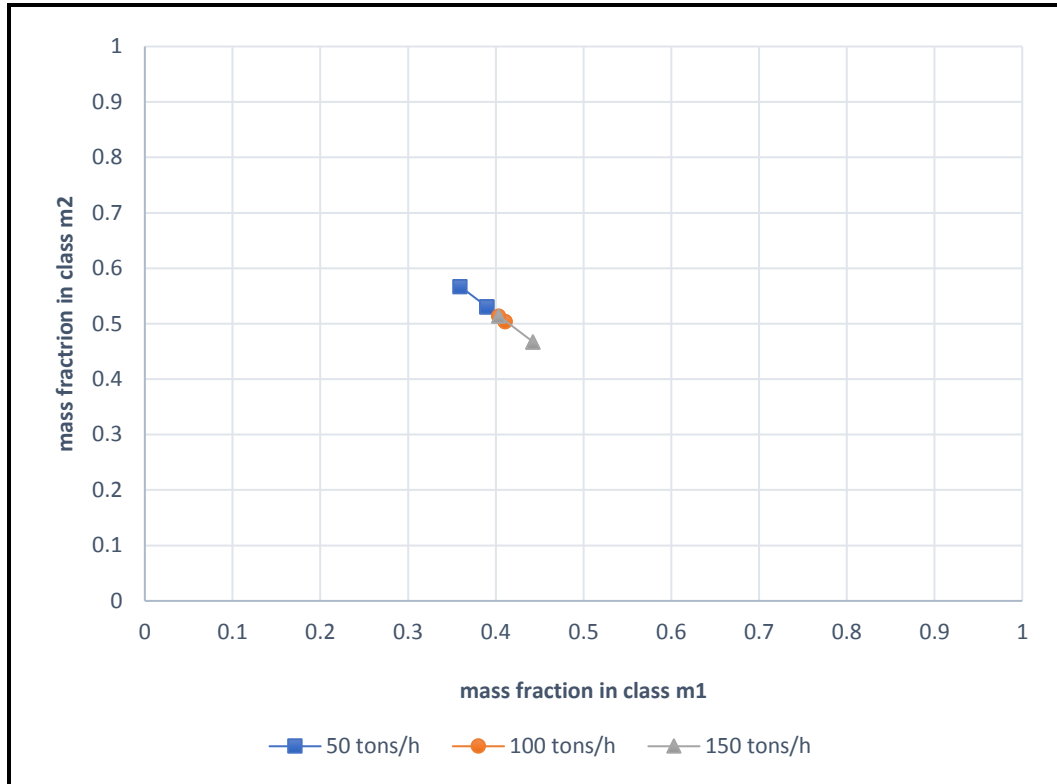


**Figure 5.9** The Attainable Region summary presenting the effects of ore feed of a SAG mill in an SABC circuit under simulated conditions  $J_T = 30\%$ ,  $J_B = 10\%$ ,  $d_B = 50\text{mm}$ ,  $\Phi_c = 65\%$  and grate opening 40 mm.

### 5.5 Effects of mill filling on the performance of the circuit

The results represent the scenarios that were simulated at mill filling 30%, 35% and 40% for feed flow rate of 100 tph. The purpose was to investigate the effects of load volume around the SAG mill in closed circuit. Figures 5.10 – 5.12 represent the different ore feed sizes that were simulated at -200 +100 mm, -400 +200 mm and -600 +400 mm respectively.

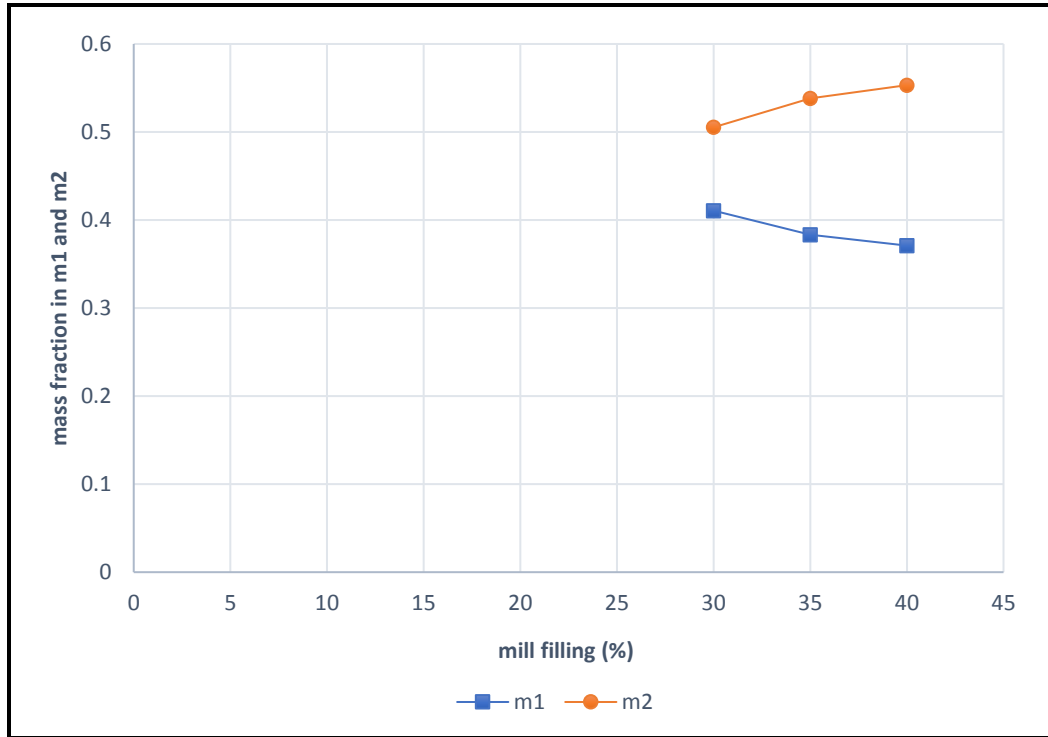


**Figure 5.10** Milling kinetics of a SAG mill in a SABC circuit as a function of an ore size of -200+100mm under the conditions  $J_B = 10\%$ ,  $d_B = 50$  mm,  $\Phi_C = 65\%$  and grate opening 40 mm with a feed flow of 100 tons/hr.

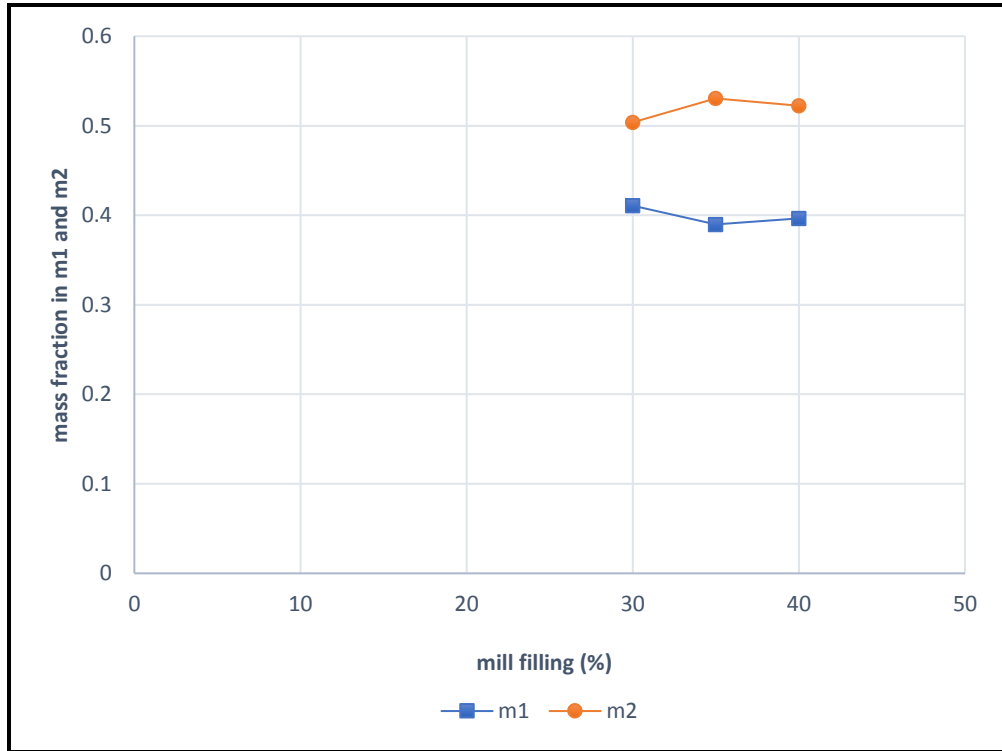


**Figure 5.11** Milling kinetics of a SAG mill in a SABC circuit as a function of an ore size of -400+200 mm under the conditions  $J_B = 10\%$ ,  $d_B = 50$  mm,  $\Phi_c = 65\%$  and grate opening 40 mm with a feed flow rate of 100 tons/hr.

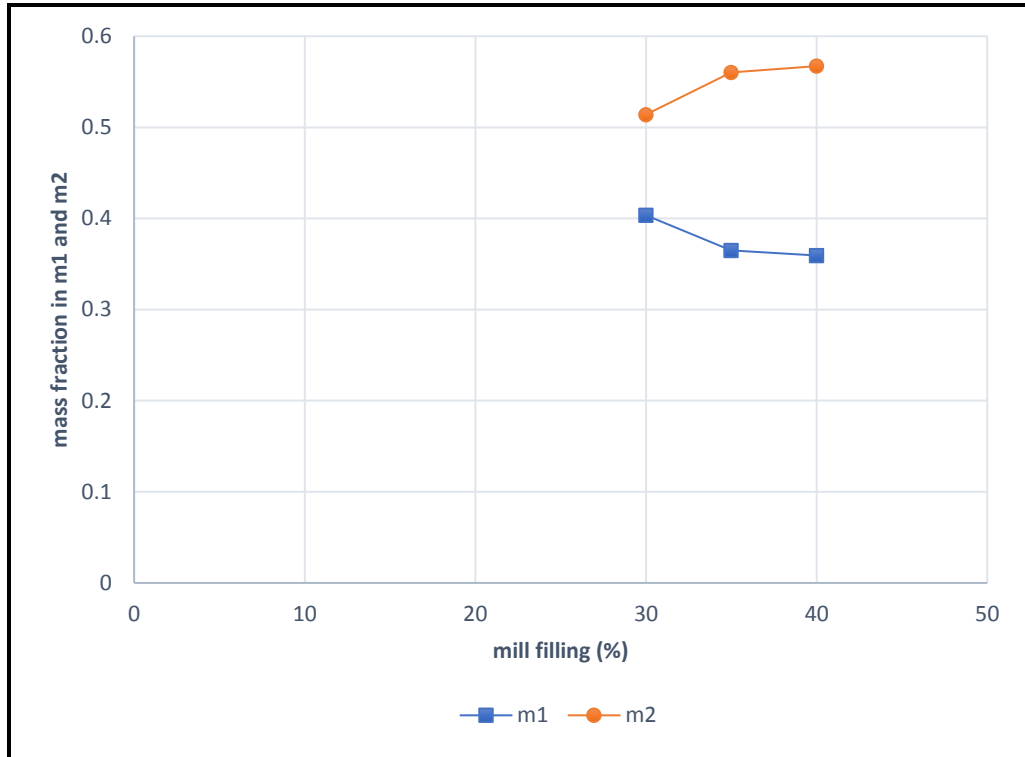


**Figure 5.12** Milling kinetics of a SAG mill in a SABC circuit as a function of an ore size of -600+400 mm under the conditions  $J_B = 10\%$ ,  $d_B = 50$  mm,  $\Phi_c = 65\%$  and grate opening 40 mm with a feed flow rate of 100 tons/hr.

Using the results from Figures 5.10, 5.11 and 5.12, the attainable region was formed as seen in Figure 5.13. It represents 9 simulations with a constant feed flow rate of 100 tph and operating on the same conditions with ball filling of 10%, ball size of 50 mm, mill speed of 65% and grate opening of 40 mm, however, they had different ore feed size. Based on the graph, the formation of critical sized material was at its highest on an ore feed size of -400 +200 mm representing 41% of  $m_1$ . In contrast, the maximised point for the section was 57% which represents the scenario with a load mill of 40% and an ore feed of -600 +400 mm. The bigger ore sized material experiences a different breakage mechanism than the smaller sized material in the SAG mill and at a higher mill filling. This data signifies that the increased volume of the media and capacity in the mill increases the rate breakage. This mechanism favours breakage by impact on the bigger sized material rather than attrition breakage consequently generating lower critically sized material.

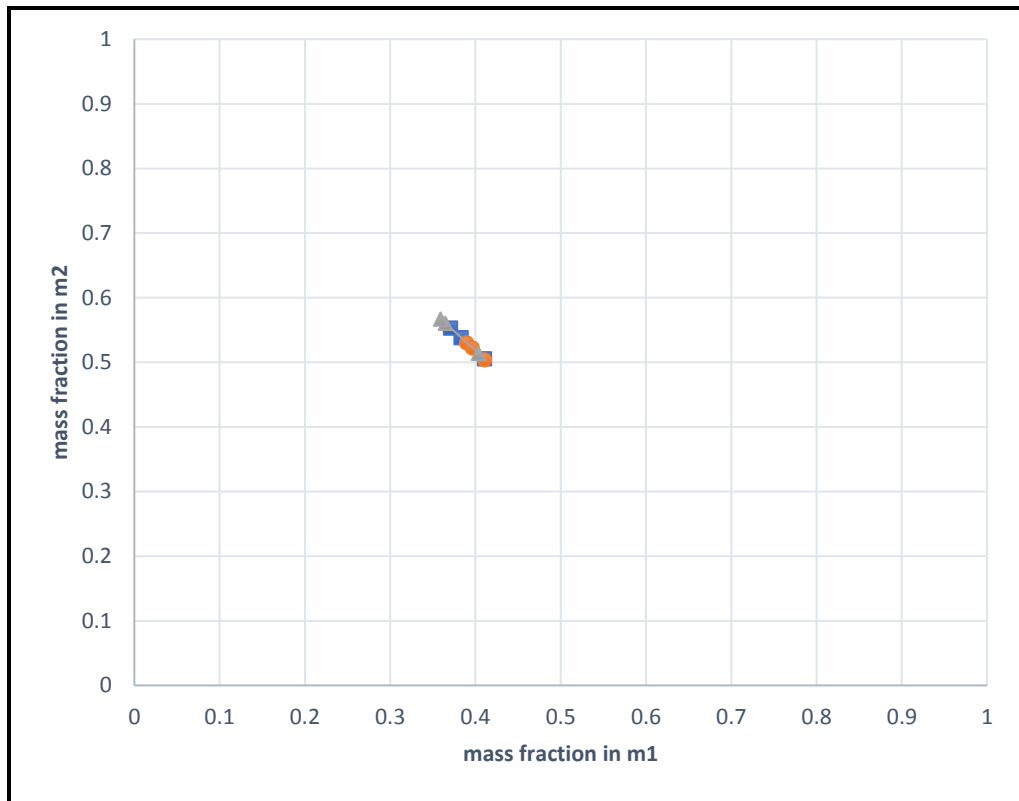
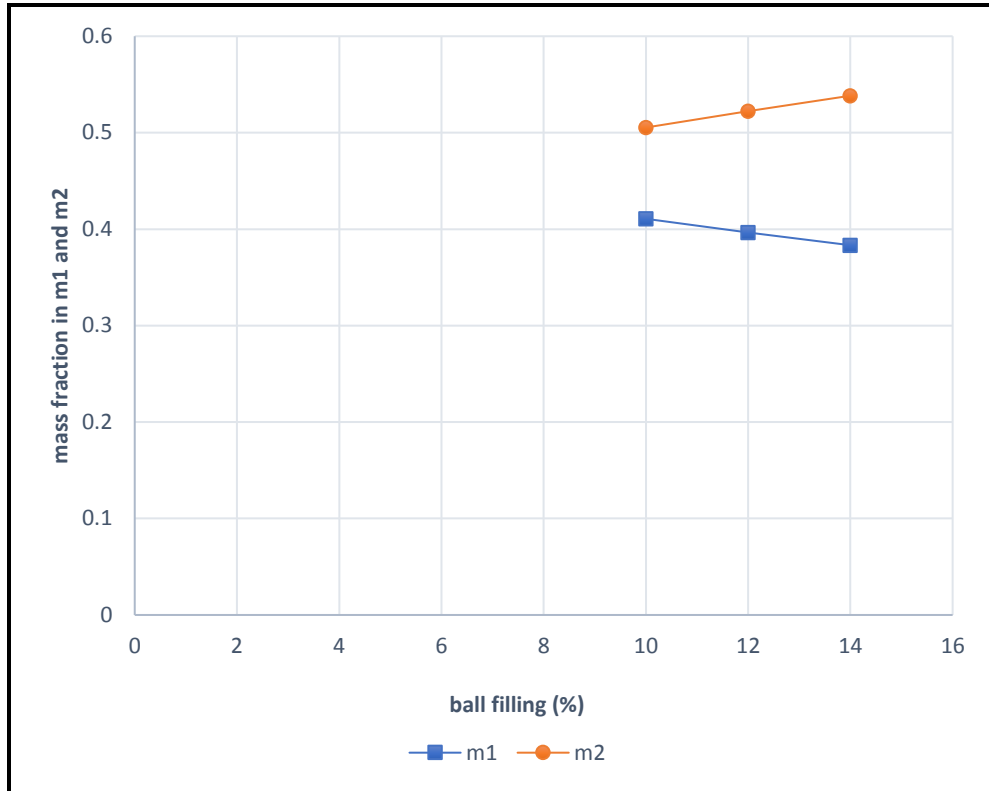


Figure 5.13 The Attainable Region summary presenting the effects of load volume of a SAG mill in an SABC circuit under simulated conditions  $J_B = 10\%$ ,  $d_B = 50$  mm,  $\Phi_c = 65\%$  and grate opening 40 mm.

## 5.6 Effects of ball filling on the performance of the circuit

The results represent the scenarios that were simulated at ball fillings of 10%, 12% and 14% for a feed flowrate of 100 tph. The purpose was to see the effects of ball filling around a SAG mill closed circuit. Figures 5.14, 5.15 and 5.16 represent the different ore feed size that were simulated at -200 +100 mm, -400 +200 mm and -600 +400 mm respectively.



**Figure 5.14** Milling kinetics of a SAG mill in a SABC circuit as a function of an ore size of -200+100 mm under the conditions  $J_T = 30\%$ ,  $d_B = 50$  mm,  $\Phi_c = 65\%$  and grate opening 40 mm with a feed flow rate of 100 tons/hr

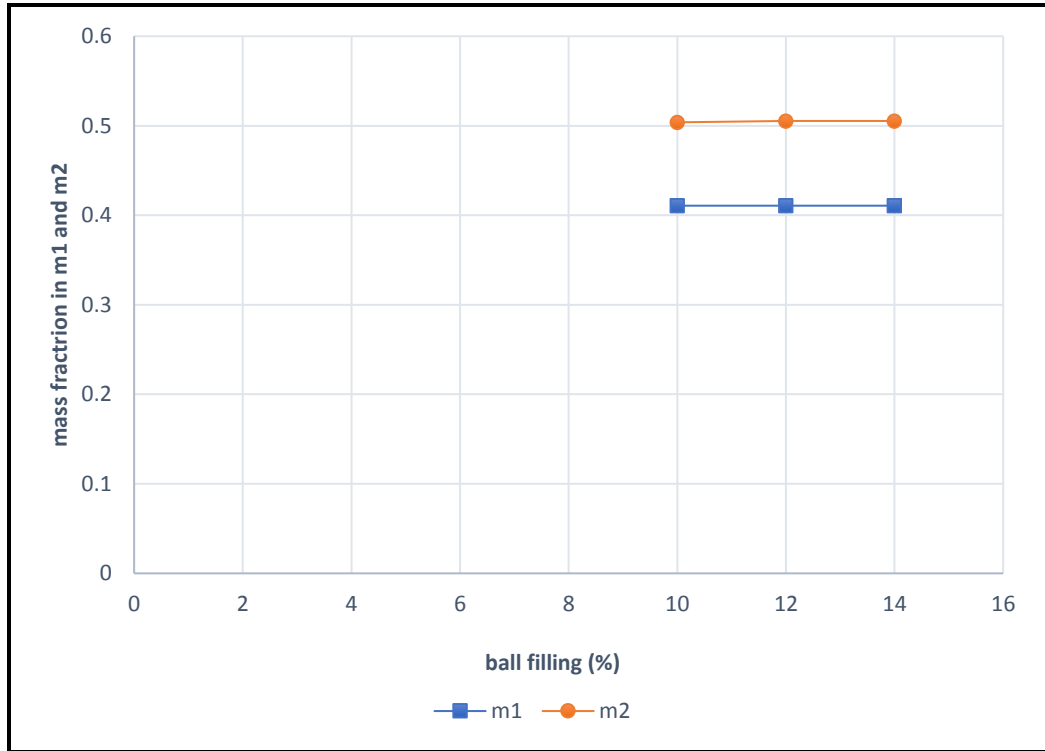


**Figure 5.15** Milling kinetics of a SAG mill in a SABC circuit as a function of an ore size of -400+200 mm under the conditions  $J_T = 30\%$ ,  $d_B = 50$  mm,  $\Phi_c = 65\%$  and grate opening 40 mm with a feed flow rate of 100 tons/hr.

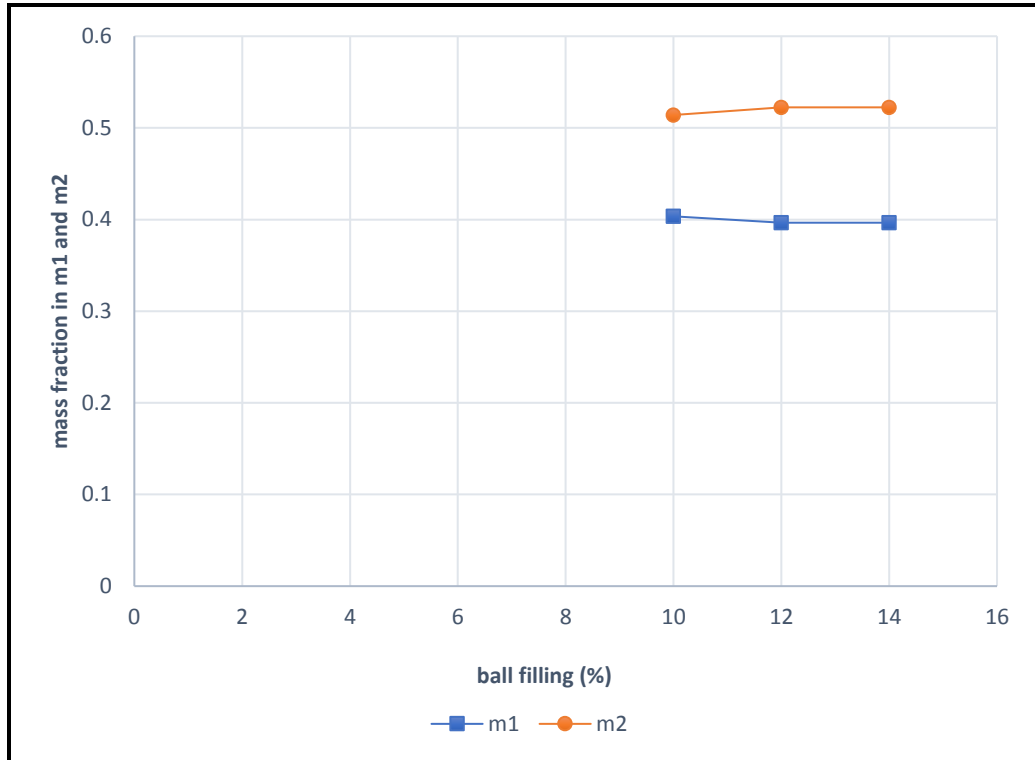


**Figure 5.16** Milling kinetics of a SAG mill in a SABC circuit as a function of an ore size of -600+400 mm under the conditions  $J_T = 30\%$ ,  $d_B = 50$  mm,  $\Phi_c = 65\%$  and grate opening 40 mm with a feed flow of 100 tons/hr.

Using the results from Figures 5.14 – 5.16, the attainable region path was generated as seen in Figure 5.17. It represents 9 simulations with a constant feed flow rate of 100 tph and operating on the same conditions with a mill filling of 30%, ball size of 50 mm, mill speed of 65% and grate opening of 40 mm, however, they had different ore feed size. Based on the graph, the formation of critical sized material was at its highest on an ore feed size of -400 +200 mm and 10% ball volume representing 41% of  $m_1$ . In contrast, the maximised point for the section was 54% which represents the scenario with a ball volume of 54% and an ore feed of -200 +100 mm. Unlike AG mills, steel balls are used to assist the breakage of media in SAG mills and based on the data in Figure 5.17, it appears that the reduction of ball filling favoured the formation of critically sized material. This was due to the breakage mechanisms experienced in the mill as it favoured the attrition between the ore particles rather than breakage by impact from the steel balls.

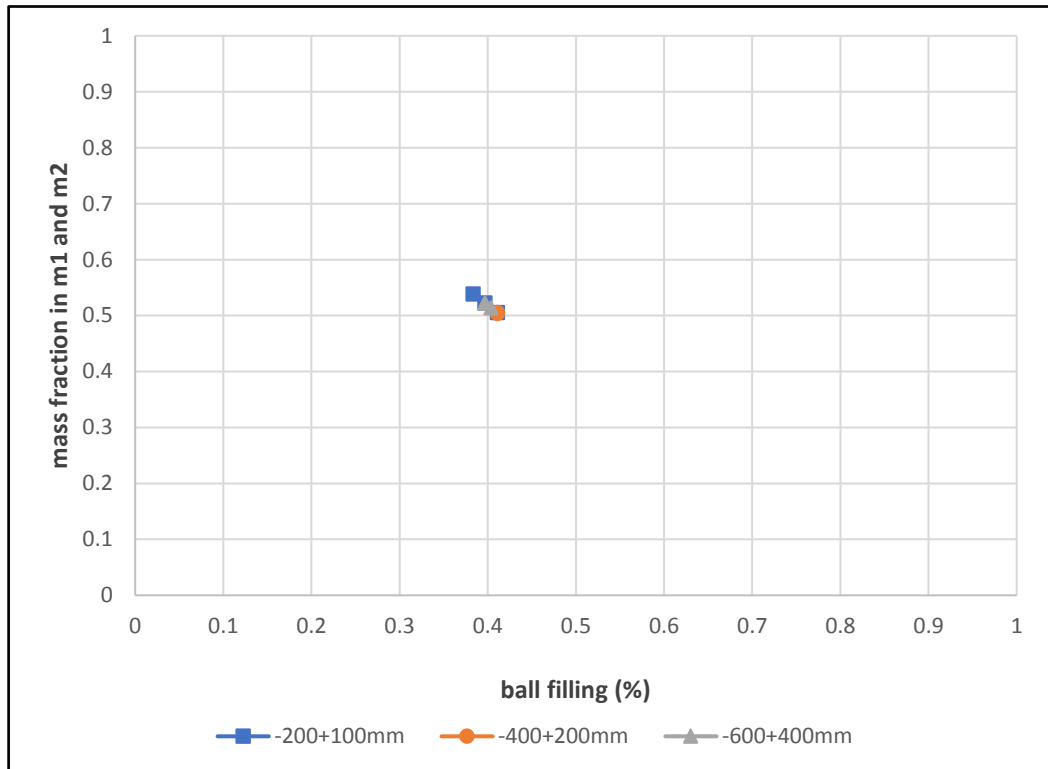


**Figure 5.17** The Attainable Region summary presenting the effects of ball volume of a SAG mill in an SABC circuit under simulated conditions  $J_T = 30\%$ ,  $d_B = 50$ ,  $\Phi_c = 65\%$  and grate opening 40 mm.

### 5.7 Effects of ball size on the performance of the circuit

The results represent the scenarios that were simulated at ball sizes 50 mm, 75 mm and 100 mm for a feed flowrate of 100 tph. The purpose was to observe the effects of ball size around a SAG mill closed circuit. Figures 5.18 – 5.20 represent the different ore feed sizes that were simulated at -200 +100 mm, -400 +200 mm and -600 +400 mm respectively.

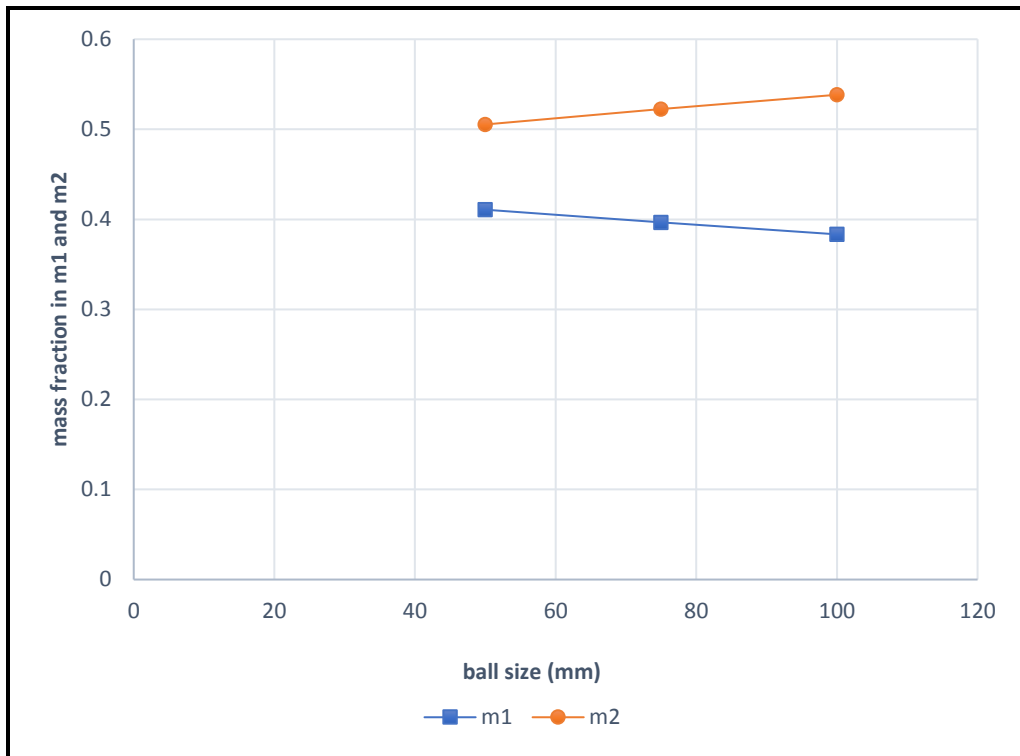


**Figure 5.18** Milling kinetics of a SAG mill in a SABC circuit as a function of an ore size of +200-100 mm under the conditions  $J_T = 30\%$ ,  $J_B = 10\%$ ,  $\Phi_c = 65\%$  and grate opening 40 mm with a feed flow of 100 tons/hr.

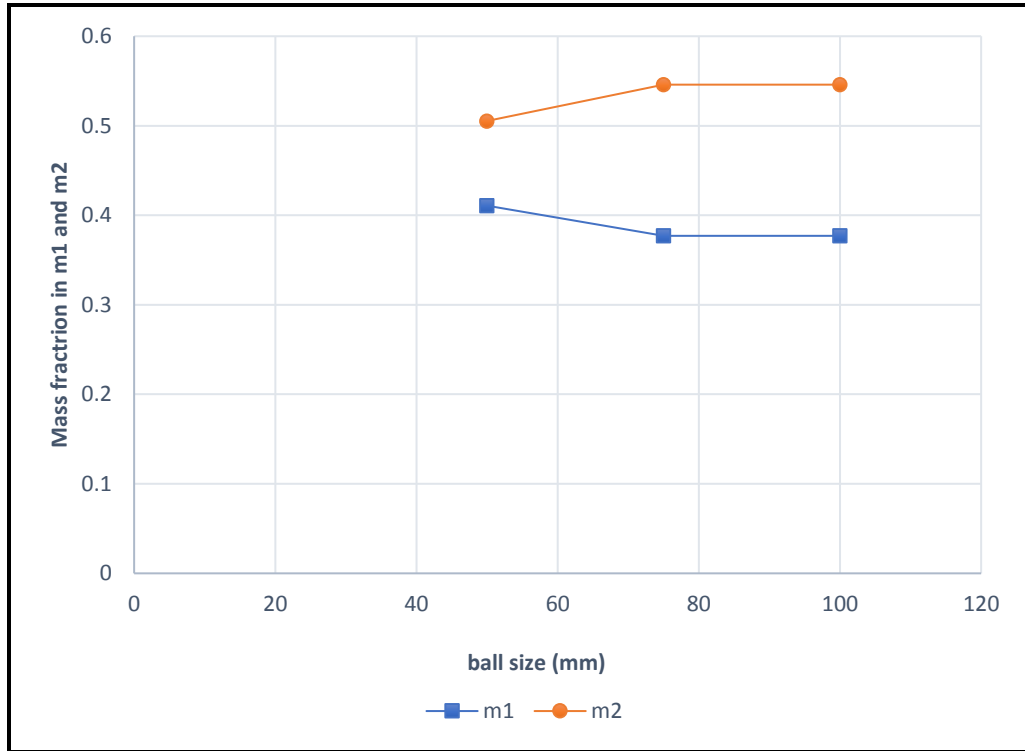


**Figure 5.19** Milling kinetics of a SAG mill in a SABC circuit as a function of an ore size of +400-200 mm under the conditions  $J_T = 30\%$ ,  $J_B = 10\%$ ,  $\Phi_c = 65\%$  and grate opening 40 mm with a feed flow of 100 tons/hr.

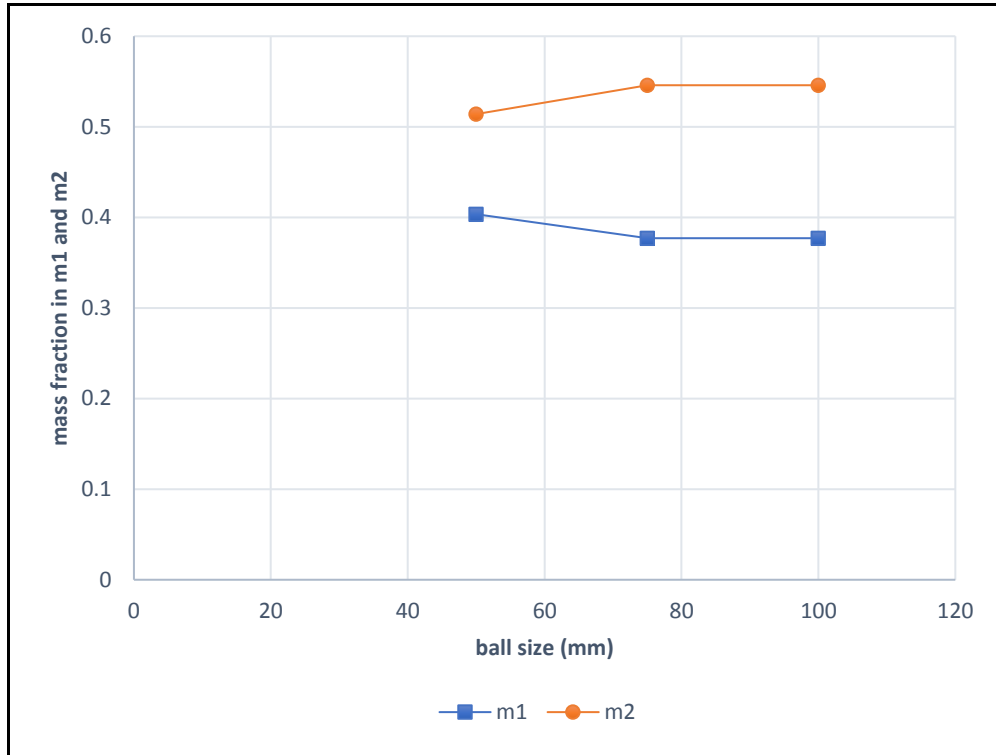


**Figure 5.20** Milling kinetics of a SAG mill in a SABC circuit as a function of an ore size of +600-400 mm under the conditions  $J_T = 30\%$ ,  $J_B = 10\%$ ,  $\Phi_c = 65\%$  and grate opening 40 mm with a feed flow of 100 tons/hr.

Figure 5.21 represents the attainable region that was formed by the results of Figures 5.19 – 5.20. It represents 9 simulations with a constant feed flow rate of 100 tph and operating on the same conditions with mill filling of 30%, ball filling of 10%, mill speed of 65% and grate opening of 40 mm, however, they had different ore feed size. Based on the graph, the formation of critical sized material was at its highest on an ore feed size of -400 +200 mm and 50 mm ball size representing 41% of  $m_1$ . In contrast, the maximised point for the section was 55% which represents the scenario with a ball size of 100 mm and an ore feed of -600 +400 mm. The mass of the bigger sized balls resulted in a higher impact on the particles. This force formed smaller particles thus creating fewer critical sized material.

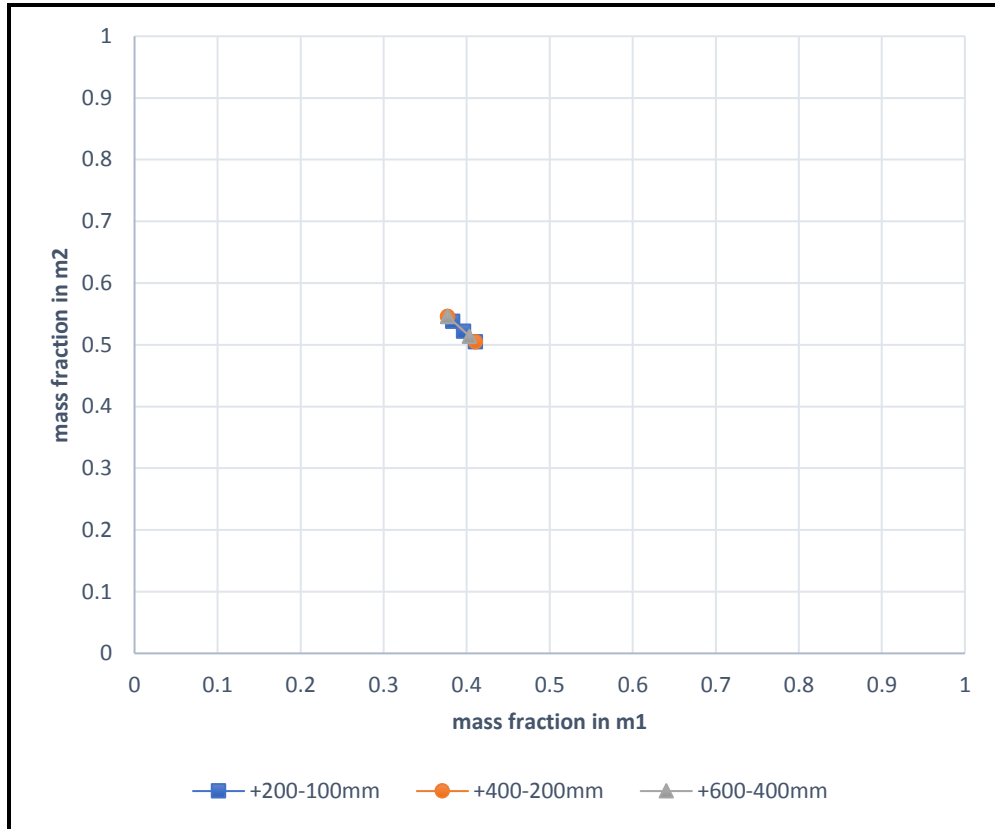


**Figure 5.21** The Attainable Region summary presenting the effects of ball size of a SAG mill in an SABC circuit under simulated conditions  $J_T = 30\%$ ,  $J_B = 10\%$ ,  $\Phi_c = 65\%$  and grate opening 40 mm.

## 5.8 Effects of mill speed on the performance of the circuit

The results represent the scenarios that were simulated at mill speed of 65%, 70% and 75% for a feed flowrate of 100tph. The purpose was to observe the effects of mill speed around a SAG mill closed circuit. Figures 5.22 – 5.24 represent the different ore feed sizes that were simulated at -200 +100 mm, -400 +200 mm and -600 +400 mm respectively.

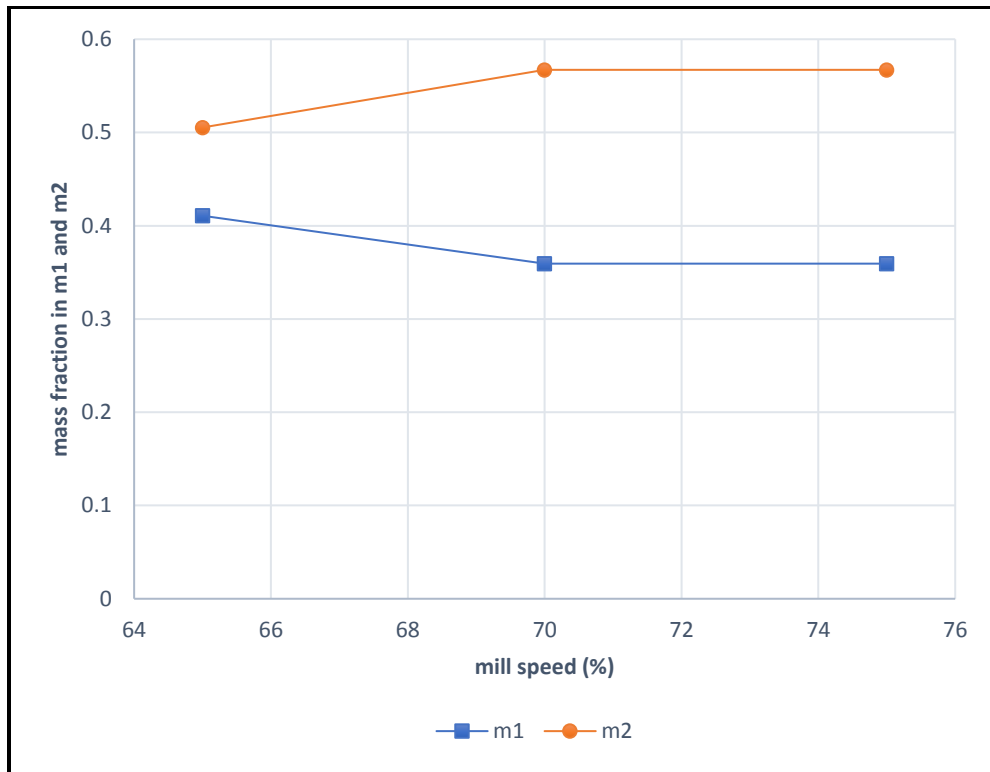


**Figure 5.22** Milling kinetics of a SAG mill in a SABC circuit as a function of an ore size of -200+100 mm under the conditions  $J_T = 30\%$ ,  $J_B = 10\%$ ,  $d_B = 50$  mm and grate opening 40 mm with a feed flow of 100 tons/hr.

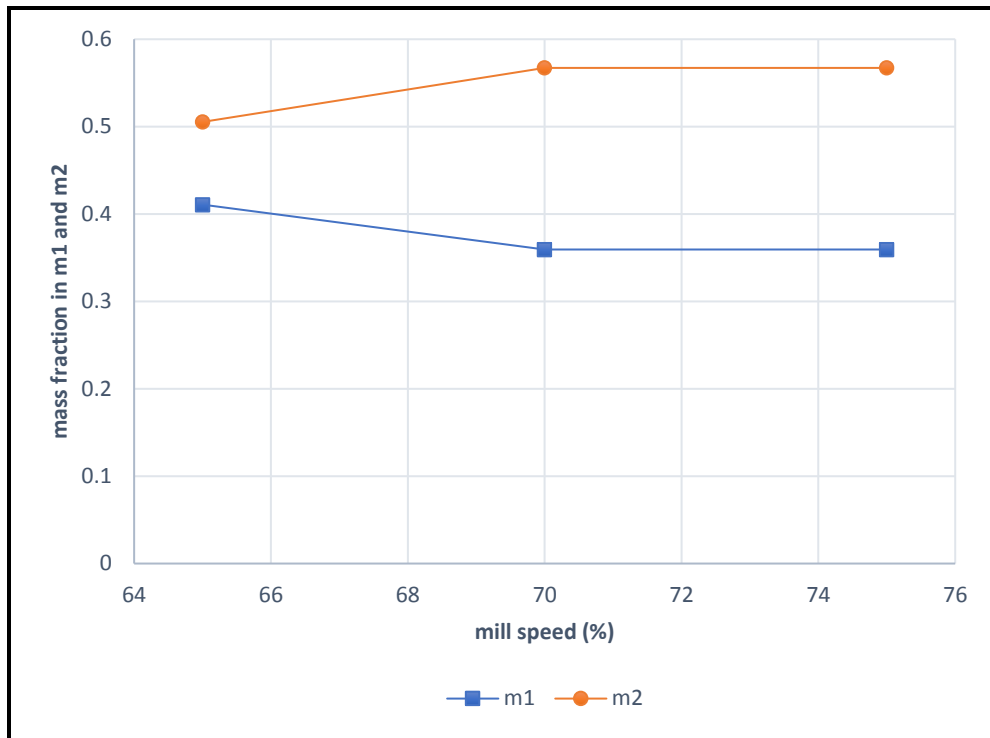


**Figure 5.23** Milling kinetics of a SAG mill in a SABC circuit as a function of an ore size of -400+200 mm under the conditions  $J_T = 30\%$ ,  $J_B = 10\%$ ,  $d_B = 50$  mm and grate opening 40 mm with a feed flow of 100 tons/hr.

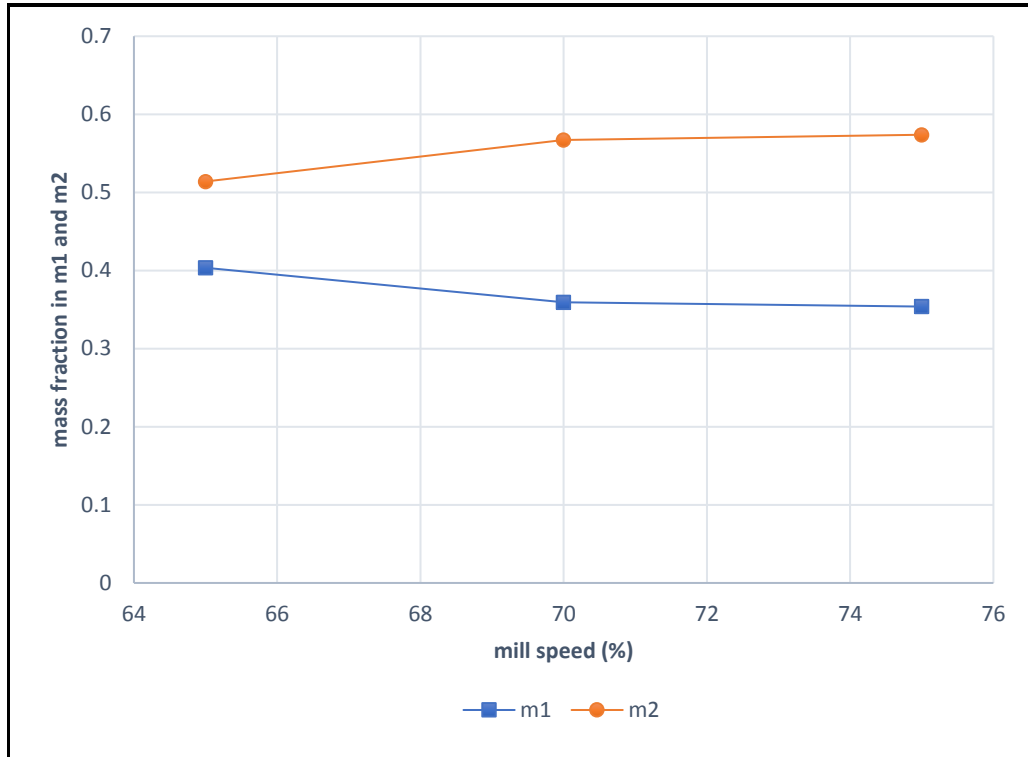


**Figure 5.24** Milling kinetics of a SAG mill in a SABC circuit as a function of an ore size of -600+400 mm under the conditions  $J_T = 30\%$ ,  $J_B = 10$ ,  $d_B = 50$  mm and grate opening 40 mm with a feed flow of 100 tons/hr.

Using the data from Figures 5.22 – 5.24 the attainable region was formed as seen in Figure 5.25. It represents 9 simulations with a constant feed flow rate of 100 tph and operating on the same conditions with mill filling of 30%, ball filling of 10%, ball size of 50 mm and grate opening of 40 mm, however, they had different ore feed size. Based on the graph, the formation of critical sized material was at its highest on a mill speed of -200 +100 mm and -400 +200 mm both at 60% mill speed representing 40% of  $m_1$ . In contrast, the maximised point for the section was 58% which represents the scenario with a ball volume of 54% and an ore feed of -600 +400 mm.

Based on Figure 5.25, the mill speed of 70 and 75% formed identical results on the different ore feed sizes. It would be recommended from an energy consumption perspective, to operate the mill speed at 70% rather than 75% due to this efficiency. It is clear that mill speed of 65% was operating at a different load

behaviour to that of 70 and 75%. The load behaviour of 65% mill speed was that of a cascading mode and the 70 and 75% mill speed favoured the cataracting mode.

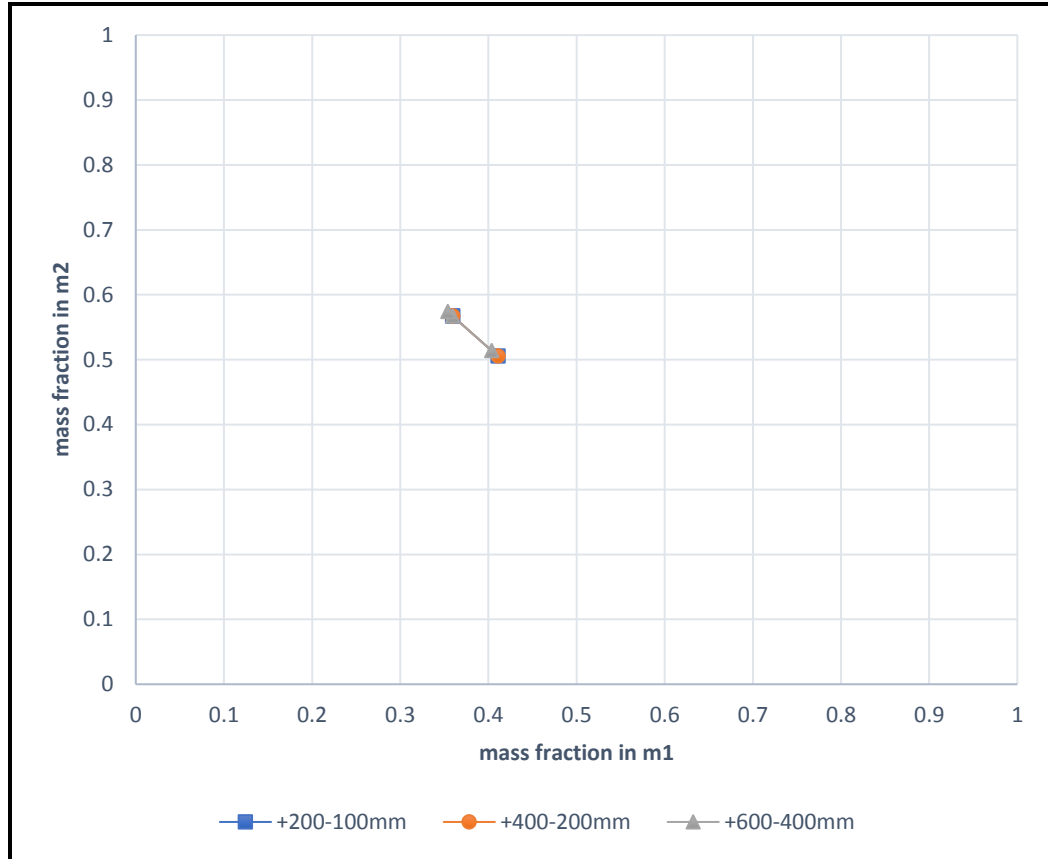


**Figure 5.25** The Attainable Region summary presenting the effects of ball size of a SAG mill in an SABC circuit under simulated conditions  $J_T = 30\%$ ,  $J_B = 10\%$ ,  $d_B = 50$  mm and grate opening 40 mm.

## 5.9 Concluding remarks

The attainable region analysis of the different scenarios illustrates the operation of the SAG mill in closed circuit. The focus was on the formation of the critical sized material in the simulated scenarios. Mass fraction  $m_1$  represented particles in the size class -100 +23 mm and  $m_2$  represented those in class -23 +4.7 mm, i.e. the critical sized material. The aim was to establish the most ideal operating system from these scenarios that would maximise size class  $m_2$  ultimately, reducing the

critical sized particles in a SAG mill. The feed flow rate and ore feed size were examined at different scenarios in the first section. For the second section, subsequent to monitoring input variables the operating parameters were additionally considered, which covered the mill filling, ball milling, ball size and mill speed. In total, there were 81 scenarios simulated at various inputs and operating parameters.

Based on the AR technique, the established results from the various scenarios were associated with Chapter 2 of this research. An increase in mill filling in the SAG mill produced less pebbles. The effects of an increase in ball filling in a SAG mill generate fewer pebbles. An increase in ball size reduces the formation of pebbles in a SAG mill. A reduction in pebble formation in a SAG mill was produced when the mill speed was operating at 70% and 75%.

## Chapter 6 Conclusion and recommendations

### 6.1. Introduction

This dissertation explored the performance of an SABC circuit using a simulation tool to improve its operation. The purpose of a milling circuit is to ensure product size requirements are met for downstream processes. The principal objective of this dissertation was then to apply the attainable region technique to find optimal operating conditions of an SABC circuit. The outcomes of this investigation are summarized in this chapter.

Computer simulation data were generated and employed for the attainable region analysis. The goal was to minimize critical sized material from a SAG mill operated in an SABC circuit by systematically adjusting key operating variables. A summary of the results and observations arising from the study undertaken are presented in the subsequent section. This is done in line with the objectives and research questions set out in the first chapter of the dissertation. Finally, conclusions and suggestions for future work also proposed.

### 6.2. Overall summary of findings

The aim of the study was to apply the attainable region technique to the classical SABC circuit. The idea was to determine the operating conditions that may eliminate the formation of pebble. The following objectives guided the research:

- ✓ To investigate the effects of feed size distribution on the formation of the critical sized particles and on the performance of the SABC circuit.
- ✓ To investigate the effects of feed rate on the energy consumption and throughput of the SABC circuit.
- ✓ To determine the milling conditions that may guarantee the optimal production of a material of a certain fineness using the attainable region technique.

The formation of critical sized pebbles in AG and SAG mills were noted as the most frequent bottleneck in its operation. The pebbles are commonly known as a fraction of material that does not self-break as readily as other sizes. There are various recommendations made to reduce this phenomenon such as the addition of pebble steel balls in the mill and the recycling of the critical sized fraction through a dedicated crusher back into the mill (Rosario, 2010). The optimization of critically sized pebbles should hypothetically improve the overall performance of the SABC circuit. This improvement is important, as the SABC circuit has many advantages such as a simple flow sheet arrangement, a small footprint, easy expansion and high potential for energy-efficient operation.

Modelling and simulation are valuable tools that are safe and economical to perform tests on the model using computer simulations rather than carrying repetitive experimentations and observations on the real system. This simulation experiment was a series of tests in which significant variations to the input variables of a simulation model were applied so that we may observe and identify the reasons for changes in the performance measures. The number of experiments in this simulation study was enough in order to determine the significant findings of the system.

The construction of the computer simulation model of the SABC circuit involved 10 units connected through 13 streams. Then, a detailed mass balance was performed for the various scenarios. In total, 81 scenarios were simulated with the focal units in the circuit being the SAG mill, the vibrating screen and the cone crusher. Based on published research, it was decided to set the critical size of the pebbles at -100 +23 mm.

The simulation program was divided into three sections. The first section looked at the performance of the SABC circuit at three feed flowrates: 50 tph, 100 tph, and 150 tph. The second section investigated the effects of ore feed size for various starting feed sizes ranging between 100 mm and 600 mm. The last section

reported on the combined effects of load volume, ball volume, ball size and mill speed on the performance of the circuit.

The results projects similar mass balance trends from the jaw crusher and stockpile. However, varies from the SAG mill as it has different operating conditions. The simulation program displays the unit equipment data that presents the operational conditions and the stream description in sizes. The energy consumption was relatively the same in the jaw crusher based on the circuit feed. However, in the SAG mill, the energy consumption significantly increased as the ore feed coarsened. This means that the mill was applying a greater power at the higher feed flow and greater ore feed size. The cone crusher was used to reduce the critical size pebbles also increased on the higher feed flow and greater ore size. In contract, the ball mill had similar energy usage throughout the scenarios.

The state variables characterizing the output of the SABC circuit was the ore size as mass fraction. The attainable region was applied by grouping the ore material into 3 size classes: the feed size class  $m_1$  for  $-100 +23$  mm, the middlings size class  $m_2$  for  $-23 +4.7$  mm and the fines size class  $m_3$  for  $-4.7$  mm. The first part was to project  $m_1$  over operational units that involved size reduction and classification from the SAG mill, vibrating screen and cone crusher. The second section was to repeat this method for  $m_2$ . Finally, on a geometric space of  $m_1$  representative for the x-axis and  $m_2$  for the y-axis the data projected on a graph to form an attainable region curve.

From the attainable region analysis, it was found that the effects of feed flow rate on the SAG mill in closed circuit were pronounced at the lowest feed of 50 tph. At an ore feed size of  $-600+400$ mm generates the least critically sized material. This is due to the breakage mechanism experienced in the mill by that particular ore feed size, together with the lower volume required for particle size reduction Furthermore, the scenarios with a feed flow rate of 150 tph with an ore feed size of  $-200 +100$  mm and  $-400 +200$  mm formed the most critical sized material. Based

on these results, the AR theory revealed that the formation of critically sized material was influenced by the increase in feed flowrate. Therefore, an increase in circuit throughput increases the generation of pebbles in a SAG mill.

Using the attainable region technique on the results for the effects of ore feed size on a SAG mill in closed circuit illustrates that the different scenarios display a consistent trend at -200 +100 mm and -400 +200 mm. However, a decline in the formation of critically sized material was observed for a feed -600 +400 mm at feed-rates 50 tph and 150 tph.

It is known that the operating parameters of a SAG mill affect the results of a system therefore to identify the ideal limits is significant. The results from the AR analysis of the effects of load volume on a SAG mill in closed circuit shows that a higher load volume produces lower critically sized material. Analysing the effects of ball volume on a SAG mill in closed circuit from an AR point of view shows a decline in critically sized material at higher ball volumes. This was demonstrated at different ore feed sizes. In terms of the effects of ball size, it was found that larger balls are prone to producing the least amount of critically sized material. The literature, however, indicates that smaller ball sizes in a mill are favoured for producing finer sized particles. The results from the AR analysis of the effects of mill speed indicated that the formation of critically sized material decreases as the mill speed increases. This can be due to the different modes of operation experienced by the media in the SAG mill. As the media experienced cascading at 65% of the critical speed, they later experienced cataracting at 70 – 75% of the critical speed; thus, increasing size reduction. Notably, the mill speed set at 70% and 75% of the critical produced similar sized material. Therefore, in order to reduce the energy usage in the circuit, the mill speed operated at 70% of the critical speed would be preferable.

### 6.3. Future outlook

This research has highlighted the importance of an SABC circuit in comminution. Future works to motivate the application of the attainable region technique for optimizing the operation of an SABC circuit would be:

- To systematically test the explorative idea covered in this simulation-based research in a real-life industrial setting. The experiment would however be aimed at validating and consolidating the attainable region findings reported in this dissertation.
- To consider the overall circuit and expand on the current simulation scenarios with varied ball mill operating parameters.
- To alter the configuration of the SABC circuit from the existing ones and determine significant findings on the modifications.

## List of references

Austin, L.G., Klimpel, R.R., Luckie, P.T., 1984. Process engineering of size reduction: Ball milling. Society of Mining Engineers of the AIME, New York

Bepswa, P.A. Mainza, A.N., Powell, M., Mwansa, S., Phiri, M., Chongo, C., van der Merwe, C., Delainey, A., Mande, P., Mulenga, D., Batubenga, L., 2015. Insights into different operating philosophies – Influence of a variable ore body on comminution circuit design and operation. SAG Conference, 20 – 23 September 2015, Vancouver, Canada

Bilgili, E., Scarlett, B., 2005. Population balance modeling of non-linear effects in milling processes. Powder Technology, vol. 153, pp. 59 – 71

Chimwani, N., Glasser, D., Hildebrandt, D., Metzger, M.J., Mulenga, F.K., 2013. Determination of the milling parameters of a platinum group minerals ore to optimize product size distribution for flotation purposes. Minerals Engineering, vol. 43 – 44, pp. 67 – 78

Chimwani, N., 2014. An attainable region approach to optimizing product size distribution for flotation purposes. PhD thesis, University of the Witwatersrand, Johannesburg

Curry, J.A., Ismay, M.J.L., Jameson, G.J., 2014. Mine operating costs and the potential impacts of energy and grinding. Minerals Engineering, vol. 56, pp. 70 – 80

Dance, A., Atheis, D., Williems, S., Taplin, D., 2014. Grinding circuit improvements at evolution mining's Edna May operation

Danha, G., Hildebrandt, D., Glasser, D., Bhodayi, C., 2015. A laboratory scale application of the attainable region on a platinum ore. Powder Technology, vol. 274, pp. 14 – 19

Dindarloo, S.R., Siami-Irdemoosa, E., 2016. Merits of discrete event simulation in modeling mining operations. SME Annual Meeting, 21 – 24 February 2016, Phoenix, Arizona, United States of America

- Epstein, B., 1947. The material description of certain breakage mechanisms leading to the logarithmic-normal distribution. *Journal of the Franklin Institute*, vol. 244, no. 12, pp. 471 – 477
- Evertsson, M., 2000. Cone crusher performance. PhD thesis, University of Technology Goteborg, Sweden
- Gupta, A., Yan, D.S. 2006. Mineral processing design and operation: an introduction. Elsevier, Perth
- Hart, S., Valery, W., Clements, B., Reed, M., Song, M., Dunne, R., 2001. Optimisation of the Cadia Hill SAG mill circuit. *Mining and Mineral Process Engineering*, University of British Columbia, Vancouver, Canada
- Hlabangana, N., Danha, G., Hildebrandt, D., Glasser, D., 2016. Use of the attainable region approach to determine major trends and optimize particle breakage in a laboratory mill. *Powder Technology*, vol. 294, pp. 414 – 419
- Hlabangana, N., Danha, G., Bwalya, M.M., Hildebrandt, D., Glasser, D., 2017. Application of the attainable region method to determine optimal conditions for milling and leaching. *Powder Technology*, vol. 317, pp. 400 – 407
- Hlabangana, N., Danha, G., Muzenda, E., 2018. Effect of ball and feed particle size distribution on the milling efficiency of a ball mill: An attainable region approach. *South African Journal of Chemical Engineering*, vol. 25, pp. 79 – 84
- Kawatra, S.K., Eisele, T.C., Walqui, H.J., 2001. Optimization of comminution circuit throughput and product size distribution by simulation and control. *Quarterly Technical Process Report*, Michigan Technological University, Houghton, United States of America
- Khumalo, N., 2007. The application of the attainable region analysis in comminution. PhD thesis, University of the Witwatersrand, Johannesburg
- King, R.P., 2001. Modelling and simulation of mineral processing systems. Butterworth-Heinemann, Oxford

King, R.P., 2012. Modeling and simulation of mineral processing systems – 2nd Edition. C.L. Schneider and E.A. King (Eds.), Society for Mining, Metallurgy, and Exploration, Colorado, United States of America

Lehohla, P., 2017. Mining industry 2015. Statistics South Africa

Lynch, A.J., Morrison, R.D., 1999. Simulation in mineral processing history, present status and possibilities. *Journal of South African Institute of Mining and Metallurgy*, vol. 99, no. 6, pp. 283– 288

Malhotra, D., Taylor, P.R., Spiller, E., LeVier, M., 2009. Recent advances in mineral processing plant design. Society for Mining, Metallurgy and Exploration, Colorado, United States of America

Makokha, A., 2011. Measuring, characterisation and modelling of load dynamic behaviour in a wet overflow-discharge ball mill. PhD thesis, University of the Witwatersrand, Johannesburg

Maria, A., 1997. Introduction to modeling and simulation. State University of New York, Binghamton, United States of America

McCaffery, K., Jankovic, A., Valery, W., La Rosa, D., Burger, B., McGaffin, I., 2006. Batu Hijau model for throughput forecast, mining and milling optimisation and expansion studies. Metso Minerals Process Technology, Brisbane, Australia

Metzger, M.J., Glasser, D., Hausberger, B., Hildebrandt, D., Glasser, B.J., 2009. Use of the attainable region analysis to optimize particle breakage in a ball mill. *Chemical Engineering Science*, vol. 64, no. 17, pp. 3766 – 3777

Mulenga, F.K., Bwalya, M.M., 2015. Application of the attainable region technique to the analysis of a full-scale mill in open circuit. *Journal of the Southern African Institute of Mining and Metallurgy*, vol. 115, no. 8, pp. 729 – 740

Mulenga, F.K., Mkonde, A.A., Bwalya, M.M., 2016. Effects of load filling, slurry concentration and feed flowrate on the attainable region path of an open milling circuit. *Minerals Engineering*, vol. 89, pp. 30 – 41

Napier-Munn, T.J., Morrell, S., Morrison, R.D., Kojovic, T., 1996. Mineral Comminution Circuits – Their Operation and Optimisation. JKMRC Monograph, University of Queensland, Australia

Staples, P., Lane, G., Braun, R., Foggiatto, B., Bueno, M.P., 2015. Are SAG mills losing market confidence?. SAG Conference. Vancouver, Canada

Tondo, L.A, Valery, W., Peroni, R., La Rosa, D., Silva, A., Jankovic, a., Colacioppo, J., 2006. Kinross' Rio Paracatu Mineracao (RPM) mining and milling optimisation of the existing and new SAG mill circuit. International Conference on Autogenous and Semiautogenous Grinding Technology, SAG2006, University of British Columbia, Vancouver, Canada

Umucu, Y., Deniz, V., Bozkurt, V., 2012. The evaluation of grinding process using MODSIM©. Journal of Mining and Geoengineering, vol. 36, no. 2, pp. 187 – 200

Verma, R., Rajamani, R.K., 2002. Effect of milling environment on the breakage rates in dry and wet grinding. In S.K. Kawatra (Ed.), Comminution: Theory and practice, pp. 261 – 271

Whiten, J.W., Narayanan, S.S., 1983. Breakage characteristics for ores for ball mill modelling. The Australasian institute of mining and metallurgy. No 286, pp 31-39

Wills, B.A., Napier-Munn, T.J., 2005. Wills' mineral processing technology: An introduction to the practical aspects of ore treatment and mineral recovery, 7th Edition. Elsevier, London

Zhang, W., 2016. Optimizing performance of SABC comminution circuit of the Wushan porphyry copper mine – A practical approach. Minerals, vol. 6, pp. 127 – 135

## Appendices

Appendix A: Simulation programme of the SAG mill closed circuit.

| Input parameters     |               |                | Operating parameters |                  |                |                |                    |                      |              |
|----------------------|---------------|----------------|----------------------|------------------|----------------|----------------|--------------------|----------------------|--------------|
| Independent variable |               | Fixed variable | SAG Mill             |                  |                |                |                    | Screen               | Cone crusher |
| Plant feed (tph)     | Ore size (mm) | Water feed (%) | Mill filling (%)     | Ball filling (%) | Ball size (mm) | Mill speed (%) | Grate opening (mm) | d <sub>50</sub> (mm) | CSS (mm)     |
| 100                  | -200+100      | 60             | 30                   | 10               | 50             | 65             | 40                 | 0.023                | 0.001        |
| 100                  | -400+200      | 60             | 30                   | 10               | 50             | 65             | 40                 | 0.023                | 0.001        |
| 100                  | -600+400      | 60             | 30                   | 10               | 50             | 65             | 40                 | 0.023                | 0.001        |
| 100                  | -200+100      | 60             | 35                   | 10               | 50             | 65             | 40                 | 0.023                | 0.001        |
| 100                  | -400+200      | 60             | 35                   | 10               | 50             | 65             | 40                 | 0.023                | 0.001        |
| 100                  | -600+400      | 60             | 35                   | 10               | 50             | 65             | 40                 | 0.023                | 0.001        |
| 100                  | -200+100      | 60             | 40                   | 10               | 50             | 65             | 40                 | 0.023                | 0.001        |
| 100                  | -400+200      | 60             | 40                   | 10               | 50             | 65             | 40                 | 0.023                | 0.001        |
| 100                  | -600+400      | 60             | 40                   | 10               | 50             | 65             | 40                 | 0.023                | 0.001        |
| 100                  | -200+100      | 60             | 30                   | 12               | 50             | 65             | 40                 | 0.023                | 0.001        |
| 100                  | -400+200      | 60             | 30                   | 12               | 50             | 65             | 40                 | 0.023                | 0.001        |
| 100                  | -600+400      | 60             | 30                   | 12               | 50             | 65             | 40                 | 0.023                | 0.001        |
| 100                  | -200+100      | 60             | 30                   | 14               | 50             | 65             | 40                 | 0.023                | 0.001        |
| 100                  | -400+200      | 60             | 30                   | 14               | 50             | 65             | 40                 | 0.023                | 0.001        |
| 100                  | -600+400      | 60             | 30                   | 14               | 50             | 65             | 40                 | 0.023                | 0.001        |
| 100                  | -200+100      | 60             | 30                   | 10               | 75             | 65             | 40                 | 0.023                | 0.001        |
| 100                  | -400+200      | 60             | 30                   | 10               | 75             | 65             | 40                 | 0.023                | 0.001        |
| 100                  | -600+400      | 60             | 30                   | 10               | 75             | 65             | 40                 | 0.023                | 0.001        |
| 100                  | -200+100      | 60             | 30                   | 10               | 100            | 65             | 40                 | 0.023                | 0.001        |
| 100                  | -400+200      | 60             | 30                   | 10               | 100            | 65             | 40                 | 0.023                | 0.001        |
| 100                  | -600+400      | 60             | 30                   | 10               | 100            | 65             | 40                 | 0.023                | 0.001        |
| 100                  | -200+100      | 60             | 30                   | 10               | 50             | 70             | 40                 | 0.023                | 0.001        |
| 100                  | -400+200      | 60             | 30                   | 10               | 50             | 70             | 40                 | 0.023                | 0.001        |
| 100                  | -600+400      | 60             | 30                   | 10               | 50             | 70             | 40                 | 0.023                | 0.001        |
| 100                  | -200+100      | 60             | 30                   | 10               | 50             | 75             | 40                 | 0.023                | 0.001        |
| 100                  | -400+200      | 60             | 30                   | 10               | 50             | 75             | 40                 | 0.023                | 0.001        |
| 100                  | -600+400      | 60             | 30                   | 10               | 50             | 75             | 40                 | 0.023                | 0.001        |